

AN ABSTRACT OF THE THESIS OF

DAVID LEE BRENCHLEY for the Ph. D.
(Name) (Degree)

in MECHANICAL ENGINEERING presented on March 7, 1968
(Major) (Date)

Title: AN EXPERIMENTAL INVESTIGATION OF COMBUSTION
PRODUCTS THROUGH A FLAT, LAMINAR, PREMIXED HYDRO-
CARBON-AIR FLAME

Abstract approved: _____
J. G. Mingle/

Flat, laminar, premixed hydrocarbon-air flames were stabilized on a porous-plate burner. In addition to temperature profiles, concentration profiles were measured for methane, ethane, ethylene, propane, acetylene, propylene, carbon monoxide, carbon dioxide and oxides of nitrogen. Dead space thickness, luminous flame zone thickness and hydrocarbon disappearance point responses were also monitored. The experimental parameters investigated were hydrocarbon fuel type: propane and propylene; equivalence ratio: .90 to 1.10; plate temperature: 600°F to 800°F; and sampling position: .005 to .335 cm.

A completely randomized nonreplicated factorial experiment was used to statistically detect the presence of main and two-factor interaction effects. Higher order three and four-factor interaction terms were pooled as an estimate of the error term. Null and alternative hypotheses were proposed concerning the presence of main and two-factor effects. The results of these tests indicate:

1. Stable species hydrocarbons exist in the reaction zone under all of the conditions investigated. Their concentration is a function of fuel type, equivalence ratio, sampling position and in some cases plate temperature. Several significant interaction terms are also present.

2. Ethylene is the major stable hydrocarbon species for both propane and propylene as fuels. The quantitative ranking of the other hydrocarbon species is a function of fuel type, equivalence ratio, and plate temperature.

3. Dead space thickness is a function of fuel type, equivalence ratio, and plate temperature but no significant two-factor interaction terms are present. For each fuel, dead space thickness may be expressed in the functional form

$$Y = \beta_0 + \beta_1 X_1 + \beta_2 X_2 + \beta_3 X_1^2 + \beta_4 X_2^2$$

where,

X_1 plate temperature °F.

X_2 equivalence ratio.

β 's constants.

4. Luminous flame zone thickness is a function of fuel type only. Propylene exhibits a greater flame zone thickness than propane.

5. Hydrocarbon disappearance point is a function of

equivalence ratio and plate temperature. Its response may be expressed in the function form

$$Y = \beta_0 + \beta_1 X_1 + \beta_2 X_1^2 + \beta_3 X_2^2$$

where,

X_1 plate temperature °F.

X_2 equivalence ratio.

β 's constants.

6. Oxides of nitrogen concentration is a function of fuel type, equivalence ratio, plate temperature, and sampling position.

Several significant interaction terms are also present. In order to examine the true fuel structure effect, the predominant covariant flame temperature effect must be removed.

One-dimensional flame equations were applied to the experimental data. Sample calculations indicate that the presence of carbon monoxide and carbon dioxide concentrations at the surface of the burner cannot be completely attributed to diffusion processes. Therefore, one must conclude that chemical reaction takes place within the dead space.

An Experimental Investigation of Combustion
Products Through a Flat, Laminar,
Premixed Hydrocarbon-Air Flame

by

David Lee Brenchley

A THESIS

submitted to

Oregon State University


in partial fulfillment of
the requirements for the
degree of

Doctor of Philosophy

June 1968

APPROVED:

Redacted for privacy

 _____
Professor of Mechanical Engineering
in charge of major

Redacted for privacy

Head of Department of Mechanical Engineering

Redacted for privacy

Dean of Graduate School

Date thesis is presented MARCH 7, 1968

Typed by Marion F. Palmateer for David L. Brenchley

ACKNOWLEDGMENTS

The student-professor relationship is capable of encompassing many extremes. I am grateful to Professor Mingle for exercising a philosophy which allows the student responsibility and flexibility yet provides the required friendship, encouragement and logistic support.

During the past four years Dr. Richard Boubel has had an instrumental influence on my graduate program. For his interest, help, concern and friendship I extend a simple but sincere "thank you".

I wish to acknowledge the following for contributions which expedited the completion of this work: Public Health Service for financial assistance under fellowship 5 F3 AP 30,827-02; Professors L. S. Slotta and D. C. Phillips of the Civil Engineering Department for loaning critical equipment; Jack Kellogg, mechanic, for his craftsmanship and ingenuity in construction of test equipment; fellow graduate students for their friendship and keen competitiveness; Dr. G. D. Faulkenberry of the Statistics Department for needed consultation; and David Neiss of the Computer Center for his efficient handling of the computer work.

Special thanks to my family and parents for much needed encouragement.

Doctoral Committee: J. G. Mingle, R. W. Boubel, J. R. Welty, D. C. Phillips, L. D. Calvin, and W. A. Davies.

NOMENCLATURE

A	experimental factor A: hydrocarbon fuel type.
B	experimental factor B: equivalence ratio.
C	experimental factor C: plate temperature, °F.
D	experimental factor D: sampling position, cm.
a, b, c, d	number of levels of factors A, B, C, and D respectively.
n	number of replications.
Y	dependent response.
Z	independent variable (sampling position, cm.)
A/F	air-fuel ratio.
ϕ	equivalence ratio; $\phi = (A/F)/(A/F)_{\text{stoichiometric}}$
X_i	mole fraction of species i.
F_t^s	critical variance ratio with s and t degrees of freedom.
ppm	parts per million by volume.
NO _x	oxides of nitrogen.
σ^2	population variance.
β	polynomial coefficients.

TABLE OF CONTENTS

<u>Chapter</u>		<u>Page</u>
I	INTRODUCTION	1
	The Problem	1
	Purpose of Study	2
	Objective of Study	4
II	LITERATURE REVIEW	6
	Flame Propagation	6
	Flame Quenching	10
III	EXPERIMENTAL PROGRAM	19
	Factors Leading to Experimental Program	19
	Purpose of Experimental Program	20
	Experimental Parameters	20
	Experimental Techniques	22
	Experimental Apparatus	28
	Experimental Procedures	36
	Statistical Design	39
IV	RESULTS	46
	Experimental Data	46
	Results of Statistical Analysis	47
	Application of Laboratory Flame Equations	82
	Discussion of Experimental Data	96
	Discussion of Experimental Design	102
	Discussion of Experimental Equipment	103
V	CONCLUSIONS AND RECOMMENDATIONS	107
	Conclusions	107
	Recommendations	108
	BIBLIOGRAPHY	110
	APPENDICES	116
	APPENDIX A: QUARTZ SAMPLING PROBE TECHNIQUE	116

	<u>Page</u>
APPENDIX B: RADIATION LOSS CORRECTION FOR THERMOCOUPLE READINGS	1 20
APPENDIX C: CALIBRATION OF DISA MODEL 55 A01 HOT-WIRE ANEMOMETER	1 23
APPENDIX D: OPERATION AND CALIBRATION OF PERKIN-ELMER MODEL 810 GAS CHROMATOGRAPH	1 26
APPENDIX E: CALIBRATION OF BECKMAN CARBON MONOXIDE AND CARBON DIOXIDE ANALYZERS	1 29
APPENDIX F: CONSTRUCTION DETAILS OF TEST EQUIPMENT	1 32
APPENDIX G: DETERMINATION OF AIR AND FUEL MASS FLOW RATES	1 35
APPENDIX H: CALIBRATION OF PACE MODEL KP 15 PRESSURE TRANSDUCERS	1 38
APPENDIX I : ONE-DIMENSIONAL FLAME EQUATIONS	1 39
APPENDIX J : METHOD FOR CALCULATING BINARY DIFFUSION COEFFICIENTS	1 44
APPENDIX K: EXPERIMENTAL DATA	1 49
APPENDIX L: TWO-WAY TABLES OF MEANS FOR THREE-FACTOR AND FOUR- FACTOR ANALYSES OF VARIANCE	1 79

LIST OF TABLES

<u>Table</u>		<u>Page</u>
1	Analysis of variance of four-factor factorial experiment.	43
2	Four-factor analysis of variance for methane response.	51
3	Four-factor analysis of variance for ethane response.	52
4	Four-factor analysis of variance for ethylene response.	53
5	Four-factor analysis of variance for propane response.	54
6	Four-factor analysis of variance for acetylene response.	55
7	Four-factor analysis of variance for propylene response.	56
8	Four-factor analysis of variance for carbon monoxide response.	57
9	Four-factor analysis of variance for carbon dioxide response.	58
10	Four-factor analysis of variance for oxides of nitrogen response.	59
11	Mean values for four-factor main effects.	60
12	Three-factor analysis of variance for dead space thickness response.	74
13	Three-factor analysis of variance for flame zone thickness response.	75
14	Three-factor analysis of variance for point of hydrocarbon disappearance response.	76
15	Actual versus predicted values for dead space and point of hydrocarbon disappearance response.	83

<u>Table</u>		<u>Page</u>
16	Derived specie diffusion velocities for operating conditions of fuel: propane; equivalence ratio: 1.05; plate temperature: 800°F.	86
Appendix		
<u>Table</u>		
C-1	Calibration data for Disa Model 55 A01 anemometer.	125
G-1	Calibration of air flowmeter for Equation (3-1).	136
G-2	Calibration of fuel flowmeter for Equation (3-1).	137
J-1	Potential parameters for Lennard-Jones (12-6) Potential.	148
K-1 to K-30	Experimental data.	149
L-1 to L-12	Two-way tables of means for three-factor and four-factor analyses of variance.	179

LIST OF FIGURES

<u>Figure</u>		<u>Page</u>
1	Side view of porous-plate, flat-flame burner.	4
2	A generalized temperature distribution across the flame front.	6
3	Tip of quartz sampling probe.	23
4	Tip of thermocouple probe.	24
5	Burner system.	29
6	Fuel and air flow apparatus.	32
7	Sampling and analytical system.	35
8	General response profiles of methane, ethane, and acetylene.	62
9	General response profile of ethylene.	63
10	General response profiles of carbon monoxide and carbon dioxide.	64
11	General response profile of hydrocarbon fuel.	65
12	General response profile of oxides of nitrogen.	66
13	Effect of equivalence ratio on ethylene response for propane and propylene fuels.	67
14	General response profiles of ethylene for propane and propylene fuels.	68
15	General ethylene response profiles for equivalence ratios of .90, .95, 1.00, 1.05 and 1.10.	69
16	General effect of equivalence ratio on ethylene response for plate temperatures of 600° F, 700° F and 800° F.	70
17	General ethylene response profiles for plate temperatures of 600° F, 700° F and 800° F.	71

<u>Figure</u>		<u>Page</u>
18	General effect of equivalence ratio on dead space response for propane and propylene fuels.	78
19	General effect of plate temperature on dead space response for propane and propylene fuels.	79
20	General effect of equivalence ratio and plate temperature on point of hydrocarbon disappearance.	80
21	Derived gas flow and ethylene diffusion velocities for operating conditions of fuel: propane; equivalence ratio: 1.05; plate temperature: 800° F.	88
22	Ethane response mass fraction profiles for operating conditions of fuel: propane; equivalence ratio: 1.05; plate temperature: 800° F.	90
23	Ethylene response mass fraction profiles for operating conditions of fuel: propane; equivalence ratio: 1.05; plate temperature; 800° F.	91
24	Propane response mass fraction profiles for operating conditions of fuel: propane; equivalence ratio: 1.05; plate temperature: 800° F.	92
25	Carbon monoxide response mass fraction profiles for operating conditions of fuel: propane; equivalence ratio: 1.05; plate temperature: 800° F.	93
26	Carbon dioxide response mass fraction profiles for operating conditions of fuel: propane; equivalence ratio: 1.05; plate temperature: 800° F.	94
 Appendix		
<u>Figure</u>		
D-1	Hydrocarbon calibration curves for Perkin-Elmer Model 810 gas chromatograph.	127
E-1	Carbon dioxide calibration curve. Beckman IR-215.	130
E-2	Carbon monoxide calibration curve. Beckman IR-15A.	131

<u>Figure</u>		<u>Page</u>
F-1	Details of thermocouple probe.	132
F-2	Details of quartz sampling probe.	133
F-3	Details of burner assembly.	134
J-1	Parameters of Lennard-Jones Potential.	146

AN EXPERIMENTAL INVESTIGATION OF COMBUSTION PRODUCTS THROUGH A FLAT, LAMINAR, PREMIXED HYDROCARBON-AIR FLAME

I. INTRODUCTION

The Problem

During the past two decades combustion research has been expanding at an accelerated rate. The combined activities of scientists with varying backgrounds--chemists, physicists, engineers, mathematicians--have led to a rapid growth of fundamental knowledge of the complex phenomena which constitute the subject of combustion.

It is hardly necessary to remark that all combustion processes are of the nature of chemical reactions with net heat evolution. Furthermore, it is clear that the attainment of conditions for reaction is necessarily preceded by physical processes governing the motion of reactants into the zone of combustion. Thus, in general, combustion phenomena involve the interaction between chemical and transport processes, i. e. aerothermochemistry.

A number of conflicting theories have been put forth to explain the mechanism of flame propagation. These involve the simultaneous solution of continuity, momentum and energy equations with consideration of the effect of chemical reactions. If a theory of the mechanism of combustion fails to predict flame speed in agreement with observations, the theory is immediately open to question. A sound theory of

flame propagation should explain the relationship between flame speed and the fundamental physical and chemical properties of fuels. However, since the early attempts late in the 19th Century, all attempts to develop such a theory have led to failure. This situation results from both an insufficient knowledge of the chemical processes occurring in the flame and the complex nature of the problem with its associated mathematical difficulties. The simple models of combustion have proved to be inadequate. The mathematical models being studied at the present are complex, involving many parameters whose values are unknown. Additional experimental data are needed for a better understanding of the combustion process and for assisting the theorist in the formulation of mathematical descriptions of flame behavior.

Purpose of Study

The primary purpose of this study was to provide experimental data which may help elucidate the mechanism of flame propagation and, in particular, the associated phenomenon termed flame quenching. Flame propagation is a progressing chemical reaction enhanced by diffusion of heat and/or chemically active species into the adjacent layers of the mixture. Flame quenching may be defined as the effect of a relatively cool combustion chamber wall in suppressing flame propagation and retarding chemical reaction in the immediate vicinity

of the wall. The behavior of flames in the neighborhood of solid boundaries is of great interest in the study of the mechanism of combustion. Visual evidence of quenching by a wall surface is generally manifested by a dark zone or "dead space" between the luminous part of the flame and the wall. While the dead space is of the order-of-magnitude of only a flame thickness, the influence of heat and species transfer through the dead space can extend into the adjacent reaction zone to a distance several times the flame thickness.

This study encompassed the use of a controlled laboratory combustion system. The operating parameters investigated were: (1) type of fuel, (2) equivalence ratio, (3) wall temperature, and (4) sampling position. In order to avoid the myriad of problems associated with studying the transient flame quenching process, a steady-state model was used. This consisted of a porous-plate, flat-flame burner enclosed in a chamber. As shown in Figure 1, this model produced a one-dimensional, steady-state flame propagating toward a relatively cool wall.

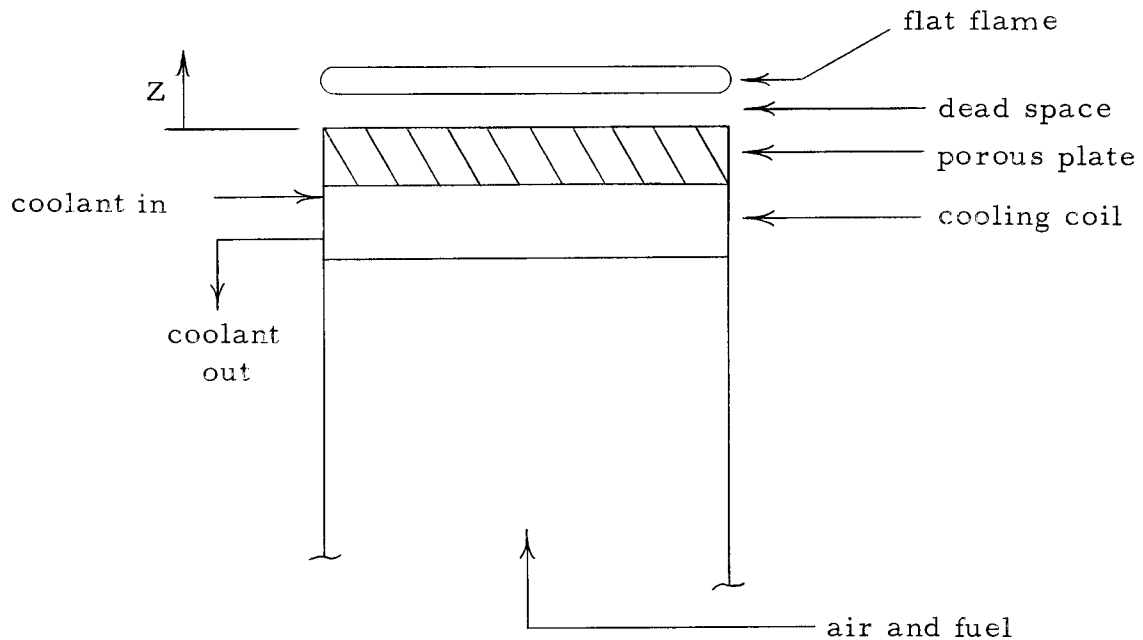


Figure 1. Side view of porous-plate, flat-flame burner.

Objectives of Study

The objectives of this experimental study were:

1. To measure the quantity of methane, ethane, ethylene, propane, propylene, acetylene, carbon monoxide, carbon dioxide and oxides of nitrogen in the vicinity of the wall under controlled variations of hydrocarbon fuel type, equivalence ratio, wall temperature, and sampling position. Use standard statistical techniques to test for main effects and two factor interaction effects.
2. To make linear measurements of dead space thickness and luminous flame zone thickness under controlled

variations of hydrocarbon fuel type, equivalence ratio, and wall temperature. Statistically test for presence of main effects and two factor interaction effects.

3. To observe the point in the flame zone where the hydrocarbon concentration approaches zero. Determine how this point is influenced by the controlled variation of the combustion parameters.
4. To measure the temperature profiles through the flame zone.
5. To gain a better understanding of flame propagation and flame quenching.

II. LITERATURE REVIEW

Flame Propagation

The theories advanced to explain flame propagation may be conveniently classified into three categories: (1) thermal theories, (2) diffusion theories, and (3) "mixed" theories. A comprehensive review of these general classes of theories has been made by Evans (13) and von Karman (51).

At one extreme, the so-called thermal theories postulate that continuity of reaction in a flow system is maintained by propagation of heat from the high-temperature reaction zone, thus raising the temperature of the approaching flow to a critical value (ignition temperature) necessary for initiating the reaction. These thermal theories are developed from a generalized temperature distribution as shown in Figure 2.

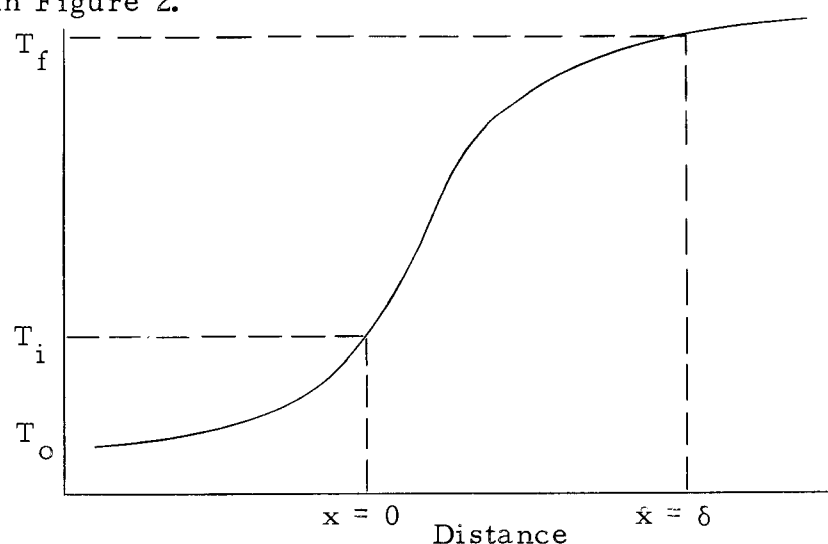


Figure 2. A generalized temperature distribution across the flame front.

The flame front is considered to be stationary at $x = 0$; and the reaction zone extends a distance δ . The energy equation, Equation (1-1), applied under steady-state conditions, is fundamental to the thermal theories. Differences in the various thermal theories result from different assumptions introduced to make a solution feasible.

$$\frac{d^2 T}{dx^2} - \frac{F \rho C_p}{\lambda} \frac{dT}{dx} + \frac{rQ}{\lambda} = 0 \quad (1-1)$$

where

T temperature.

x distance.

ρ gas density

C_p specific heat.

F flame speed.

r reaction rate.

Q heat of reaction.

λ thermal conductivity.

In solving this equation two important assumptions which strongly influence any solution are usually introduced. These are (1) below T_i , no reaction occurs; and (2) above T_i , the reaction proceeds at a constant rate. Concerning the first assumption, the combustion reaction is a continuous process, going from a slow oxidation to a cool flame region under proper conditions, and finally to the

hot-flame, fast reaction. To say that no reaction occurs is equivalent to saying that there is no slow oxidation. But slow oxidations and cool flames do occur, do have exothermic heats of reaction, and, therefore, contribute to raising the gases to the ignition temperature T_i , in addition to the heating effect due to conduction from the flame front. Concerning the second assumption, kinetic studies show that the rate of oxidation is a function of temperature, pressure, and concentration; therefore, the rate is a function of distance within the flame front. But, until the mechanism of hydrocarbon combustion is better understood, it is possibly preferable and certainly easier to obtain formal mathematical solutions to Equation (1-1) by considering the term $\frac{rQ}{\lambda}$ to be constant.

For $T < T_i$, Equation (1-1) is solved with $\frac{rQ}{\lambda}$ equal to zero. For $T > T_i$, $\frac{rQ}{\lambda}$ takes a constant value. At T_i , the temperature and heat flow of the two equations are equated. The flame speed relationship shown in Equation (1-2) is then obtained.

$$F = \sqrt{\frac{\lambda r}{\rho C_p a_o} \frac{T_f - T_o}{T_i - T_o}} \quad (1-2)$$

where a_o is the mole concentration of the combustible. Equation (1-2) is the form of solution obtained by many early workers including Daniell (10), using the thermal theory approach.

Another extreme view is represented by the so-called diffusion

theory according to which, in the steady-state combustion zone, active particles such as hydrogen atoms and hydroxyl radicals, present in the high temperature burned mixture, diffuse upstream into the fresh combustible and serve as ignition centers. Because of the mathematical similarities between the equations which govern thermal conduction and those which govern particle diffusion, the flame speed equations derived on the basis of either thermal or diffusion mechanisms are similar in form. A major difference in the results is in the predicted effect of pressure on burning velocity. The effect is negligible in thermal theories, but important in diffusion theories. Equation (1-3), which is of the form used by Simon (47), is typical of that obtained by using the diffusion theory

$$F = \sqrt{\frac{\sum_i \frac{K_i C P_i D_i L}{Q B_i}}{1}} \quad (1-3)$$

where the subscript i refers to the species under consideration and

- C initial mole fraction of combustible.
- Q mole fraction of potential combustion products, carbon dioxide and water vapor.
- L molecules per cc of gas at mean temperature.
- K_i rate constant for interaction of radical with one combustible.
- P_i equilibrium partial pressure in the burned gas.

D_i coefficient of diffusion into unburned gas.

B_i term where value depends upon the rate of radical recombination.

The controversy between the thermal and radical diffusion theories is far from being resolved. Often is the case that any arguments used to defend one theory can readily be applied with a few assumptions to also defend the other theory. As one studies the arguments for either the thermal or diffusion mechanisms, it becomes apparent that the actual combustion process probably depends on both mechanisms to some extent. There have been at least three developments using the "mixed" theory approach: Hirschfelder and Curtiss (30), von Karman and Penner (53), and Boys and Corner (5). As one might expect, these approaches are quite sophisticated and certainly too extensive to discuss here. Any attempt to condense these complex mathematical developments would be grossly inadequate.

Flame Quenching

Flame quenching (wall quenching) has been studied by many research workers from both theoretical and experimental approaches. Although these researchers' interests arose from various fields of application, they were primarily studying wall quenching as a natural phenomenon.

Various methods were used to indicate the extent of the

quenching effect. Two of the principal methods were: (1) linear measurement of the dark zone or dead space between the wall and the luminous part of the flame, and (2) measurement of the minimum opening through which a flame will propagate. As was the case with flame propagation, the thermal and particle diffusion theories have been offered as mechanisms explaining the flame quenching phenomenon. In the thermal theory, the cooling effect of the wall is the principal deterrent to flame propagation. But, in the diffusion theory, free radical chain carriers necessary for propagation are said to be deactivated by the wall. Before the importance of free radicals and atoms in flames was fully appreciated, it was accepted that quenching was entirely governed by heat conduction from the flame to the cold surface, the chemical reaction being able to proceed only in those regions of the gas where the temperature was greater than a vaguely defined "ignition temperature." Now in the light of present knowledge of chain reactions it appears that diffusion of free radicals to the wall may well play significant roles in flame quenching.

In studies by von Karman and Millan (52) on laminar flames near a cold wall, a flame was assumed to be propagating in a large diameter tube filled with a combustible gaseous mixture. A thermal theory was used; diffusion between various species and the possible chain breaking effect on the wall were neglected. It was assumed

that a one dimensional theory of the laminar flame front could be applied, with the exception of a domain near the wall in which approximately a two dimensional form can be assumed. In these studies, dead space was defined as the distance between the wall and a point in the flame front corresponding to the "ignition temperature." Predicted dead space values for methane, propane and ethylene did not agree well with measured values. However, von Karman noted that the ratio of these terms remained constant and, therefore, felt this somewhat substantiated the thermal conduction theory for explaining flame shape near a cool wall.

In a case considered by Wohl (57) a flame was assumed to be established parallel to a cool wall by igniting a combustible gaseous mixture passed through a cooled porous wall. A visible flame zone is established parallel to the plate. If the flow velocity is decreased, the visible flame zone will approach the plate. At a certain low velocity and distance, cooling will be so strong as to extinguish the flame. The dead space is directly accessible to observation as the distance between the visible upstream boundary of the flame front and the plate. Wohl found that the distance from the wall at which a flame can be maintained is a function of the amount of heat transferred to the wall. Thus, if the heat transfer is increased, then a greater distance would be necessary to reduce the heat transfer and maintain the flame, otherwise the flame would be quenched.

In Potter's and Berlad's (41) theoretical study of flame quenching in tubes, it was assumed that the flame was quenched when the amount of heat retained by the flame is equal to or less than a constant fraction of the total heat produced by the flame. From this study Equation (1-4) for quenching distance was derived

$$d = \sqrt{\frac{FGNK_T X_f}{C_p W}} \quad (1-4)$$

where,

- C_p heat capacity in reaction zone.
- d quenching diameter.
- F constant that relates total heat produced by combustion to heat which must be retained by flame for it to exist.
- G dimensional factor dependent only upon chamber geometry.
- N Avogadro's Number
- W rate of reaction in reaction zone.
- X_f mole fraction of fuel in unburned gas.
- K_T mean thermal conductivity in reaction zone.

Friedman (16) derived an equation for quench distance in a rectangular opening between two plates based on the assumption that quenching occurs when the rate of heat generation in the flame is equal to or less than the rate of heat transfer to the walls. This distance between the two plates at the quenching condition which

Friedman called the quenching distance, is expressed as Equation (1-5).

$$X = \frac{2K}{U_f C_p} \sqrt{\frac{1}{f} \frac{T_f - T_i}{T_i - T_o}} \quad (1-5)$$

where,

- X quenching distance.
- U_f burning velocity.
- C_p specific heat of gaseous mixture.
- T_f flame temperature.
- T_i ignition temperature.
- T_o cold gas temperature.
- K thermal conductivity of gaseous mixture.
- f dimensionless geometrical factor.

The effect of wall temperature and mixture pressure on the quench distance was studied experimentally by Friedman and Johnston (20). Measurements were made by measuring the minimum spacing between parallel plates through which flash-back can occur with a given air-fuel ratio, pressure, ambient temperature, and wall temperature. Propane was chosen as the fuel because of its availability in pure form and its similarity to higher saturated hydrocarbons with regard to burning velocity, minimum ignition energy, and flame temperature. The procedure for determining the quenching distance consisted in producing a flame stabilized on a

rectangular port. When the flow to the burner is quickly reduced to zero, the flame is either quenched by the plates or will flash back through the slit, depending upon the conditions. Using this test equipment Friedman found the relationship shown as Equation (1-6

$$X \propto \frac{1}{P^a T^b} \quad (1-6)$$

where,

X quenching distance, inches.

P absolute chamber pressure, atmospheres.

T plate temperature, °F

$$\left. \begin{array}{l} a = 0.76 \\ b = 0.85 \end{array} \right\} \quad A/F = 22.0$$

$$\left. \begin{array}{l} a = 0.91 \\ b = 0.50 \end{array} \right\} \quad A/F = 11.5$$

Simon and Belles (48) examined an active particle mechanism of quenching. Active particles were considered to be generated in the flame and destroyed on the container walls. Equation (1-7) was derived which related the limiting diameter to the concentration of active particles, the diffusion coefficients for the particles, the time between effective collisions of an active particle and a gas molecule, the efficiency of the wall to destroy chain carriers, the pressure, and a constant depending on the shape of the duct through which the

flame is propagating. The equation for quenching diameter was derived on the hypothesis that in order for the flame to propagate through a tube, the number of effective collisions per unit volume in the gas ahead of the burning zone must not fall below some critical value.

$$d = \sqrt{\frac{32 AP}{P_i \sum \frac{D_i \tau_i e_i}{P_i}}} \quad (1-7)$$

where,

- d diameter of tube.
- A fraction of molecules present in gas phase which must react for flame to continue to propagate.
- P total pressure.
- P_i partial pressure of one kind of active particle.
- D_i diffusion coefficient of active particle of one kind into gas.
- τ_i time between effective collisions for active particles of one kind.
- e_i efficiency of wall to prevent active particles which collide with it from returning to gas phase as chain carriers.

The mechanism of Simon and Belles (48) indicates that the nature of the surface should be important. This is expressed by the coefficient "e". There is little information available on this term. The results of experiments to determine the effect of the nature of

the surface conflict. In general, either no surface effect or only a slight surface effect has been observed. Belles and Berlad (2) suggest that a wall that has been exposed to hot combustion products cannot be expected to remain uncontaminated. It may be that the efficiency of removal of chain carriers from the gas phase by any surface at flame temperature may be the same. These are probably the reasons for the usual failure to observe any effect of different wall materials on quenching distance. However, Lewis and von Elbe (37) report experiments in flame tubes, which were carefully treated before the passage of each flame, did indicate that wall effects can be observed if the work is done properly.

Recently Gad El-Mawla (28) has reported studies on wall quenching. This work was motivated out of a genuine interest to determine what extent this phenomenon contributes to unburned hydrocarbon emissions from an internal combustion engine. A sintered bronze, porous-plate, flat-flame burner was used. This steady-state model was selected to simulate the transient quenching conditions which exist at the walls of an internal combustion engine. Gad El-Mawla found that the quenching effect extends beyond the dead space and that some chemical reaction takes place in the dead space.

To compare the thermal and diffusion theories with experimental results Potter and Berlad (42), using argon-oxygen-propane flame, replaced argon with helium. If argon is replaced by helium,

while the combustible and oxygen concentrations are held constant, only diffusion coefficients and thermal conductivities are affected; equilibrium flame temperatures and composition remain unchanged. The simple experiment of flame propagation up a tube was used. The ability of a flame to get through the tube depends on several factors: (1) pressure, (2) temperature, (3) kind of fuel, oxidant, and inert diluents, (4) relative concentrations of fuel, oxidant and inert diluent and (5) the cross-sectional shape and size of the tube. It was found that the thermal equation proposed by Potter and Berlad, Equation (1-4), satisfactorily predicted the effect of the replacement of argon with helium. The diffusion theory equation of Simon and Belles, Equation (1-7), did not satisfactorily predict the effect. Potter and Berlad contend, however, that the success of the thermal equation should not be interpreted as conclusive evidence that flame quenching is entirely a thermal process because many approximations and assumptions were made in deriving the expressions for both theories. Thus, at the present neither the thermal theory nor the diffusion theory is established as the exclusive process by which wall quenching occurs. As was suggested in the case of flame propagation, it may well be that indeed both mechanisms contribute to the phenomenon of wall quenching.

III. EXPERIMENTAL PROGRAM

Factors Leading to Experimental Program

As indicated in the previous chapter, in order to completely describe a laminar flame system by theoretical methods, it would be necessary to have the following information: (1) the step-by-step mechanism by which reaction occurs in the flame, (2) the rates of all the reactions occurring in the flame and their dependence on temperature and concentration, (3) the transport properties of all components of the mixture and their dependence on temperature, (4) the effect of the wall in breaking chain carriers, and (5) the "environmental conditions" for which the information is desired.

Most of this information just is not available. For example, consider the first factor listed. In spite of extensive research efforts reported in references (3, 14, 22, 23, 26, 29, 32, 55), the mechanism for methane-oxygen combustion still is not definitely established. There is little doubt that free radicals and chain reactions are involved. At the present time not enough facts are known. Thus there are several detailed proposed reaction mechanisms which are concordant with the experimental data.

Problems of similar magnitude exist for satisfying the other factors. Thus theoretical approaches have had only limited success. Investigators must continue to record more facts so that more

accurate theories may be developed.

Purpose of Experimental Program

The purpose of this experimental program was to provide some pertinent data which may be used to further the understanding of flame propagation and flame quenching. Temperature profiles and concentration profiles were to be measured through the reaction zone for controlled variation of combustion parameters. Using one-dimensional flame equations, species diffusion velocities, mass flux fraction profiles, and rate constants may be derived from the experimental data. The specific details concerning test conditions, experimental equipment and techniques, and data analysis are described in the following sections.

Experimental Parameters

The experimental parameters investigated in this study were: (1) hydrocarbon fuel type, (2) equivalence ratio, (3) wall temperature, and (4) sampling position in flame with respect to burner surface. The levels for equivalence ratio, wall temperature, and sampling position were selected as a result of extensive preliminary tests on the burner system. The gas mixture velocity was chosen so that it would produce a stable flame under partial quenching conditions. Propane and propylene were selected as typical representatives of

two common types of fuel structure.

1. Fuel Type:

a) propane (paraffin)

b) propylene (olefin)

2. Equivalence Ratio:

a) $\phi = 0.90$

b) $\phi = 0.95$

c) $\phi = 1.00$

d) $\phi = 1.05$

e) $\phi = 1.10$

3. Wall Temperature:

a) $T = 600^{\circ}\text{F}$

b) $T = 700^{\circ}\text{F}$

c) $T = 800^{\circ}\text{F}$

4. Sampling Position:

a) 0.005 cm g) 0.185 cm

b) 0.035 cm h) 0.215 cm

c) 0.065 cm i) 0.245 cm

d) 0.095 cm j) 0.275 cm

e) 0.125 cm k) 0.305 cm

f) 0.155 cm l) 0.335 cm

5. Chamber Pressure: 1 atmosphere

6. Oxidant: air

7. Inert: nitrogen in air
8. Wall Material: stainless steel
9. Mixture Velocity: 7.5 feet per minute

Experimental Techniques

Flame Stability

The success of the following experimental techniques requires a stable flame. Therefore, the levels of the experimental parameters were selected to meet this requirement. The presence of flame perturbation was detected with a precision Gaertner Model M-912 cathetometer. Under thermal equilibrium conditions no short or long-term drift was observed during a six-hour period. Fristrom (24) has reported that with a propane-air flame at 1/4-atmosphere pressure, the maximum variation during a five-minute period was only 0.03 mm. Photographs did not reveal any long-term change.

Gas Sampling

Gas samples were taken from the flame zone with a special quartz microprobe. The tip of this probe as shown in Figure 3 is constructed such that it does not cause aerodynamic disturbance in the flame and the stable sample constituents are "frozen" from further reaction. No attempt was made to sample unstable free

radical particles with this system.

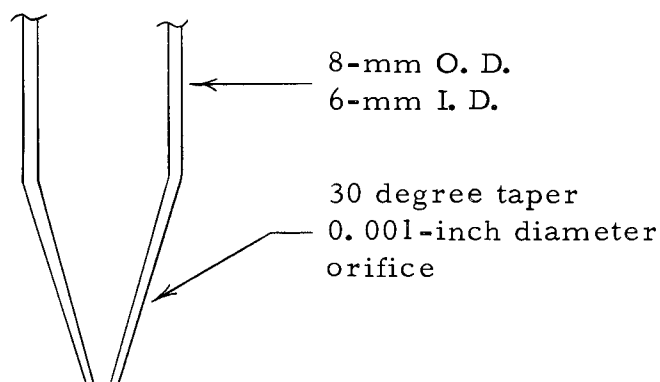


Figure 3. Tip of quartz sampling probe.

Probe sampling is a straight forward process--the gas sample is withdrawn, quenched, and then analyzed. Critical flow sampling conditions are maintained at the probe orifice. The contoured nozzle and large pressure drop effectively quench the flame reaction so that a reliable sample reaches the analytical instruments. Such a probe withdraws only a few micrograms of sample per second and does not visually disturb the flame structure. This type of sampling probe has been successfully used by other investigators (19, 23, 24, 25, 43, 50). Further details justifying the use of this probe are presented in Appendix A.

Flame Temperature Measurements

The temperature profile through the flame zone was measured with a platinum-platinum ten percent rhodium microminiature thermocouple. The thermocouple method has been reported by a number of

investigators (15, 17, 18, 21, 23, 35, 40, 55). The thermocouple probe, as shown in Figure 4, was designed to minimize aerodynamic disturbances in the flame.

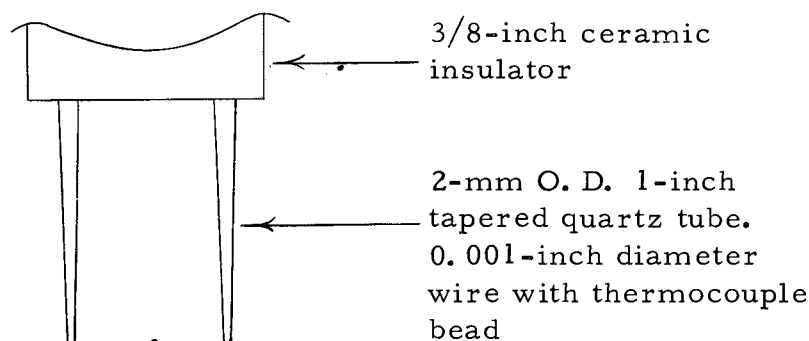


Figure 4. Tip of thermocouple probe.

A bare platinum-platinum ten percent rhodium thermocouple cannot be used for flame temperature measurements because it acts as a catalyst in the reacting chemical system. This causes undesirable surface reactions at the thermocouple bead and gives erroneous results. A non-catalytic ceramic coating has been developed by the National Bureau of Standards which solves this problem. This material, known as NBS A-418, consists of a mixture of eight oxides plus a small proportion of enameled clay. A thin coating may be applied which does not appreciably change the thermocouple bead diameter. Friedman (17) has reported satisfactory results using this non-catalytic ceramic coating.

The thermocouple temperature readings must be corrected for radiation losses. Conduction losses may be neglected since the wires

adjacent to the thermocouple junction, as shown in Figure 4, are exposed to the same temperature region in the flat flame. Detailed calculations for correcting for radiation losses are given in Appendix B.

Probe Position Measurements

The positions of the quartz sampling probe and the thermocouple probe were measured with a Gaertner Model M-912 cathetometer. This optical instrument provides a vernier readout to 0.01 mm. This method eliminates the thermal expansion errors inherent with mechanical micrometer-type measuring systems. According to references (18, 19, 23, 25) the cathetometer is the preferable method for flame zone measurements. Optical aberrations of the telescope and distortion due to density gradients in the flame are only small sources of error.

Mixture Velocity Measurements

The gas velocity profile above the sintered stainless steel plate was measured with a Disa Model 55 A01 constant-temperature hot-wire anemometer. This measurement was made (1) to insure that the gas velocity was of the proper magnitude and (2) to insure that a flat velocity profile existed. The latter requirement is imperative for developing a flat flame. The calibration data for the Disa

instrument are shown in Appendix C.

Hydrocarbon Analysis

A Perkin-Elmer Model 810 gas chromatograph with flame ionization detector was used for the quantitative analysis for methane, ethane, ethylene, propane, propylene and acetylene. A constant-volume (1 cc) sampling valve insured constant sample size. Output from the chromatograph was recorded by a Honeywell Model Elektronik 15 recorder equipped with a Disc Model 201-B integrator. Pertinent operating conditions and calibration procedures are presented in Appendix D.

Carbon Monoxide and Carbon Dioxide Analysis

Non-dispersive infrared analyzers were used to measure carbon monoxide and carbon dioxide concentrations. The carbon monoxide analyzer was a Beckman Model IR-15A while the carbon dioxide analyzer was a Beckman Model IR-215. Typical calibration curves for these instruments are shown in Appendix E.

Oxides of Nitrogen Analysis

The Saltzman colorimetric method (46) was applied in determining oxides of nitrogen concentrations. Thirty milliliter gas samples at one-third atmosphere total pressure were brought to one

atmosphere by adding oxygen. This excess oxygen enhanced the conversion of nitric oxide to nitrogen dioxide. The nitrogen dioxide was then absorbed into one milliliter of Saltzman reagent for color development. A Bausch and Lomb Model Spectronic 20 colorimeter was used to determine the amount of nitrite ion present. Due to the small sample size, the Spectronic 20 had to be modified so that quartz microcells with 0.2 milliliter capacity could be used.

Analysis for Alcohols, Aldehydes, and Acids

No attempt was made to analyze for oxygen-containing intermediates such as alcohols, aldehydes, ketones, and acids. Although these are definitely stable intermediates in cool flames and in slow oxidation of hydrocarbons, this apparently is not the case in a relatively high-temperature, fast-reacting system as this. Using mass spectrometer analysis Fristrom (25) has found that these intermediates are not present in a propane-air flame at 1/4-atmosphere pressure. In order to establish that this absence was not due to faulty sampling, poor analytical equipment or abnormally high disappearance rates, both methyl alcohol and formaldehyde were introduced into the incoming gas and were successfully detected. Smith (49) has reported similar results for a methane diffusion flame system. Only very trace amounts of formaldehyde were detected using the mass spectrometer.

Experimental Apparatus

Several pieces of apparatus were fabricated specifically for this project. Detailed sketches of the burner assembly, quartz sampling probe, and thermocouple probe are shown in Appendix F while general descriptions of test equipment are given in the following sections.

Burner Assembly

The schematic diagram in Figure 5 shows the general features of the test apparatus.

A two-inch diameter sintered stainless steel burner was enclosed in an air-tight chamber. This housing, which consisted of a six-inch diameter pyrex cross-section, allowed access for the quartz sampling probe, thermocouple probe, coolant lines, ignition probe and also an observation port.

The quartz sampling probe and thermocouple probe were placed in stationary positions. Traverses through the flame zone were accomplished by use of a micrometer which moved the burner relative to the probes. The distance between the probes and the burner surface was measured optically with a Gaertner Model M-912 cathetometer.

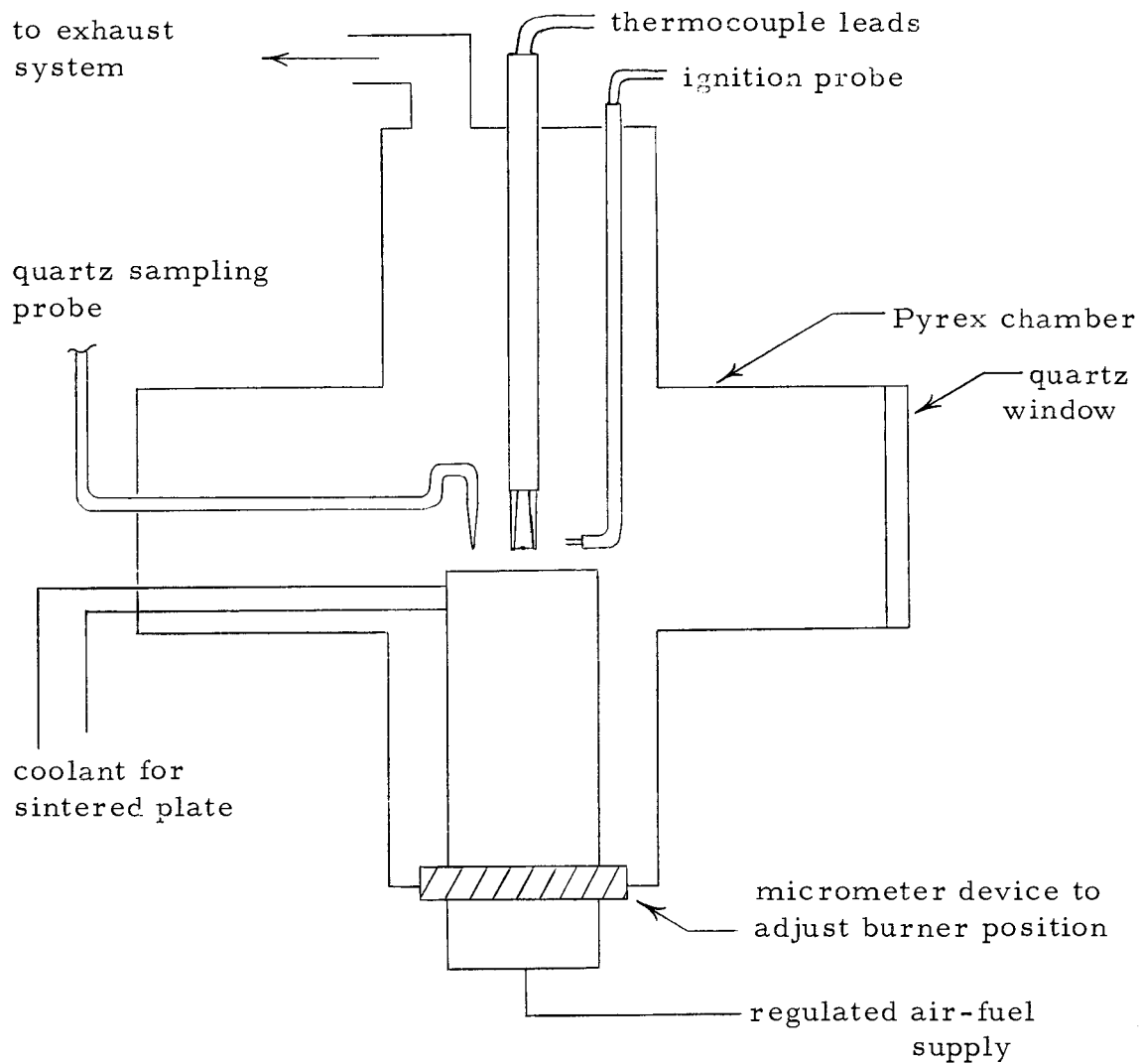


Figure 5. Burner system.

The ten-inch sampling probe was fabricated from (8-mm O. D. and 6-mm I. D.) quartz tubing. The internal taper at the tip was 30 degrees while the sampling orifice was 0.001-inch diameter. This probe was built to specifications by Thermal American Fused Quartz Company of Montville, New Jersey.

The 20-inch platinum-platinum ten percent rhodium thermocouple probe used 0.001-inch diameter wire. The details of the tip

of this probe are revealed in Figure 4. The quartz tips for this probe were also made by Thermal American Fused Quartz Company while the remainder of the probe fabrication was performed by Omega Engineering Inc. of Springdale, Connecticut. The thermocouple junction was coated with NBS A-418 by Ceramic Coating Company of Newport, Kentucky.

A thermocouple probe similar to the one shown in Figure 4 was used in some cases to monitor flame temperatures. The 0.003-inch diameter platinum-platinum ten percent rhodium couple was "flame plated" with a silica coating to minimize catalytic effects. Dow Corning Type 307 silicone oil and the "flame plating" method of Kaskan (34) were used.

The sintered disc was 1/4-inch thick, 20 percent porosity, and made of 316 stainless steel. The process used by Panoramic Corporation of Janesville, Wisconsin, provided extremely uniform porosity. This produced the desired flat velocity profile.

During burner operation the disc was cooled by placing a copper cooling coil on the bottom side of the disc. This coil, which was made of 1/8-inch copper tubing, was sanded down to increase the contact area. The coolants, water and air, were regulated by use of a Nupro Model 2M2 micrometer valve.

The temperature of the porous plate was determined by use of a 0.005-inch iron-constantan thermocouple placed at the surface.

Output from this thermocouple was read on a Leeds and Northrup Model 8686 millivolt potentiometer.

The ignition probe was built to function similar to a spark plug. It consisted of two 1/16-inch diameter copper wires enclosed in a two-hole glass rod. The gap between the ends of the wires was about 1/8-inch. Using a spring loaded off-on switch, the input leads were hooked to a Powerstat Type 126 and Mullenbach Model G-BFE ignition transformer. This arrangement provided control of arc intensity and duration.

Fuel and Air Supply

High purity propane (99.5 percent minimum) and propylene (99.5 percent minimum) fuels were obtained from The Matheson Company. The specifications indicated: (1) propane may contain small quantities of ethane and isobutane as well as up to 0.005 weight percent sulfur, and (2) propylene may contain small amounts of propane and ethane and a trace quantity of carbon dioxide. A gas chromatography analysis revealed: (1) the propane contained only a trace amount of ethane, and (2) the propylene possessed 0.158 percent by volume propane but no measureable ethane.

The required air supply was provided by a compressor, storage tank, and desiccant tank system. This provided the needed dry air and eliminated being dependent upon the building air supply system

which had gross pressure fluctuations.

Air and Fuel Flow Measurement

The air and fuel flow control systems used identical equipment. This arrangement is illustrated in Figure 6.

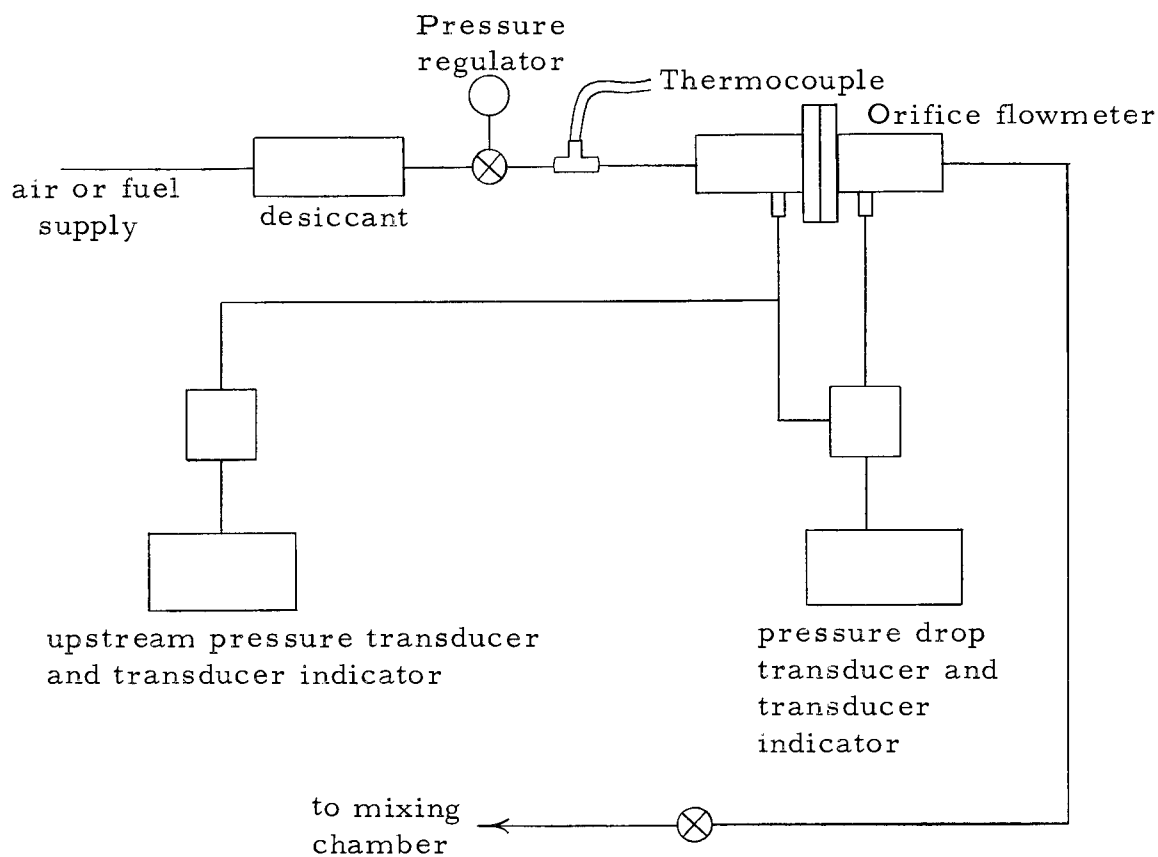


Figure 6. Fuel and air flow apparatus.

The air and fuel mass flow rates were determined using orifice flowmeters which were constructed according to American Society of Mechanical Engineers Code. Orifice plates with holes of 0.010, 0.0135, 0.016, 0.025, 0.035, and 0.045-inch diameters were made.

The holes were drilled by a jeweler and the plate surfaces were finished in the metallography laboratory to insure a sharp edge orifice. Orifices were inspected under high magnification.

The basic equation used for air and fuel flow is shown as Equation (3-1). Further discussion of this equation and calibration data are given in Appendix G.

$$M = K \sqrt{\frac{P_1 \Delta P}{T_1}} \quad (3-1)$$

where,

K constant.

P_1 upstream pressure, psia.

ΔP orifice pressure drop, inches of water.

T_1 upstream temperature, °R.

M mass flow rate, lbs/sec.

Upstream pressures of the fuel and air were set at sufficiently high values to maintain critical flow conditions across the Nupro Model 2S metering valves. This was a necessity so that any variation of operating parameters downstream would not in turn affect changes in the fuel and air flow. Tests for critical flow conditions were conducted by increasing the backpressure below the Nupro valve until finally a change in the orifice pressure drop occurred. In this manner, the required upstream conditions to maintain critical

flow for micrometer valve settings were determined.

Any moisture present was removed by anhydrous calcium sulfate desiccant. The upstream temperature was monitored by using an iron-constantan thermocouple and a Leeds and Northrup Model 8686 potentiometer.

Upstream pressures and pressure drops across the orifice plate were determined with Pace Model KP15 pressure transducers and Pace Model CD25 transducer indicators. These Pace Units provided extreme convenience in that they have a linear response, can be over-pressured without damage, and unlike liquid manometers have no tendency to leak, blow-over, or blow-up. The calibration procedure for the Pace units is given in Appendix H.

A Republic Model 310-3-1/4 D two-way valve allowed using the same Pace unit to monitor both fuel and air upstream pressures. Similarly a Republic Model A331-202 double two-way valve made it possible to measure the air and fuel orifice meter pressure drops with the same Pace unit. These valves are both spring-loaded teflon-plug valves which exhibit negligible leak rates. The complete air and fuel flow system was extensively tested for leaks using Snoop Leak Detector.

Sampling and Analytical System

A schematic of the sampling and analytical system is shown

in Figure 7. The total volume of this system was minimized in order to reduce the total sampling time required. Extreme care was taken to eliminate leaks; use of high vacuum leak sealant proved to be a necessity. Whenever possible stainless steel tubing and Swagelok fittings were used.

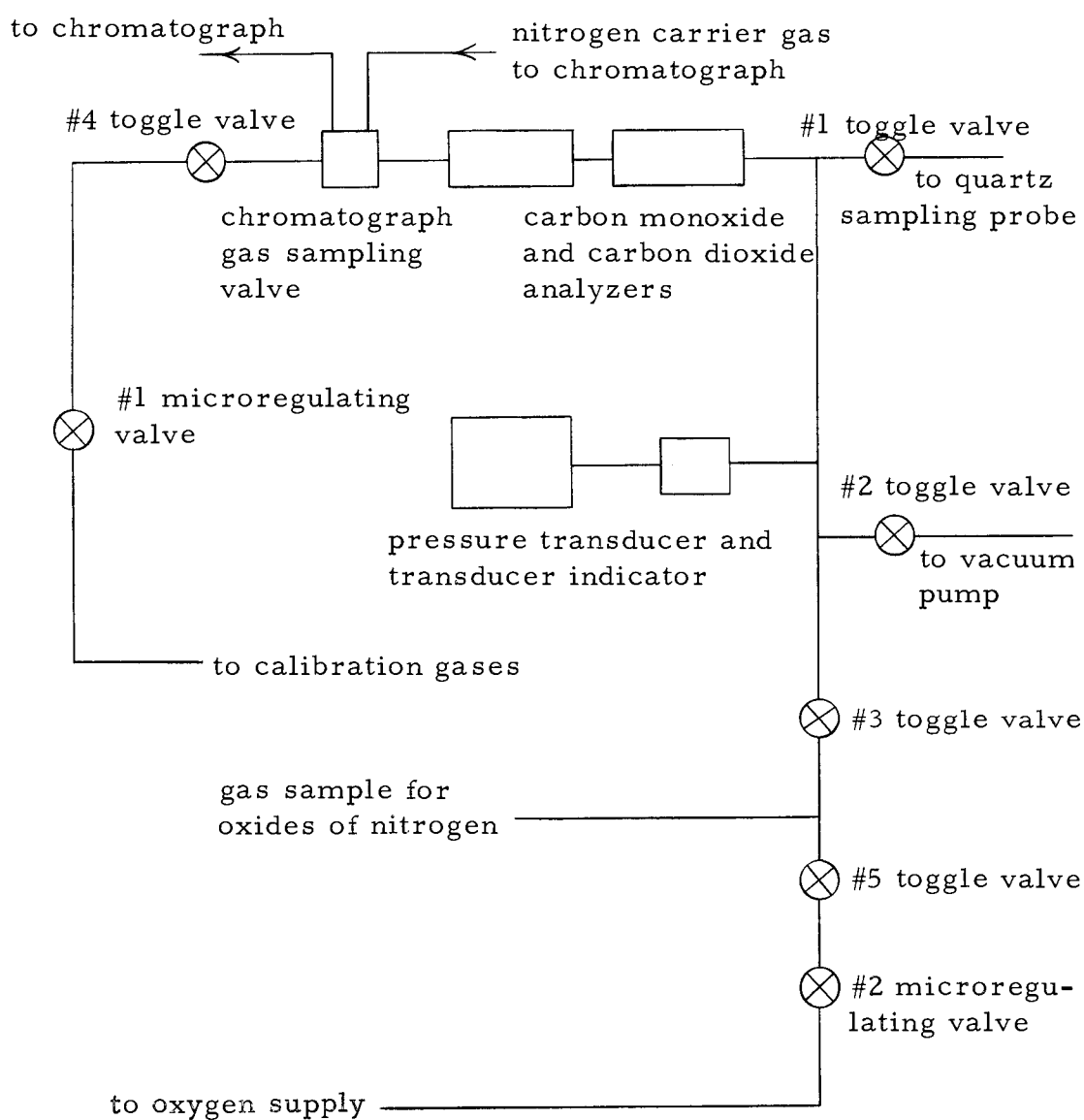


Figure 7. Sampling and analytical system.

A Pace Model KP15 transducer and Pace Model CD25 indicator unit was used to monitor the total pressure of the system. This method offered several distinct advantages: (1) possessed a minimal internal volume (< 0.1 cc), (2) eliminated possible sample contamination due to presence of a manometer fluid, (3) offered inherent design conducive to eliminating leaks and (4) system pressure could be rapidly changed without worry of blowing a manometer. In addition, this unit could handily note a pressure change of $1/1000$ atmosphere. Thus, it was particularly effective in detecting leaks within the sampling and analytical system. Ultimately the system was capable of holding greater than 29 inch-mercury vacuum for at least 15 minutes with no measureable change in pressure. The calibration procedure for this instrument is given in Appendix H.

A Perkin-Elmer Model 008-0659 two-way sampling valve was used to take a constant-volume sample for hydrocarbon analysis. In position #1 the 1 cc sample loop became part of the sampling system. In position #2 the sample taken, while the valve was in position #1, was carried to the chromatograph by the nitrogen carrier gas.

Experimental Procedures

Burner Operation

Prior to igniting the burner, the chamber was evacuated with

the vacuum system to remove any fuel which may have somehow accumulated. The air flow was set at the desired rate and then the fuel flow set such that the flame would stabilize regardless of the initial burner and chamber conditions. The mixture was then ignited and the desired mixture ratio obtained. During the next two hours the system reached thermal equilibrium. Prior to taking data, final adjustments of plate temperature and chamber pressure were made. The chamber pressure was held constant at one atmosphere (14.7 psi). The small day-to-day variations were eliminated by using the appropriate adjustments of the exhaust valve and vacuum system valve.

Instrument Adjustments and Calibration

While the burner system reached thermal equilibrium, the analytical instruments were adjusted and calibrated. The gas chromatograph and nondispersive infrared instruments were left in operation constantly in order to minimize drift due to thermal instability. These instruments were handily calibrated in less than 30 minutes. This was done prior to each test. Thus, any change in instrument response with time could be detected.

Gas Sampling

In the following step-by-step description refer to Figure 7.

1. Put gas chromatograph sampling valve to position #1.
2. Close toggle valves #1 and #4.
3. Close toggle valve #5.
4. Open toggle valve #2. Start vacuum pump and allow to operate at least two minutes. Carbon monoxide and carbon dioxide analyzers should have zero output.
5. Open toggle valve #1 in order to evacuate sampling probe. Allow at least two minutes operation.
6. Close toggle valve #2 and turn off vacuum pump.
7. Draw sample into system to total pressure of 1/3 atmosphere and then shut toggle valve #1. Sampling time should be about 50 seconds. Allow sample to stabilize for two minutes.
8. Take carbon monoxide and carbon dioxide readings.
9. Turn gas chromatograph valve to position #2 for hydrocarbon analysis.
10. Close #3 toggle valve.
11. Using #2 microregulating valve add oxygen to NO_x sample bottle.
12. Add Saltzman reagent to NO_x bottle and allow 24 hours for color development before reading colorimeter.
13. Observe output from gas chromatograph and make appropriate attenuation changes.

14. Put on new NO_x gas sampling bottle and return gas chromatograph valve to position #1.
15. Evacuate sample system in preparation for next sample.

Statistical Design

Requirements

The selection of the statistical design was complicated by the fact that it must be a compromise in order to satisfy several requirements. The basic requirements of the statistical design were:

1. Must be able to detect presence of main effects of each parameter.
2. Must be able to detect the presence of two factor interaction effects between parameters.
3. Should be as simple as possible.
4. Should be an efficient design which will minimize the total number of tests to be made and still meet the other requirements.

Selected Design

A completely randomized nonreplicated factorial experiment was selected with factors as follows: (1) Factor A; hydrocarbon fuel type, (2) Factor B; equivalence ratio, (3) Factor C; plate (wall)

temperature, and (4) Factor D; sampling position with reference to plate surface. Due to the gross time requirements of the experimental procedures and the delicate nature of some of the experimental equipment and analytical instruments, replication was not considered practical. Replication is generally needed to obtain an estimate of the error term. However, as shown in the following sections, this problem can be alleviated by pooling the three and four factor interaction terms as an estimate of the error term.

Statistical Model

The form of statistical model used is one in which each observation is expressed as the sum of several component effects. In other words, it is an additive type model. The four-way classification model (with interaction) has the form shown in Equation (3-2).

$$\begin{aligned}
 Y_{ijkln} = & \mu + A_i + B_j + C_k + D_l + (AB)_{ij} + (AC)_{ik} \\
 & + (AD)_{il} + (BC)_{jk} + (BD)_{jl} + (CD)_{kl} \\
 & + (ABC)_{ijk} + (ABD)_{ijl} + (ACD)_{ikl} \\
 & + (BCD)_{jkl} + (ABCD)_{ijkl} + e_{ijkln}
 \end{aligned}
 \tag{3-2}$$

where,

μ = general mean

A, B, C, and D = main effects

AB, AC, AD, BC, BD, and CD = two factor interaction effects

ABC, ABD, ACD, and BCD = three factor interaction effects

ABCD = four factor interaction effects

e = random error term

In addition to the assumption of additivity, several assumptions are made concerning the random error terms. These have been thoroughly discussed by Davies (11) and Cochran and Cox (7) and are briefly enumerated as follows: (1) the errors are independent, (2) the variances of the errors are equal and (3) the errors are normally distributed. In actual practice it is difficult to be certain that these assumptions all hold. Another implied assumption of the statistical model is that the levels of the independent variables are measured or controlled without error. All error is assumed to be in the dependent response. This is certainly not the case in actual experiments. However, little can be done to compensate for this variability except striving to improve laboratory techniques. Box (4) has considered the transmitted error due to this variability for linear, quadratic and general polynomial response surfaces. Apparently the magnitude of the transmitted error is a function of the response surface.

The estimated maximum error present in the factor levels of this experiment are as follows:

Factor A (fuel type): no variation due to batches

Factor B (equivalence ratio): ± 0.005

Factor C (plate temperature): $\pm 5^{\circ}\text{F}$

Factor D (sampling position): $\pm 0.002\text{ cm}$

No attempt was made to precisely estimate these errors or account for their presence by altering experimental data.

The Factorial Experiment

The factorial experiment is one in which the effects of several factors are studied simultaneously. The advantages and disadvantages of this type of experiment are stressed by Cochran and Cox (7). Briefly though, the main advantages are: (1) offers considerable saving of time and material and (2) offers capability of being able to detect interaction effects. The major disadvantages are: (1) becomes large and complex as the number of factors increases, and (2) sometimes difficult to properly interpret meaning.

The expected mean square values for factorial experiments have been presented by Cornfield and Tukey (8). This study used a completely randomized non-replicated factorial experiment. The mean square values for a four-factor, fixed model experiment with replication are shown in Table 1. Actually for the fixed model each of the effect variance terms should be shown as summation expressions. For example, σ_B^2 should be shown as $\Sigma B_j^2/b-1$ but as a matter of convenience the σ^2 terms are used. The assumption is made that the three and four-factor interaction effects are negligible,

Table 1. Analysis of Variance of four-factor factorial experiment.

Source of Variance	Degrees of Freedom	Expected Mean Squares
A	$a - 1$	$\sigma_e^2 + nbcd \sigma_A^2$
B	$b - 1$	$\sigma_e^2 + nacd \sigma_B^2$
C	$c - 1$	$\sigma_e^2 + nabd \sigma_C^2$
D	$d - 1$	$\sigma_e^2 + nabc \sigma_D^2$
AB	$(a - 1)(b - 1)$	$\sigma_e^2 + ncd \sigma_{AB}^2$
AC	$(a - 1)(c - 1)$	$\sigma_e^2 + nbd \sigma_{AC}^2$
AD	$(a - 1)(d - 1)$	$\sigma_e^2 + nbc \sigma_{AD}^2$
BC	$(b - 1)(c - 1)$	$\sigma_e^2 + nad \sigma_{BC}^2$
BD	$(b - 1)(d - 1)$	$\sigma_e^2 + nac \sigma_{BD}^2$
CD	$(c - 1)(d - 1)$	$\sigma_e^2 + nab \sigma_{CD}^2$
ABC	$(a - 1)(b - 1)(c - 1)$	$\sigma_e^2 + nd \sigma_{ABC}^2$
ABD	$(a - 1)(b - 1)(d - 1)$	$\sigma_e^2 + nc \sigma_{ABD}^2$
ACD	$(a - 1)(c - 1)(d - 1)$	$\sigma_e^2 + nb \sigma_{ACD}^2$
BCD	$(b - 1)(c - 1)(d - 1)$	$\sigma_e^2 + na \sigma_{BCD}^2$
ABCD	$(a - 1)(b - 1)(c - 1)(d - 1)$	$\sigma_e^2 + n \sigma_{ABCD}^2$
Replication	$abcd (n - 1)$	σ_e^2

i. e. , ABC, ABD, ACD, BCD and ABCD are negligible. Therefore, an estimate of the error term is provided by pooling these terms. As indicated by Cochran and Cox (7) this assumption is frequently made and is not without justification since experience has often shown it to be true. However, at least two methods are available to test the validity of this assumption. Bartlett's test (38) checks for homogeneity of variances. In other words, it hypothesizes that each of these terms indeed estimates the same variance. Rejection of the hypothesis leads one to conclude that at least one of the higher order terms was not negligible. A graphical method proposed by Daniel (9) helps indicate without the use of analysis of variance techniques, which higher order effects are probably significant and should not be included in the pooled residual sum of squares.

The effect of inadvertently using a significant higher order interaction term as part of the error estimator, is to inflate the error term. This can cause one to make the error of accepting a false hypothesis.

Hypotheses Tested

A null hypothesis was made for each of the dependent responses, i. e. , that there was no difference in response at the various levels of the selected combustion parameters. The alternative hypothesis was made which stated there was a significant

difference. Similar null and alternative hypotheses were made for the two-factor interaction responses.

As an example consider the hypotheses concerning the effect of factor B, equivalence ratio, upon ethylene response.

Null Hypothesis: $\sigma_B^2 = 0$

Alternative Hypothesis: $\sigma_B^2 \neq 0$

If the null hypothesis was accepted then it was concluded that equivalence ratio had no influence on ethylene response. If the alternative hypothesis was accepted then the data used in accepting the alternative hypothesis was available to formulate prediction equations.

IV. RESULTS

Experimental Data

The 30 combinations of the levels of factors A (fuel type), B (equivalence ratio), and C (plate temperature) were randomized by the method of Quenouille (44) using a random numbers table. Factor D (sampling position) was intentionally not included for two reasons: (1) it would have made the mechanics of conducting the overall experiment unduly long and difficult, and (2) it was felt that there was little possibility of introducing systematic bias by not randomizing this factor.

There was no past evidence or reason to believe that the responses would not satisfy the assumptions in the statistical model. However, there is one point which should be mentioned concerning the use of the gas chromatograph for detecting hydrocarbon responses. This instrument has an 18-position attenuation switch ($1X \rightarrow 500,000X$) which allows a great range of flexibility. But, for any given attenuation the instrument has a maximum error which is proportional to the full scale value. Thus if a wide range of attenuations is used, an induced error is brought about which is not absolute but proportional to the response. If this problem is gross then according to Li (38) the variances may be equalized by using a log transformation on the experimental data. It was felt that this transformation was not

needed in this case. Only five of the lower attenuations (2X, 5X, 10X, 20X and 50X) were used in measuring the six hydrocarbon responses. All except propane were measured using 2X, 5X and 10X attenuations.

The raw experimental data is presented in tabular form in Appendix K. The hydrocarbon and oxides of nitrogen responses are given in parts per million while the carbon monoxide and carbon dioxide responses are in percent by volume. The listed gas temperatures have been corrected for radiation losses using the method outlined in Appendix B.

Results of Statistical Analysis

Four-factor Analysis of Variance

The four-factor analysis of variance calculations were made for the dependent responses of methane, ethane, ethylene, propane, acetylene, propylene, carbon monoxide, carbon dioxide and oxides of nitrogen. The computations were performed on the CDC 3300 computer at Oregon State University. The computer program (OSU-04) is on file in the Statistical Analysis Program Library. The obtained analyses of variance (A. O. V.) for these responses are shown as Tables 2 through 10 respectively. The corresponding means for the main effects are listed in Table 11 while the means for two-factor

effects are in Appendix L. The critical variance ratio (F-test) values at five percent level of significance are listed on the A. O. V. tables.

In several cases the (fuel) x (equivalence ratio) x (plate temperature) interaction term was not pooled with the other higher order terms to obtain an estimate of the error term. It was held out because generally it had a mean square value several times larger than any of the other higher order terms. This really did not grossly alter the estimates of the error term since this term has only eight degrees of freedom compared to 242 total degrees of freedom for the remaining higher order terms.

The mean square values in the analysis of variance tables were used to test the various null hypotheses concerning presence of main and interaction effects. If the equivalence ratio and/or plate temperature factor proved to be significant then these effects were broken down into linear and quadratic individual degrees of freedom. Since equal increments were used between factor levels these computations could be made using orthogonal multipliers and then modifying the four-factor computer program. The results of these statistical tests are included in the A. O. V. tables.

In addition to the main effects, a large number of two-factor effects were also found to be significant. This is the result of (1) having a small error term due to the refined laboratory testing conditions and techniques and (2) having such a large number of

observations. The real significance of an interaction effect is best viewed by comparing it to the magnitude of the main effects. If the main effect completely overshadows the interaction effect by orders of magnitude, then interaction effect probably isn't really of significant interest.

By definition, the physical meaning of significant main and two-factor interaction effects found in the following A.O.V. tables is briefly described as follows:

fuel: the dependent variable response is not
the same for propane and propylene.

equivalence ratio: the dependent variable response is not
the same for all five levels of equivalence ratio.

plate temperature: the dependent variable response is not
the same for all three levels of plate temperature.

sampling position: the dependent variable response is not
the same for all 12 levels of sampling position.

(fuel) x (equivalence ratio): the shape or slope of the equivalence ratio versus dependent variable curve is not the same for propane and propylene.

(fuel) x (plate temperature): the shape or slope of the plate temperature versus dependent variable curve is not the same for propane and propylene.

(fuel) x (sampling position): the shape or slope of the sampling position versus dependent variable curve is not the same for propane and propylene.

(equivalence ratio) x (plate temperature): the shape or slope of the equivalence ratio versus dependent variable curve is not the same for all three levels of plate temperature.

(equivalence ratio) x (sampling position): the shape or slope of the sampling position versus dependent variable curve is not the same for all five levels of equivalence ratio.

(plate temperature) x (sampling position): the shape or slope of the sampling position versus dependent variable curve is not the same for all three levels of plate temperature.

Table 2. Four-factor analysis of variance for methane response.

Source of Variance	Degrees of Freedom	Mean Square	Variance Ratio	Significant at 5% Level
Fuel	1	1526074.22	94.02	Yes
Equivalence Ratio	4	2366284.84	145.78	Yes
Linear	1	7923936.23	488.19	Yes
Quadratic	1	1379430.48	84.98	Yes
Plate Temperature	2	47806.17	2.95	No
Sampling Position	11	1794279.51	110.54	Yes
Fuel x Equivalence Ratio	4	57784.11	3.56	Yes
Fuel x Plate Temperature	2	9288.52	0.57	No
Fuel x Sampling Position	11	186106.87	11.47	Yes
Equivalence Ratio x Plate Temperature	8	43085.78	2.65	Yes
Equivalence Ratio x Plate Temperature	44	150009.27	9.24	Yes
Plate Temperature x Sampling Position	22	10667.05	0.66	No
Pooled terms	250	16231.20	---	---

Critical Variance Ratios at 5% Level of Significance:

$$F_{250}^1 = 3.8415$$

$$F_{250}^2 = 2.9957$$

$$F_{250}^4 = 2.3719$$

$$F_{250}^8 = 1.9384$$

$$F_{250}^{11} = 1.7914$$

$$F_{250}^{22} = 1.5439$$

$$F_{250}^{44} = 1.3788$$

Table 3. Four-factor analysis of variance for ethane response.

Source of Variance	Degrees of Freedom	Mean Square	Variance Ratio	Significant at 5% Level
Fuel	1	436392.10	142.07	Yes
Equivalence Ratio	4	75363.48	24.54	Yes
Linear	1	270397.51	88.03	Yes
Quadratic	1	27698.48	9.02	Yes
Plate Temperature	2	12441.22	4.05	Yes
Linear	1	24867.70	8.10	Yes
Quadratic	1	14.73	< 0.01	No
Sampling Position	11	298134.00	97.06	Yes
Fuel x Equivalence Ratio	4	22058.15	7.18	Yes
Fuel x Plate Temperature	2	2499.41	0.81	No
Fuel x Sampling Position	11	32107.89	10.45	Yes
Equivalence Ratio x Plate Temperature	8	21437.99	6.98	Yes
Equivalence Ratio x Sampling Position	44	8588.17	2.80	Yes
Plate Temperature x Sampling Position	22	4005.07	1.30	No
Fuel x Equivalence Ratio x Plate Temperature	8	20609.32	6.71	Yes
Pooled Terms	242	3071.59	---	---
Critical Variance Ratios at 5% Level of Significance:		$F_{242}^1 = 3.8415$	$F_{242}^2 = 2.3719$	
$F_{242}^4 = 2.3719$	$F_{242}^8 = 1.9384$	$F_{242}^{11} = 1.7914$	$F_{242}^{22} = 1.5439$	$F_{242}^{44} = 1.3788$

Table 4. Four-factor analysis of variance for ethylene response.

Source of Variance	Degrees of Freedom	Mean Square	Variance Ratio	Significant at 5% Level
Fuel	1	15190973.33	208.04	Yes
Equivalence Ratio	4	4818992.86	66.00	Yes
Linear	1	17467362.53	239.21	Yes
Quadratic	1	1372112.56	18.79	Yes
Plate Temperature	2	207331.51	2.84	No
Sampling Position	11	14764670.30	202.20	Yes
Fuel x Equivalence Ratio	4	51085.30	0.70	No
Fuel x Plate Temperature	2	27535.80	0.38	No
Fuel x Sampling Position	11	1489159.25	20.39	Yes
Equivalence Ratio x Plate Temperature	8	169350.14	2.32	Yes
Equivalence Ratio x Sampling Position	44	440122.80	6.03	Yes
Plate Temperature x Sampling Position	22	154112.40	2.11	Yes
Fuel x Equivalence Ratio x Plate Temperature	8	163919.56	2.24	Yes
Pooled Terms	242	73018.55	---	---

Critical Variance Ratios at 5% Level of Significance:		$F_{242}^1 = 3.8415$	$F_{242}^2 = 2.9957$	
$F_{242}^4 = 2.3719$	$F_{242}^8 = 1.9384$	$F_{242}^{11} = 1.7914$	$F_{242}^{22} = 1.5439$	$F_{242}^{44} = 1.3788$

Table 5. Four-factor analysis of variance for propane response.

Source of Variance	Degrees of Freedom	Mean Square	Variance Ratio	Significant at 5% Level
Fuel	1	6161540239.75	4620.94	Yes
Equivalence Ratio	4	4501261.00	3.38	Yes
Linear	1	15684566.42	11.76	Yes
Quadratic	1	592468.76	0.44	No
Plate Temperature	2	49187809.81	36.89	Yes
Linear	1	92416029.33	69.31	Yes
Quadratic	1	5959590.31	4.47	Yes
Sampling Position	11	654809891.80	491.08	Yes
Fuel x Equivalence Ratio	4	4294174.81	3.22	Yes
Fuel x Plate Temperature	2	49386121.31	37.04	Yes
Fuel x Sampling Position	11	650786708.06	488.07	Yes
Equivalence Ratio x Plate Temperature	8	5927509.59	4.45	Yes
Equivalence Ratio x Sampling Position	44	1551093.01	1.16	No
Plate Temperature x Sampling Position	22	2717786.62	2.04	Yes
Fuel x Equivalence Ratio x Plate Temperature	8	5893153.05	4.42	Yes
Pooled terms	242	1333393.00	---	---
- - - - -				
Critical Variance Ratios at 5% Level of Significance:		$F_{242}^1 = 3.8415$	$F_{242}^2 = 2.9957$	
$F_{242}^4 = 2.3719$	$F_{242}^8 = 1.9384$	$F_{242}^{11} = 1.7914$	$F_{242}^{22} = 1.5439$	$F_{242}^{44} = 1.3788$

Table 6. Four-factor analysis of variance for acetylene response.

Source of Variance	Degrees of Freedom	Mean Square	Variance Ratio	Significant at 5% Level
Fuel	1	4592321.11	203.30	Yes
Equivalence Ratio	4	2436561.14	107.88	Yes
Linear	1	8261908.51	365.83	Yes
Quadratic	1	1321889.89	58.53	Yes
Plate Temperature	2	60421.72	2.68	No
Sampling Position	11	1047645.16	46.39	Yes
Fuel x Equivalence Ratio	4	210227.14	9.31	Yes
Fuel x Plate Temperature	2	4164.59	0.18	No
Fuel x Sampling Position	11	222172.57	9.84	Yes
Equivalence Ratio x Plate Temperature	8	29934.62	1.33	No
Equivalence Ratio x Sampling Position	44	191994.01	8.50	Yes
Plate Temperature x Sampling Position	22	14976.88	0.66	No
Pooled Terms	250	22584.30	---	---
- - - - -				
Critical Variance Ratios at 5% Level of Significance:		$F_{250}^1 = 3.8415$	$F_{250}^2 = 2.9957$	
$F_{250}^4 = 2.3719$	$F_{250}^8 = 1.9384$	$F_{250}^{11} = 1.7914$	$F_{250}^{22} = 1.5439$	$F_{250}^{44} = 1.3788$

Table 7. Four-factor analysis of variance for propylene response.

Source of Variance	Degrees of Freedom	Mean Square	Variance Ratio	Significant at 5% Level
Fuel	1	13224956537.00	533.03	Yes
Equivalence Ratio	4	35457159.00	14.29	Yes
Linear	1	92080569.80	37.11	Yes
Quadratic	1	15245004.09	6.14	Yes
Plate Temperature	2	65382482.25	26.35	Yes
Linear	1	124175636.21	50.04	Yes
Quadratic	1	6589328.67	2.65	No
Sampling Position	11	1363019940.22	549.37	Yes
Fuel x Equivalence Ratio	4	37944967.00	15.29	Yes
Fuel x Plate Temperature	2	66078404.50	26.63	Yes
Fuel x Sampling Position	11	1290308108.22	520.00	Yes
Equivalence Ratio x Plate Temperature	8	6637117.47	2.67	Yes
Equivalence Ratio x Sampling Position	44	5126718.20	2.07	Yes
Plate Temperature x Sampling Position	22	4238841.70	1.71	Yes
Pooled Terms	250	2481060.00	---	---
- - - - -				
Critical Variance Ratios at 5% Level of Significance:		$F_{250}^1 = 3.8415$	$F_{250}^2 = 2.9957$	
$F_{250}^4 = 2.3719$	$F_{250}^8 = 1.9384$	$F_{250}^{11} = 1.7914$	$F_{250}^{22} = 1.5439$	$F_{250}^{44} = 1.3788$

Table 8. Four-factor analysis of variance for carbon monoxide response.

Source of Variance	Degrees of Freedom	Mean Square	Variance Ratio	Significant at 5% Level
Fuel	1	6.294	146.37	Yes
Equivalence Ratio	4	81.356	1892.00	Yes
Linear	1	231.767	5389.70	Yes
Quadratic	1	90.653	2108.13	Yes
Plate Temperature	2	0.647	15.05	Yes
Linear	1	0.938	21.81	Yes
Quadratic	1	0.356	8.27	Yes
Sampling Position	11	4.194	97.53	Yes
Fuel x Equivalence Ratio	4	1.065	24.77	Yes
Fuel x Plate Temperature	2	0.017	0.40	No
Fuel x Sampling Position	11	0.064	1.48	No
Equivalence Ratio x Plate Temperature	8	0.168	3.91	Yes
Equivalence Ratio x Sampling Position	44	1.200	27.91	Yes
Plate Temperature x Sampling Position	22	0.155	3.60	Yes
Fuel x Equivalence Ratio x Plate Temperature	8	0.199	4.63	Yes
Pooled Terms	242	0.043	---	---
Critical Variance Ratios at 5% Level of Significance:		$F_{242}^1 = 3.8415$	$F_{242}^2 = 2.9957$	
$F_{242}^4 = 2.3719$	$F_{242}^8 = 1.9384$	$F_{242}^{11} = 1.7914$	$F_{242}^{22} = 1.5439$	$F_{242}^{44} = 1.3788$

Table 9. Four-factor analysis of variance for carbon dioxide response.

Source of Variance	Degrees of Freedom	Mean Square	Variance Ratio	Significant at 5% Level
Fuel	1	11.271	37.08	Yes
Equivalence Ratio	4	8.212	27.01	Yes
Linear	1	5.832	19.17	Yes
Quadratic	1	17.540	57.69	Yes
Plate Temperature	2	6.032	19.84	Yes
Linear	1	12.060	39.67	Yes
Quadratic	1	0.004	0.01	No
Sampling Position	11	150.519	495.12	Yes
Fuel x Equivalence Ratio	4	7.467	24.56	Yes
Fuel x Plate Temperature	2	0.908	2.99	No
Fuel x Sampling Position	11	0.508	1.67	No
Equivalence Ratio x Plate Temperature	8	0.699	2.30	Yes
Equivalence Ratio x Sampling Position	44	0.345	1.13	No
Plate Temperature x Sampling Position	22	0.536	1.76	Yes
Fuel x Equivalence Ratio x Plate Temperature	8	0.705	2.32	Yes
Pooled Terms	242	0.304	---	---
- - - - -				
Critical Variance Ratios at 5% Level of Significance:		$F_{242}^1 = 3.8415$	$F_{242}^2 = 2.9957$	
$F_{242}^4 = 2.3719$	$F_{242}^8 = 1.9384$	$F_{242}^{11} = 1.7914$	$F_{242}^{22} = 1.5439$	$F_{242}^{44} = 1.3788$

Table 10. Four-factor analysis of variance for oxides of nitrogen response.

Source of Variance	Degrees of Freedom	Mean Square	Variance Ratio	Significant at 5% Level
Fuel	1	581.406	70.41	Yes
Equivalence Ratio	4	1794.654	217.34	Yes
Linear	1	6885.142	833.85	Yes
Quadratic	1	59.022	7.15	Yes
Plate Temperature	2	81.255	9.84	Yes
Linear	1	91.884	11.12	Yes
Quadratic	1	70.625	8.55	Yes
Sampling Position	11	1610.378	195.03	Yes
Fuel x Equivalence Ratio	4	124.630	15.09	Yes
Fuel x Plate Temperature	2	11.352	1.37	No
Fuel x Sampling Position	11	19.974	2.42	Yes
Equivalence Ratio x Plate Temperature	8	21.325	2.58	Yes
Equivalence Ratio x Sampling Position	44	144.763	17.53	Yes
Plate Temperature x Sampling Position	22	15.967	1.93	Yes
Fuel x Equivalence Ratio x Plate Temperature	8	53.110	6.43	Yes
Pooled Terms	242	8.257	---	---
- - - - -				
Critical Variance Ratios at 5% Level of Significance:		$F_{242}^1 = 3.8415$	$F_{242}^2 = 2.9957$	
$F_{242}^4 = 2.3719$	$F_{242}^8 = 1.9384$	$F_{242}^{11} = 1.7914$	$F_{242}^{22} = 1.5439$	$F_{242}^{44} = 1.3788$

Table 11. Mean values for four-factor main effects.

Factor \ Specie	Methane ppm	Ethane ppm	Ethylene ppm	Propane ppm	Acetylene ppm	Propylene ppm	Carbon Monoxide %	Carbon Dioxide %	Oxides of Nitrogen ppm
Fuel									
Propane	373	162	1077	8287	115	283	1.8	9.2	6.8
Propylene	243	92	667	13	341	12405	1.6	9.6	9.3
Equivalence Ratio									
0.90	609	156	1283	4451	532	7528	3.5	9.3	14.1
0.95	336	148	923	4196	256	6089	1.7	9.7	12.4
1.00	240	143	830	4259	167	6194	1.2	9.8	6.8
1.05	208	107	713	4066	121	6256	1.0	9.1	4.4
1.10	149	80	610	3778	64	5656	1.0	9.1	2.6
Plate Temperature °F									
600	325	137	913	4861	253	6968	1.8	9.2	7.1
700	286	126	830	3968	209	6536	1.6	9.4	8.7
800	314	117	873	3620	221	5530	1.6	9.6	8.4
Sampling Position cm									
.005	358	146	1067	11692	194	16456	1.4	6.1	0.8
.035	401	167	1171	10801	218	15508	1.5	6.4	1.2
.065	448	190	1285	9648	255	14285	1.6	6.9	1.5
.095	512	219	1490	7877	321	12165	1.8	7.5	1.9
.125	597	249	1744	5416	423	9146	2.1	8.3	2.5
.155	637	252	1800	2747	511	5494	2.3	9.3	3.2
.185	482	192	1262	1086	473	2282	2.3	10.6	5.6
.215	227	78	519	460	299	632	1.9	11.1	11.2
.245	35	28	107	62	36	142	1.6	11.5	15.3
.275	4	2	18	12	5	23	1.4	11.6	17.2
.305	0	0	0	0	0	0	1.3	11.7	17.8
.335	0	0	0	0	0	0	1.2	11.7	18.5

Four-factor Response Curves

It is not practical to present all of the experimental data in graphical form. However, the general response curves for each dependent variable are presented in Figures 8 through 12. These curves were obtained by averaging the responses for all levels of A (fuel type), B (equivalence ratio), and C (plate temperature) at each level of D (sampling position). At this point only general response features are of interest and therefore no attempt was made to obtain computer prediction equations using a least squares method. The main features to note are (1) stable species hydrocarbons do exist in the reacting system, (2) hydrocarbon concentrations increase as fuel concentration decreases and then experience a sharp negative gradient as the reaction proceeds, (3) carbon monoxide concentration increases to a peak value and then decreases to a lower fixed concentration, (4) carbon dioxide concentration increases to a maximum value, and (5) oxides of nitrogen concentration experiences a sharp increase in the general vicinity where carbon monoxide and hydrocarbon concentrations drop rapidly.

The general response curves for the dependent variable ethylene are shown in Figures 13 through 17. These are presented to graphically illustrate the presence of main and two-factor interaction effects.

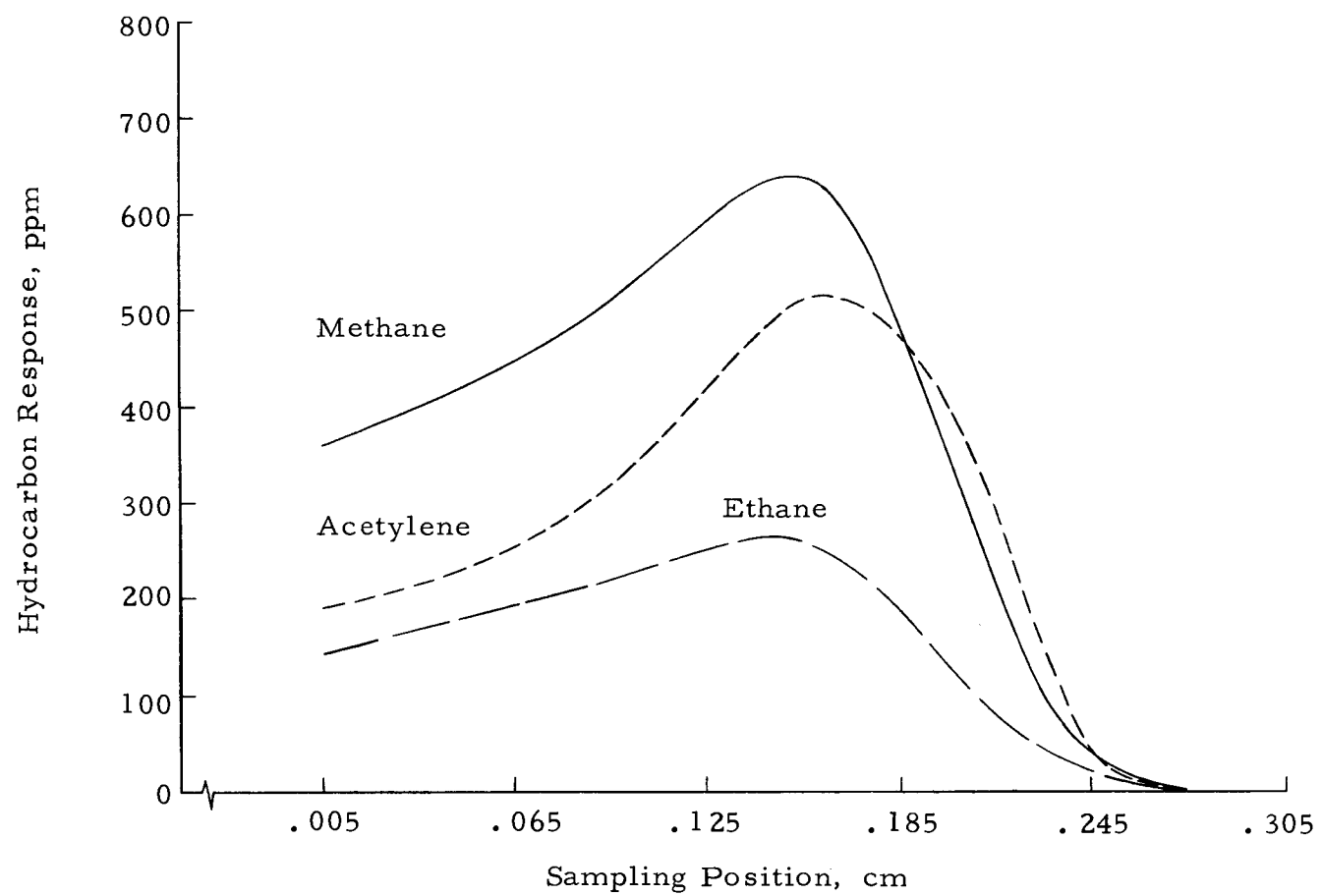


Figure 8. General response profiles of methane, ethane, and acetylene.

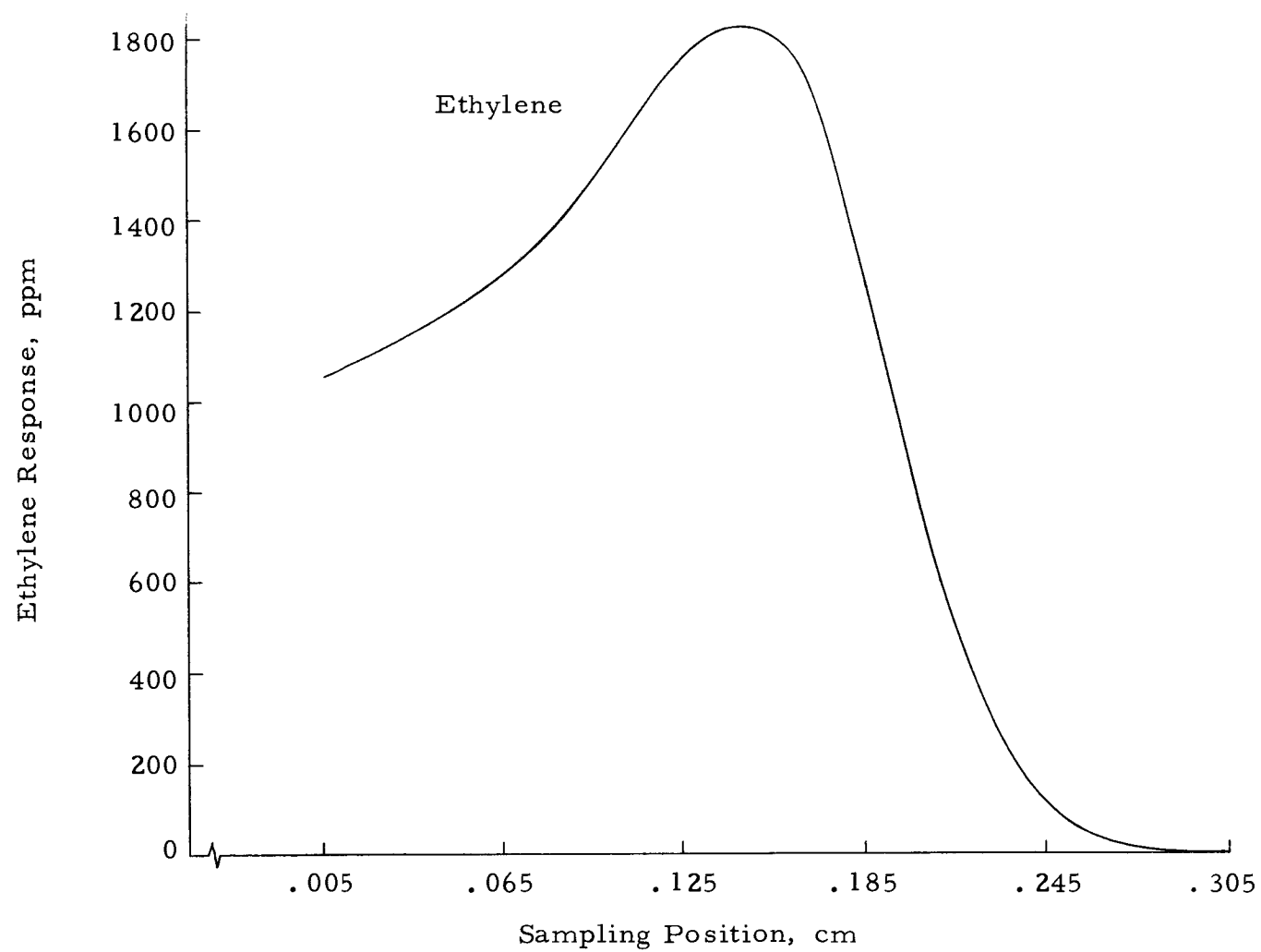


Figure 9. General response profile of ethylene.

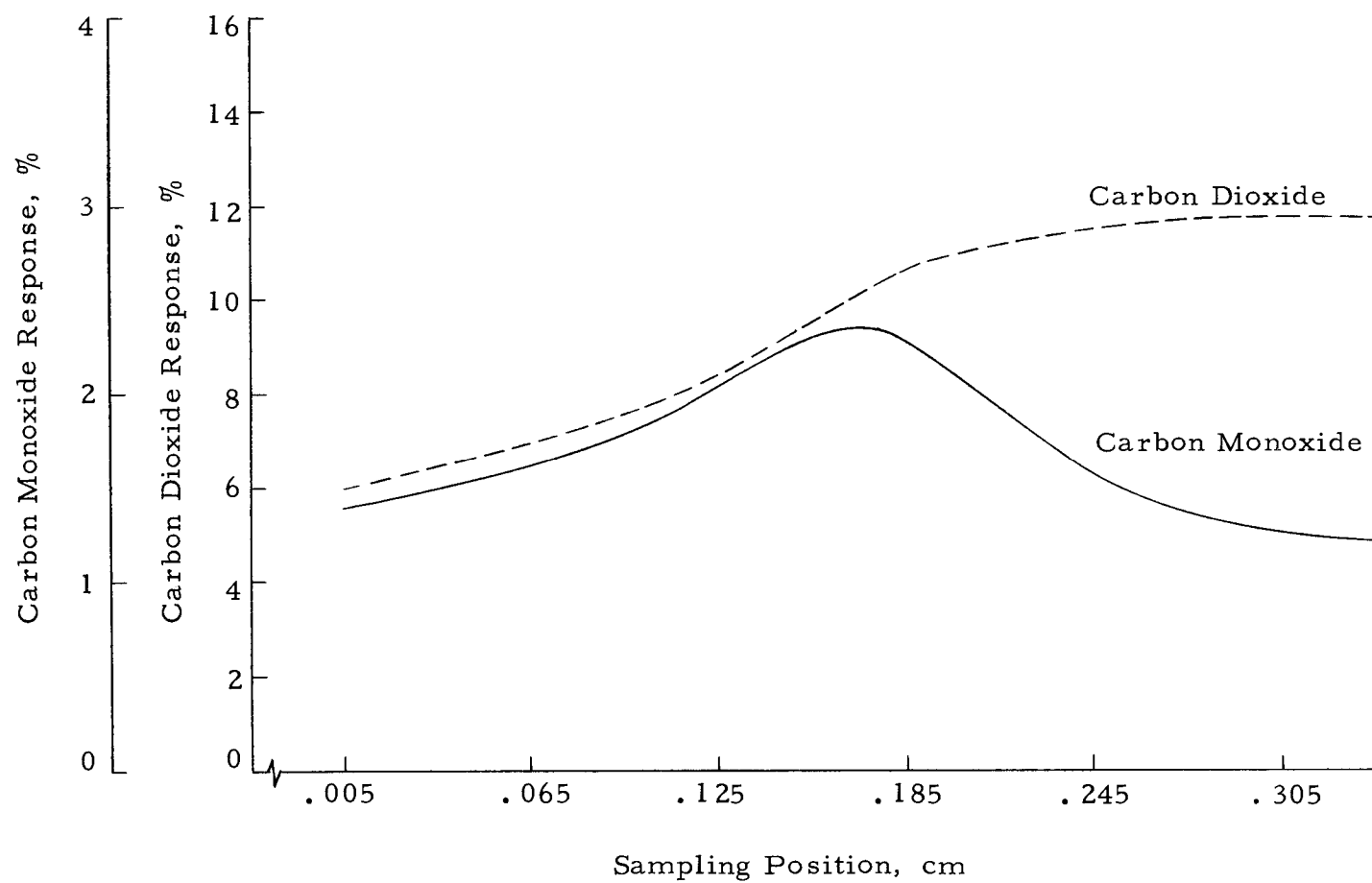


Figure 10. General response profiles of carbon monoxide and carbon dioxide.

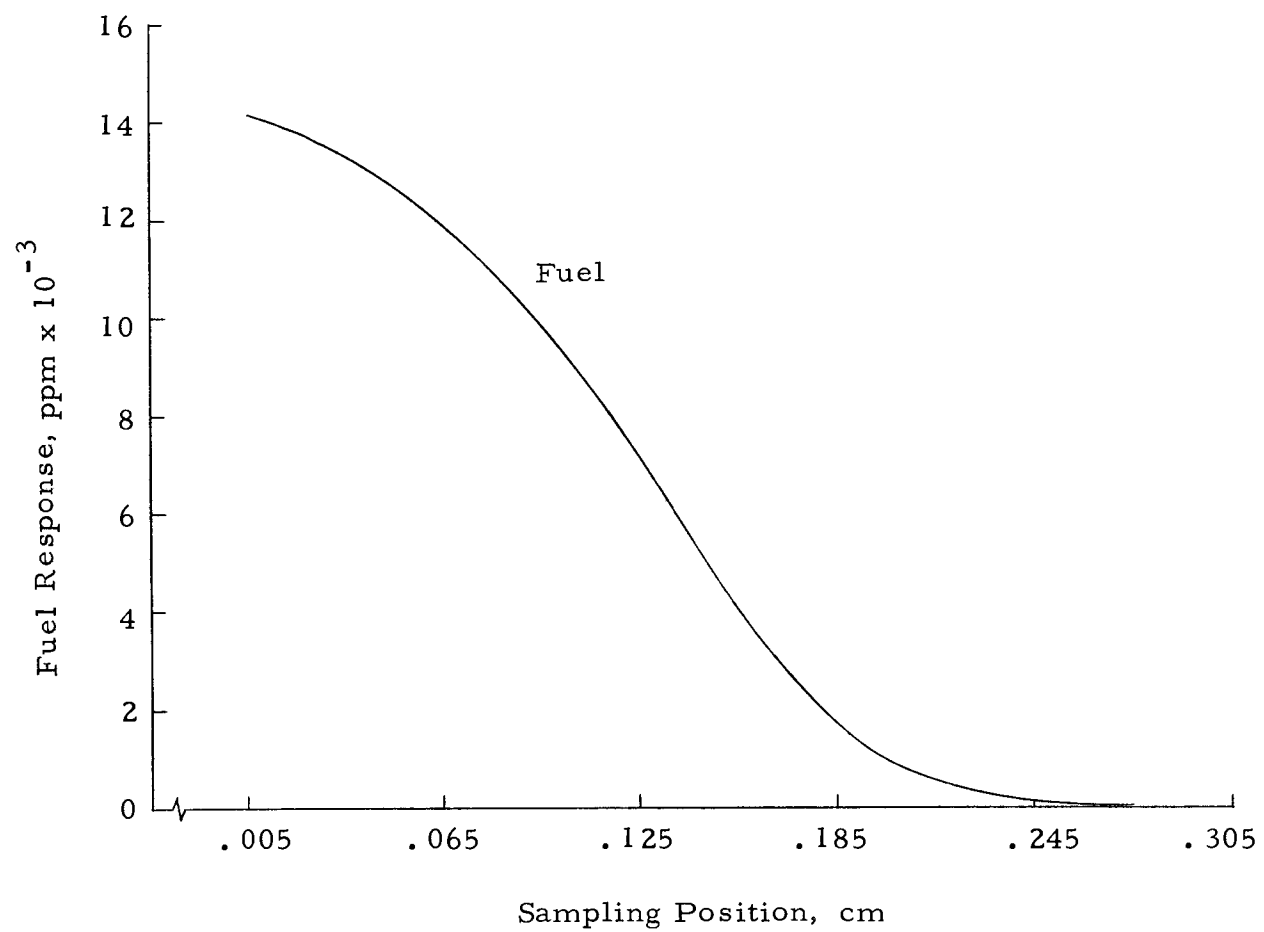


Figure 11. General response profile of hydrocarbon fuel.

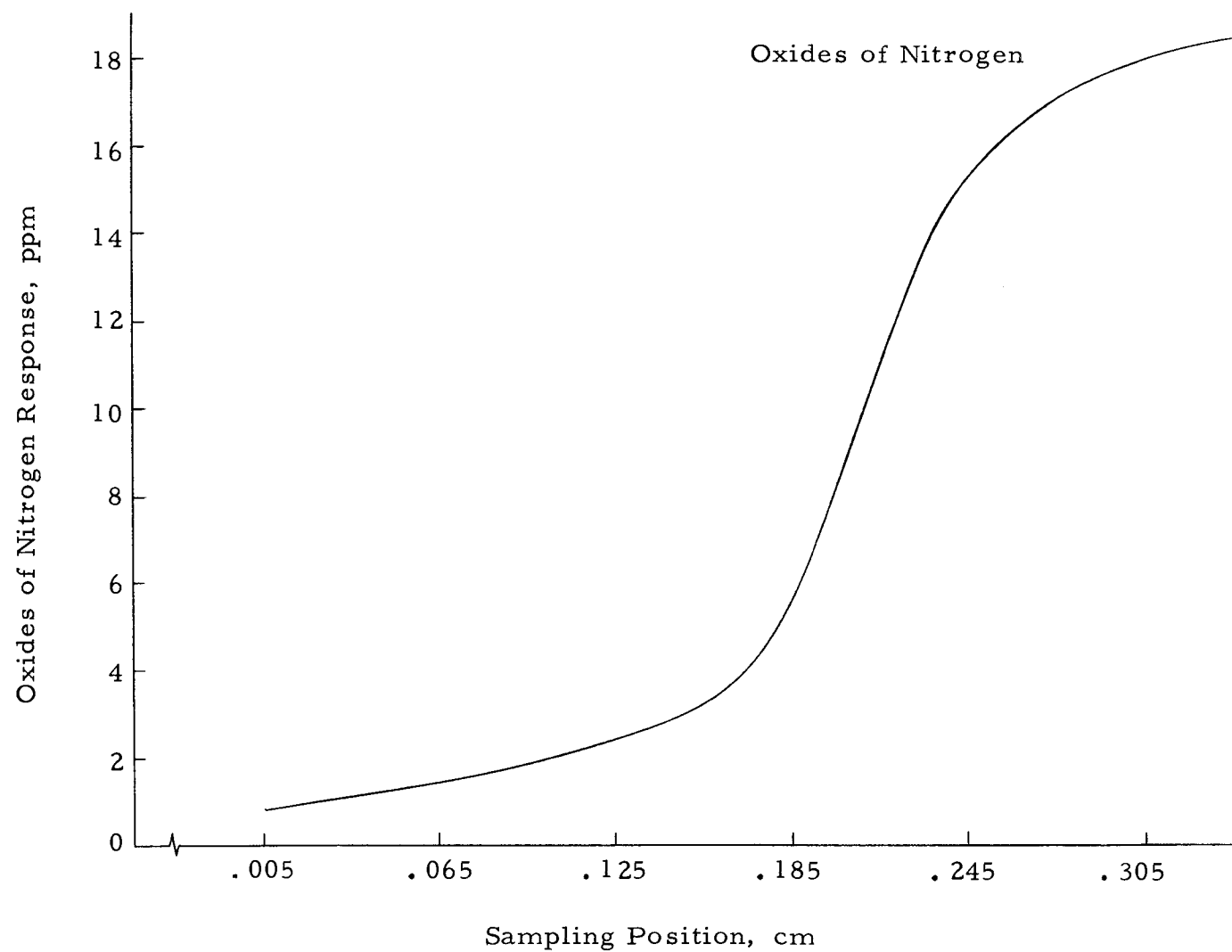


Figure 12. General response profile of oxides of nitrogen.

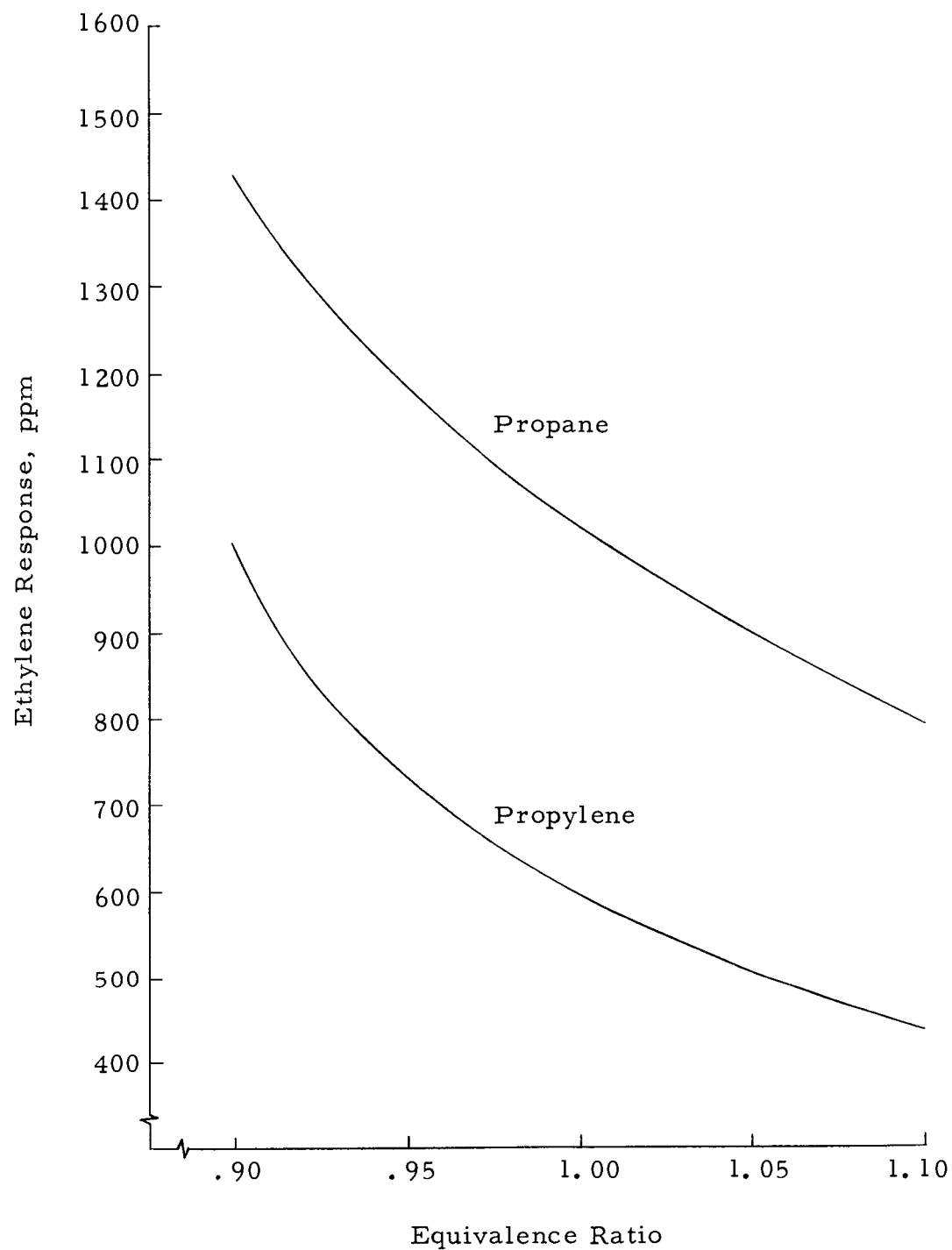


Figure 13. Effect of equivalence ratio on ethylene response for propane and propylene fuels.

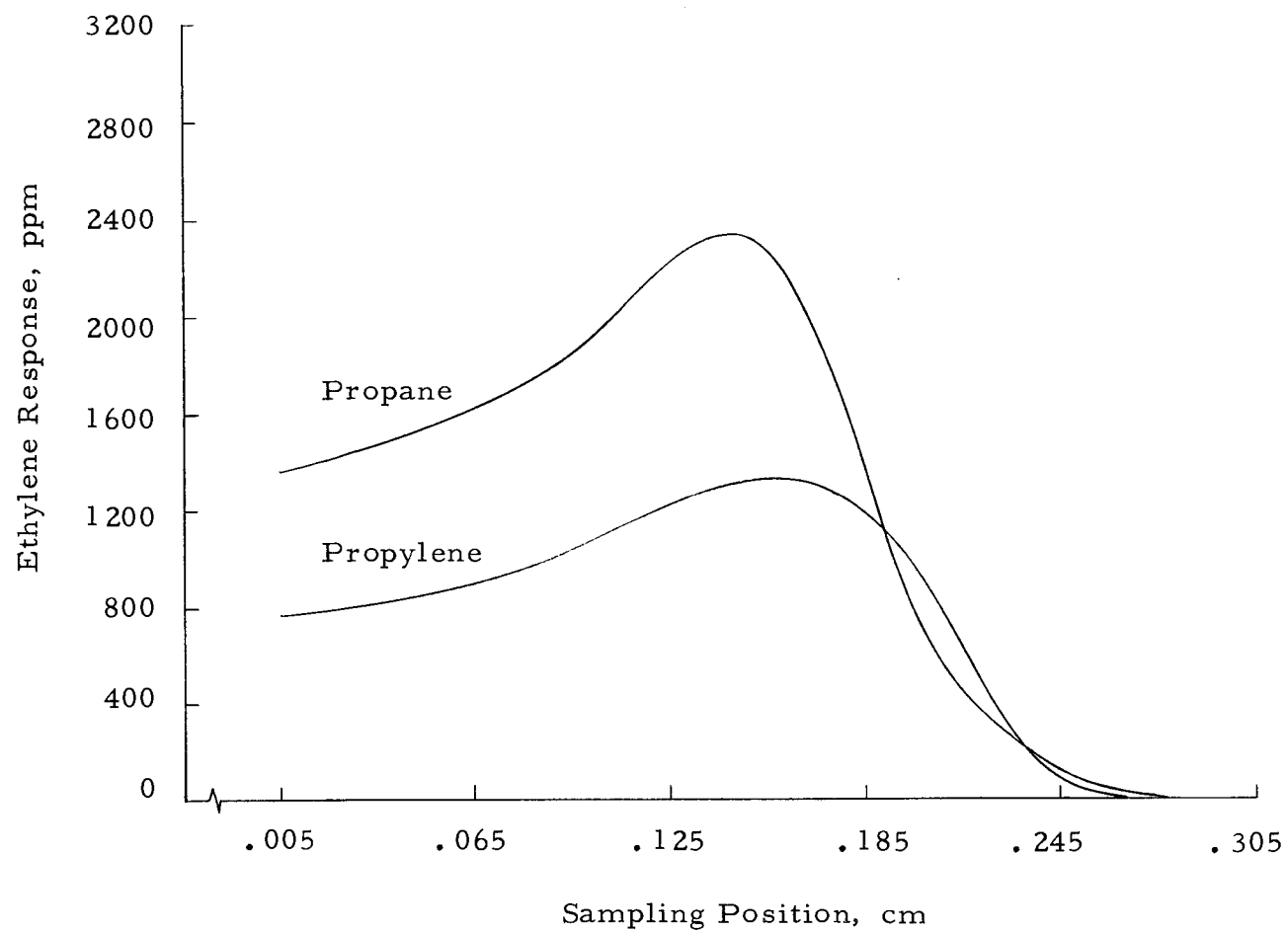


Figure 14. General response profiles of ethylene for propane and propylene fuels.

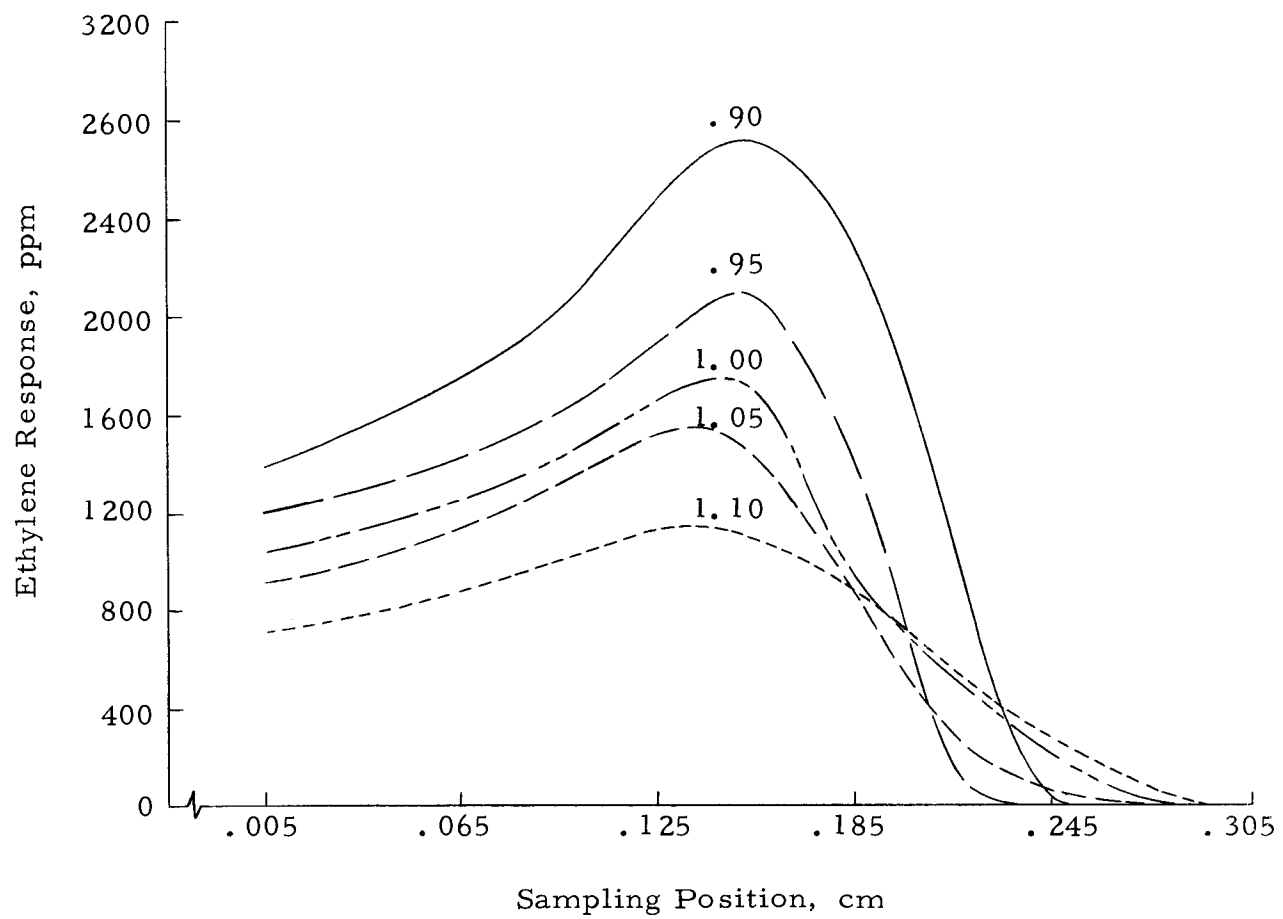


Figure 15. General ethylene response profiles for equivalence ratios of .90, .95, 1.00, 1.05 and 1.10.

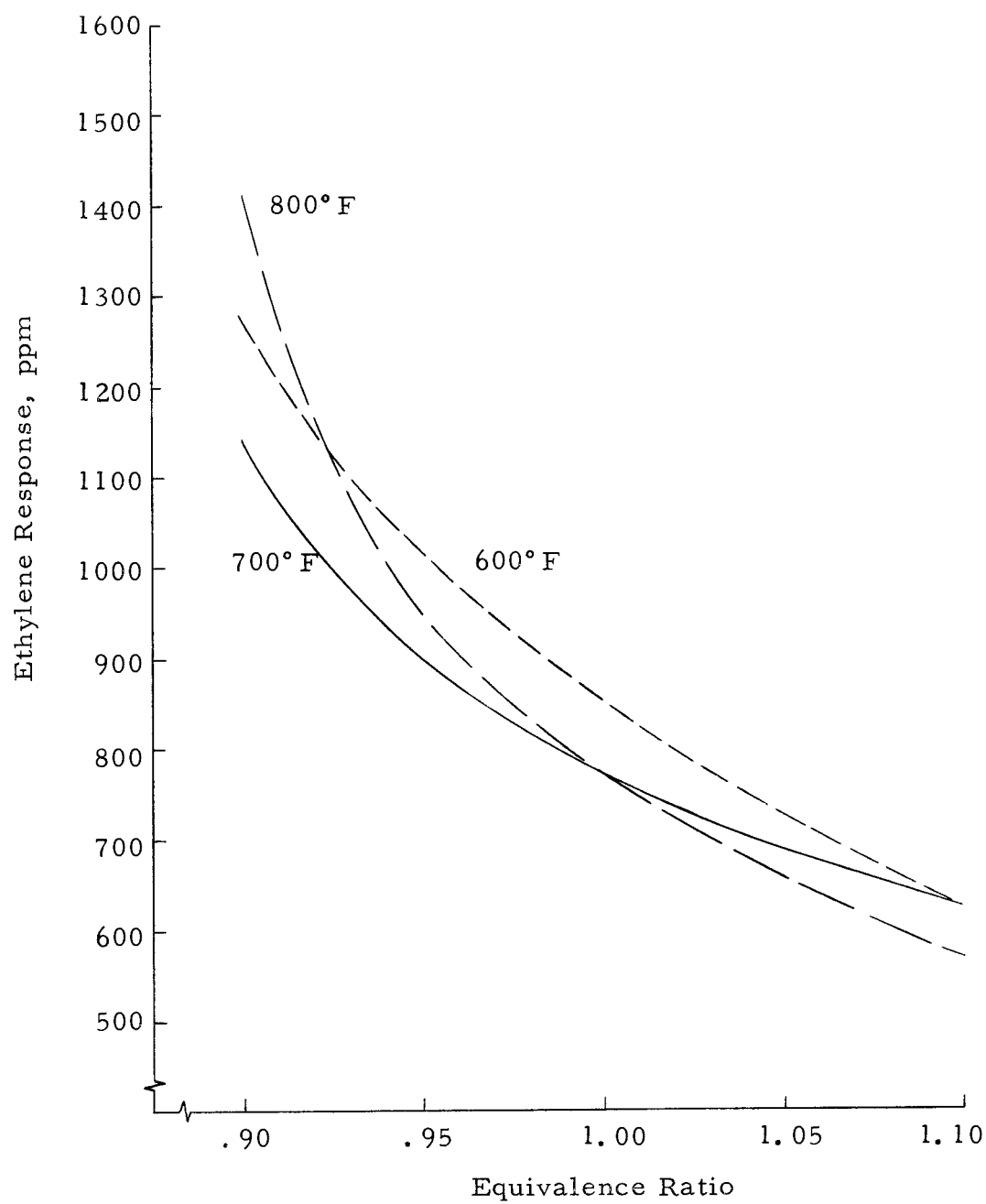


Figure 16. General effect of equivalence ratio on ethylene response for plate temperatures of 600°F, 700°F and 800°F.

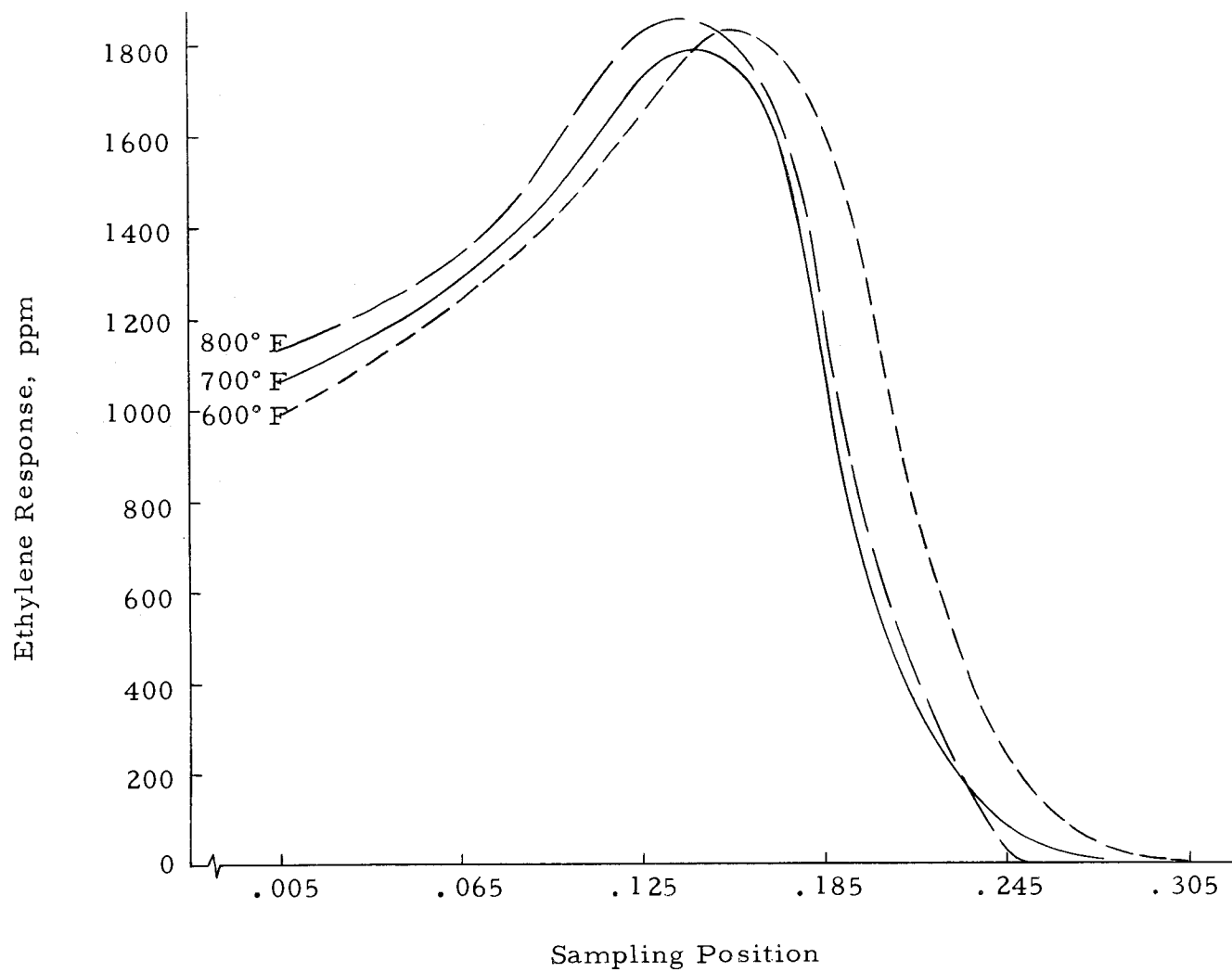


Figure 17. General ethylene response profiles for plate temperatures of 600°F, 700°F and 800°F.

Figure 13 demonstrates the difference in response for the two fuels. No (fuel) x (equivalence ratio) interaction effect was detected in the analysis of variance. This is graphically made apparent since the two response curves have about the same shape and seem to be parallel.

Figures 14, 15, 16, and 17 respectively, demonstrate the (fuel) x (sampling position), (equivalence ratio) x (sampling position), (equivalence ratio) x (plate temperature), and (sampling position) x (plate temperature) interaction effects. In each case the interaction effect is typified by overlapping response curves.

One of the prime objectives of this study was to define the concentration profile through the reaction zone for each of the dependent variables. Thus a set of profiles was to be obtained for each of the 30 combinations of fuel type, equivalence ratio and plate temperature. Twelve equal-spaced levels of sampling position were initially chosen for the four-factor experiment to accomplish this objective. However, additional levels of sampling position were needed in most cases to define the response profiles. While these additional observations could not be used in the four-factor analysis of variance, they could be used in defining equations of the form shown in Equation (4-1)

$$Y = \beta_0 + \beta_1 Z + \beta_2 Z^2 + \beta_3 Z^3 + \dots \beta_n Z^n \quad (4-1)$$

where,

Y dependent variable response.

Z sampling position (independent variable).

β 's parameters to be estimated.

The coefficients may be estimated using a Stepwise Multiple Linear Regression Analysis (OSU-01) or possibly a Non-linear Least Squares program (OSU-05). The usefulness of these curves and equations will be discussed in the Laboratory Flame Equations section of this chapter.

Three-factor Analysis of Variance

In addition to the primary gas concentration measurements, several secondary measurements were made for each of the 30 combinations of fuel type, equivalence ratio, and plate temperature. These observations included dead space thickness, luminous flame zone thickness, and the point of hydrocarbon disappearance (hydrocarbon distance). The first two have been graphically illustrated in Figure 1 while the latter is merely the lowest level of sampling position at which no hydrocarbons are detected. These dependent responses constitute a non-replicated three-factor case. Analysis of variance computations were made using computer program OSU-03 and are given in Tables 12, 13 and 14. The corresponding means for main effects and two-factor effects are in Appendix L. The

Table 12. Three-factor analysis of variance for dead space thickness response.

Source of Variance	Degrees of Freedom	Mean Square	Variance Ratio	Significant at 5% Level
Fuel	1	.000163	13.58	Yes
Equivalence Ratio	4	.000128	10.67	Yes
Plate Temperature	2	.001440	120.00	Yes
Fuel x Equivalence Ratio	4	.000022	1.83	No
Fuel x Plate Temperature	2	.000053	4.42	No
Equivalence Ratio x Plate Temperature	8	.000023	1.92	No
Fuel x Equivalence Ratio x Plate Temperature	8	.000012	---	---
- - - - -				

Critical Variance Ratios at 5% Level of Significance:

$$F_8^1 = 5.3177$$

$$F_8^2 = 4.4590$$

$$F_8^4 = 3.8378$$

$$F_8^8 = 3.4381$$

Table 13. Three-factor analysis of variance for flame zone thickness response.

Source of Variance	Degrees of Freedom	Mean Square	Variance Ratio	Significant at 5% Level
Fuel	1	.001470	38.68	Yes
Equivalence Ratio	4	.000137	3.60	No
Plate Temperature	2	.000130	3.42	No
Fuel x Equivalence Ratio	4	.000053	1.39	No
Fuel x Plate Temperature	2	.000130	3.42	No
Equivalence Ratio x Plate Temperature	8	.000022	0.58	No
Fuel x Equivalence Ratio x Plate Temperature	8	.000038	---	---
- - - - -				

Critical Variance Ratios at 5% Level of Significance:

$$F_8^1 = 5.3177$$

$$F_8^2 = 4.4590$$

$$F_8^4 = 3.8378$$

$$F_8^8 = 3.4381$$

Table 14. Three-factor analysis of variance for point of hydrocarbon disappearance response.

Source of Variance	Degrees of Freedom	Mean Square	Variance Ratio	Significant at 5% Level
Fuel	1	.000963	4.72	No
Equivalence Ratio	4	.004200	20.58	Yes
Plate Temperature	2	.002920	14.31	Yes
Fuel x Equivalence Ratio	4	.000097	0.38	No
Fuel x Plate Temperature	2	.000333	1.63	No
Equivalence Ratio x Plate Temperature	8	.000383	1.88	No
Fuel x Equivalence Ratio x Plate Temperature	8	.000204	---	---
- - - - -				

Critical Variance Ratios at 5% Level of Significance:

$$F_8^1 = 5.3177$$

$$F_8^2 = 4.4590$$

$$F_8^4 = 3.8378$$

$$F_8^8 = 3.4381$$

(fuel) x (equivalence ratio) x (plate temperature) interaction term was used as an estimate of the error term in testing the null hypotheses concerning presence of main effects and two-factor effects. The critical variance ratio (F-test) values at five percent level of significance are listed at the bottom of the analysis of variance tables.

Three-factor Response Curves

The general response curves for dead space thickness are reported in Figures 18 and 19 while the hydrocarbon distance response is shown in Figure 20. No response curves for luminous flame zone thickness are given since only the fuel effect is significant. As with the four-factor case, these curves are intended to demonstrate general response features and therefore the refinement of computer curve fitting has not been used. Note that although some divergence and overlapping is shown in Figures 18 and 19, these effects are not statistically significant. In Figure 20, the propane and propylene data were averaged because the fuel effect for point of hydrocarbon disappearance was not significant.

Using a Multiple Linear Regression Analysis (Modified Program OSU-01) the raw data for dead space thickness were forced to fit the function shown as Equation (4-2)

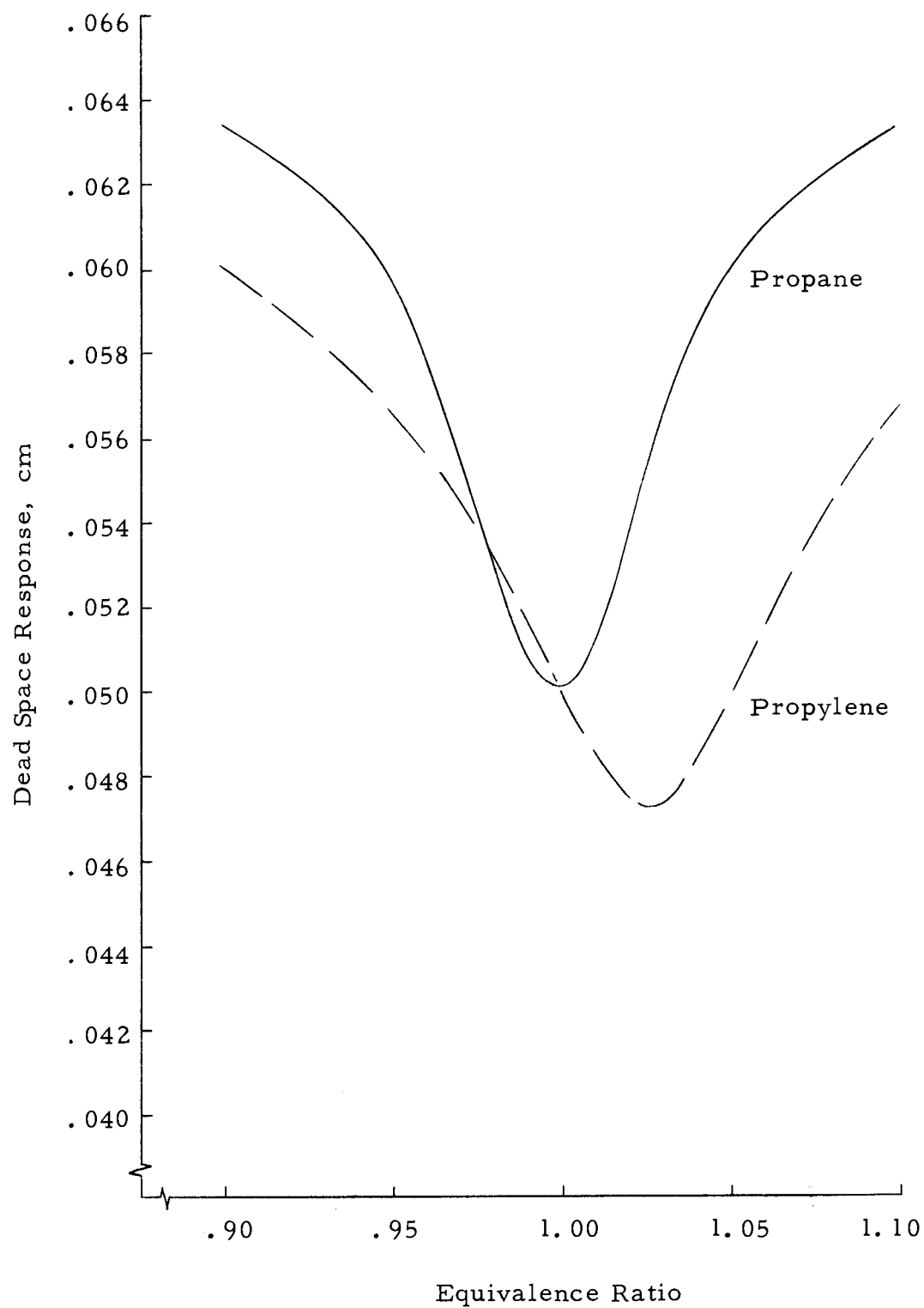


Figure 18. General effect of equivalence ratio on dead space response for propane and propylene fuels.

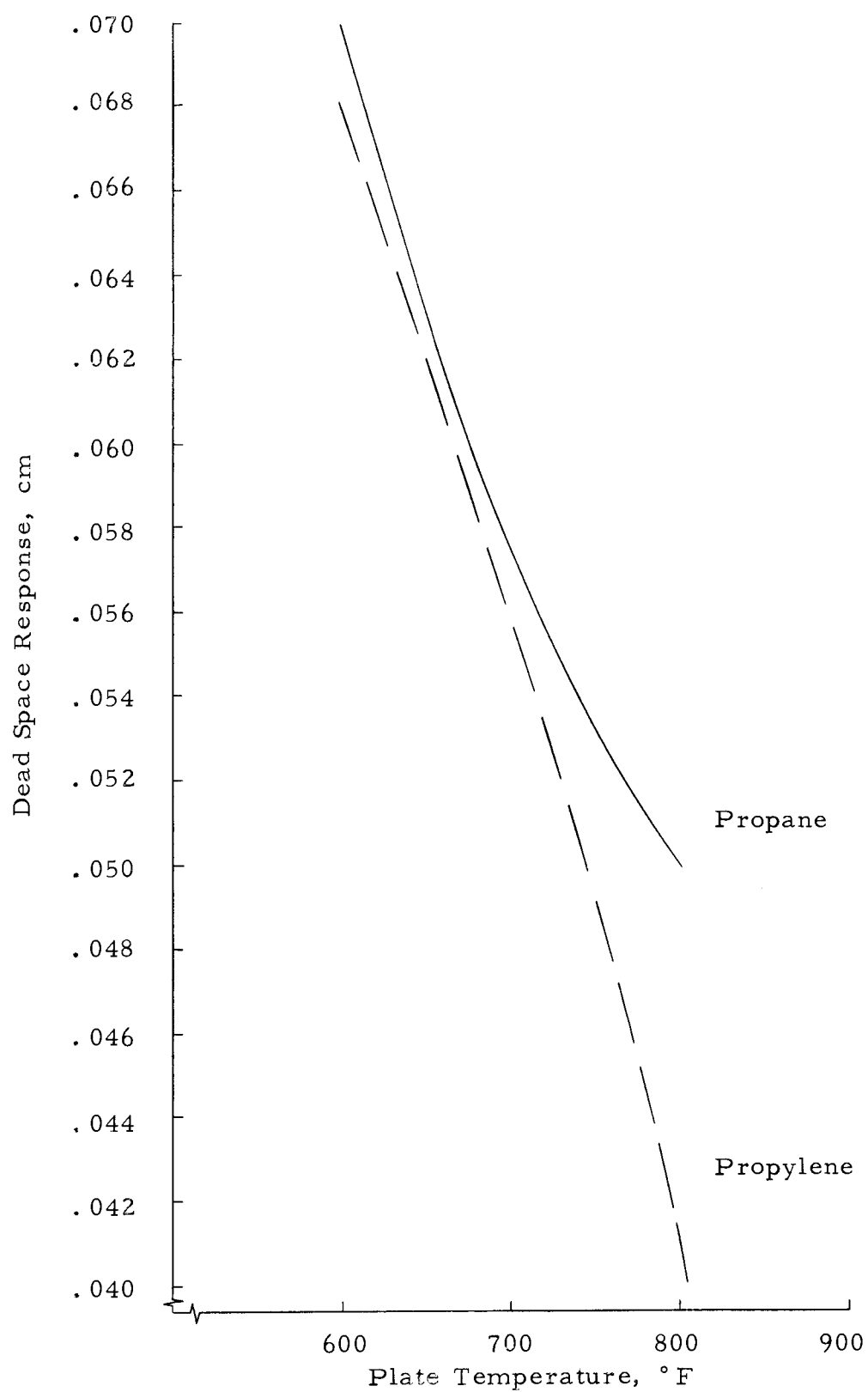


Figure 19. General effect of plate temperature on dead space response for propane and propylene fuels.

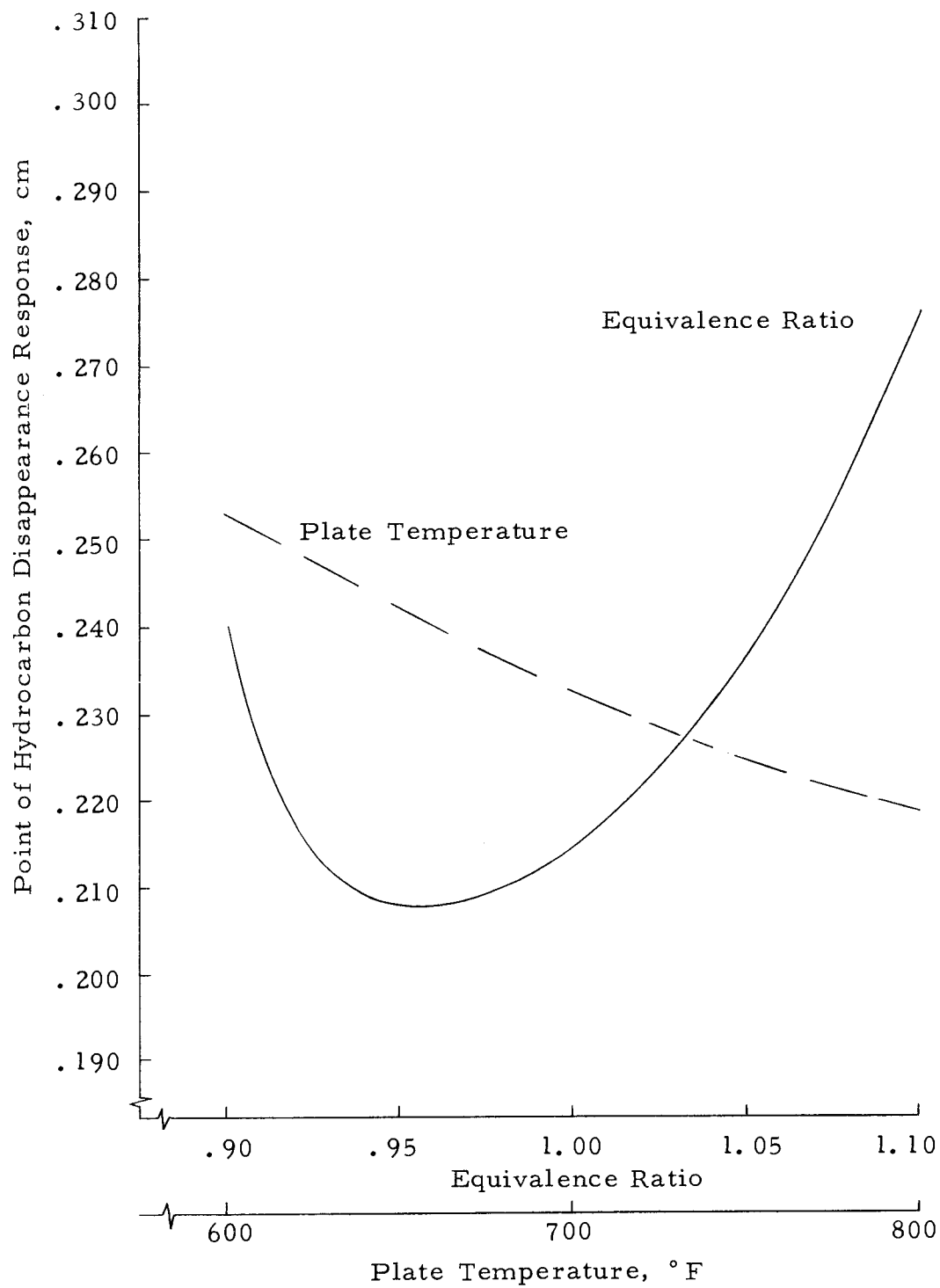


Figure 20. General effect of equivalence ratio and plate temperature on point of hydrocarbon disappearance.

$$Y = \beta_0 + \beta_1 X_1 + \beta_2 X_2 + \beta_3 X_1^2 + \beta_4 X_2^2 \quad (4-2)$$

where,

Y dependent response, cm.

X₁ plate temperature, °F.

X₂ equivalence ratio.

β's parameters to be estimated.

Due to the presence of a fuel effect on dead space response, Equations (4-3) and (4-4) are for propane and propylene, respectively.

$$Y = 1.0916594 - .0004180X_1 - 1.7102895X_2 + .00000022X_1^2 + .8571447X_2^2 \quad (4-3)$$

$$Y = .9454584 + .0003200X_1 - 1.9050130X_2 - .00000032X_1^2 + .9428398X_2^2 \quad (4-4)$$

Equation (4-5) is for the point of hydrocarbon disappearance response. It was obtained using a Stepwise Multiple Linear Regression Analysis (OSU-01) and a function of the form shown in Equation (4-2). The propane and propylene data were pooled to obtain estimates of the parameters for this expression. Only statistically significant coefficients are included.

$$Y = .4682776 - .0007750X_1 + .000000425X_1^2 + .0997252X_2^2 \quad (4-5)$$

The correlation coefficients for Equations (4-3), (4-4) and (4-5) are 0.965, 0.913 and 0.714, respectively. Some of the actual and predicted values are compared in Table 15.

Application of Laboratory Flame Equations

The one-dimensional flame equations which are given in Appendix I may be applied to the experimental data. Unfortunately, a complete description of the flame system requires in addition to the temperature profiles, concentration profiles for $n-1$ of the constituents present. Some of the major ones which were not measured in this study are hydrogen, oxygen, nitrogen and water vapor. Another term which must somehow be evaluated is the area ratio. Determining this term as a function of sampling position for each of the 30 sets of operating conditions would have indeed been a monumental effort in itself. No attempt was made to make these measurements.

Diffusion velocities, as a function of sampling position, may be calculated using Equation (I-6)

$$V_i = - \frac{D_{ij}}{X_i} \frac{dX_i}{dZ} \quad (I-6)$$

which is the basic binary diffusion velocity equation (neglecting thermal diffusion). The binary rather than multicomponent diffusion

Table 15. Actual versus predicted values for dead space and point of hydrocarbon disappearance response.

Dead Space, cm x 10 ²				Point of Hydrocarbon Disappearance, cm x 10 ² Combined Propane and Propylene Data	
Propane		Propylene			
Actual	Predicted by Equation (4-3)	Actual	Predicted by Equation (4-4)	Actual	Predicted by Equation (4-5)
8.30	7.51	3.90	4.19	2.55	2.36
6.00	6.18	6.00	5.79	2.20	2.13
4.50	5.31	6.80	6.76	2.00	2.22
7.30	6.89	3.80	3.59	2.10	2.08
5.80	5.57	5.30	5.19	2.70	2.54
4.80	4.69	6.00	6.15	2.05	2.32
5.80	6.69	4.10	3.44	2.60	2.65
5.30	5.37	4.60	5.04	2.90	2.75
4.40	4.49	5.60	6.00	2.70	2.39
6.80	6.92	3.60	3.78	3.00	2.75
5.70	5.61	5.50	5.38	2.50	2.42
5.40	4.73	6.50	6.34	2.55	2.64
7.40	7.59	4.20	4.58	2.45	2.54
6.20	6.27	6.20	6.18	2.05	2.08
5.50	5.38	7.50	7.14	2.50	2.36

expression is acceptable since nitrogen is present in excess. The additional rigor of the complex multicomponent expressions is not warranted. Each specie, i , is thus considered to be a trace component in a binary mixture with nitrogen, j . For flame temperature systems, data on multicomponent diffusion are almost completely lacking while binary diffusion coefficient data are quite limited. Therefore, binary coefficients must be calculated by the method of classical statistical mechanics as outlined in Appendix J. The method is presented in detail by Fristrom and Westenberg (27) and Hirschfelder (31).

The concentration values, X_i , are available directly from the experimental data but the concentration gradients must be calculated. This may be accomplished graphically but is a very tedious method. However, if suitable computer prediction equations have been determined then this alternative is certainly more expedient and probably more accurate.

As an example of obtaining prediction expressions, the carbon dioxide and propane response data from Table K-12 were arbitrarily fitted to the functional form shown in Equation (4-6) using a Stepwise Multilinear Regression Analysis (OSU-01)

$$Y = \beta_0 + \beta_1 Z + \beta_2 Z^2 + \beta_3 Z^3 + \beta_4 Z^4 + \beta_5 Z^5 \quad (4-6)$$

where,

Z = sampling position, cm.

The resulting expressions for propane, Equation (4-7), and carbon dioxide, Equation (4-8), have correlation coefficients of .999 and .995, respectively. Only statistically significant coefficients are included.

$$Y = 21045 - 12382Z - 831495Z^2 + 46182180Z^5 \quad (4-7)$$

$$Y = 6.357 - 16.107Z + 448.769Z^2 - 1373.975Z^3 + 2739.198Z^5 \quad (4-8)$$

Similar expressions could be obtained for the other dependent responses. Also the data could be fitted using a Non-linear Least Squares program (OSU-05) but it has the inherent disadvantage that one must have reasonably accurate initial estimates of the coefficients.

Sample Calculations

Diffusion velocity calculations were made from the experimental data listed in Table 12 of Appendix K. The operating conditions were propane as fuel, equivalence ratio of 1.05 and plate temperature of 800° F. The calculated species diffusion velocities are summarized in Table 16. Positive species diffusion velocities indicate that the component is diffusing downstream with the gas flow

Table 16. Derived specie diffusion velocities for operating conditions of fuel: propane;
equivalence ratio: 1.05; plate temperature: 800°F.

Nomenclature: Diffusion velocities cm/sec.; positive velocities downstream with gas flow.

Distance from Plate cm	Methane	Ethane	Ethylene	Propane	Acetylene	Propylene	Carbon Monoxide	Carbon Dioxide	Oxides of Nitrogen
.005	- 4.3	- 2.4	- 1.2	1.8	0	- 3.05	- 2.7	- 0.7	- 0
.035	-15.3	-11.9	- 7.4	5.3	0	- 6.9	- 6.4	- 3.0	0
.065	-16.1	-20.2	-12.3	10.7	-207.0	-12.7	-11.2	- 6.4	0
.095	-14.5	- 6.6	-16.8	17.4	-115.5	-12.9	-12.6	- 7.2	-100.0
.125	9.3	18.3	- 2.1	38.7	9.8	2.7	-13.3	- 9.2	- 63.6
.155	71.6	40.4	254.0	76.0	92.8	42.0	21.0	-10.7	- 59.6
.185	198.5	155.0	20.5	112.8	121.0	94.6	44.2	- 3.6	- 77.5
.215	0	0	0	0	0	0	40.0	- 1.0	- 33.1
.245	0	0	0	0	0	0	16.6	0	- 22.5

while negative velocities indicate the converse. Figure 21 illustrates how the ethylene diffusion velocity compares with the gas velocity.

The mass flux fraction, G_i , was calculated using Equation (I-3)

$$G_i = \frac{N_i M_i (v + V_i)}{\rho v} \quad (\text{I-3})$$

where the velocity and density values are calculated using the continuity equation and equation of state. The term G_i represents the fraction of the total mass flow at any cross section contributed by specie i , and contains terms due to both convection and diffusion.

The mass fraction, f_i , was calculated from the experimental data using Equation (I-10)

$$f_i = x_i \frac{M_i}{\bar{M}} \quad (\text{I-10})$$

where,

\bar{M} = mean molecular weight.

The area ratio, A , was assumed to be constant and equal to 1.00. This seemed acceptable in that Fristrom (23) had reported area ratio values in the range of 1.00 to 1.08 for Z values (sampling position) of 0.00 to 0.35 cm.

The mean molecular weight, \bar{M} , was also assumed to be constant but equal to the initial value of 29.5. This assumption appeared reasonable since Fristrom (25) had reported experimental

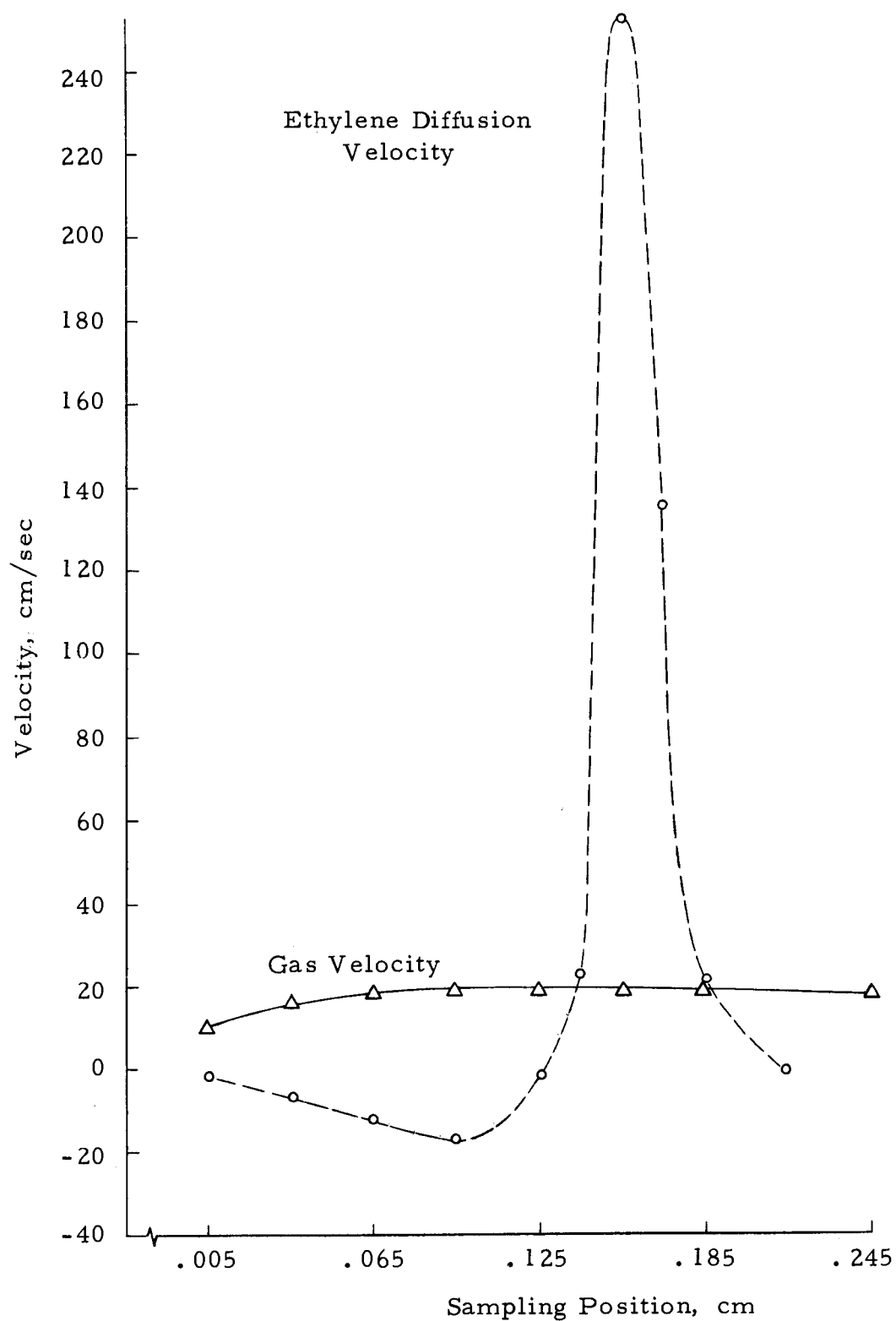


Figure 21. Derived gas flow and ethylene diffusion velocities for operating conditions of fuel: propane; equivalence ratio: 1.05; plate temperature: 800° F.

data indicating that the measured mean molecular weight through the reaction zone varied by no more than seven percent from the initial value.

The derived mass fraction and mass flux fraction profiles for ethane, ethylene, propane, carbon monoxide and carbon dioxide are presented in Figures 22 through 26, respectively. No least squares curve fitting was done. However, the general shapes of these curves graphically illustrate the need to consider the effects of species diffusion in the reacting system. If diffusion processes were not significant then the f_i and G_i curves would coincide. This is obviously not the case. For species which exhibit a maximum in the f_i curve it should be noted $f_i = G_i$ at the maxima since then the diffusion velocities are zero. It is interesting to note that the G_i curve for ethane (Figure 22) actually goes into a negative region. Physically, this means that at these points there is a net upstream flow of ethane molecules. Acetylene and oxides of nitrogen were the only other measured species to exhibit negative G_i values. This effect and the apparent maximum in the propane G_i curve in Figure 24 may be real or possibly only a result of the numerical treatment of the data.

The rate constants for each species, K_i , may be calculated using Equation (I-4)

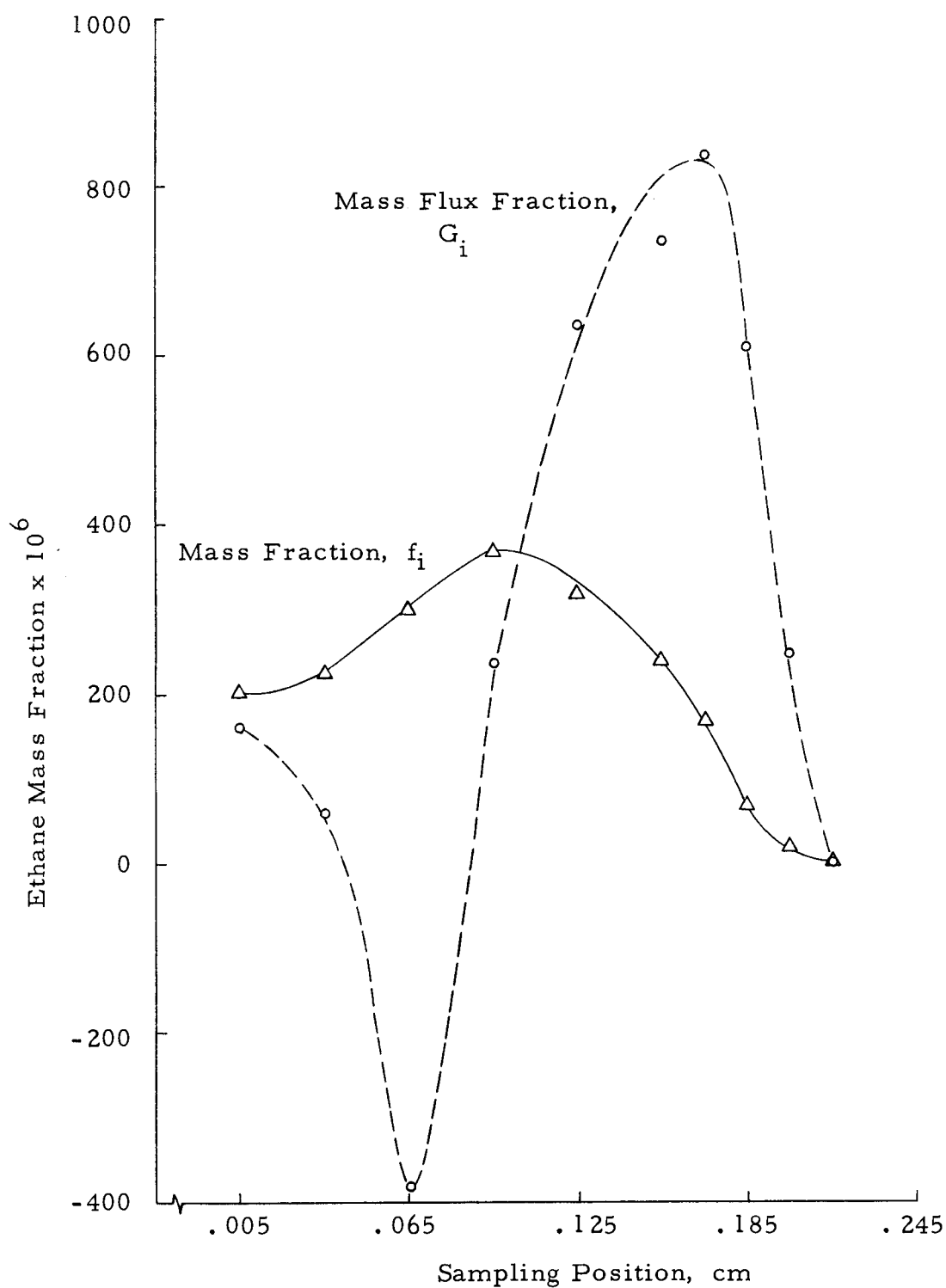


Figure 22. Ethane response mass fraction profiles for operating conditions of fuel: propane; equivalence ratio: 1.05; plate temperature: 800°F.

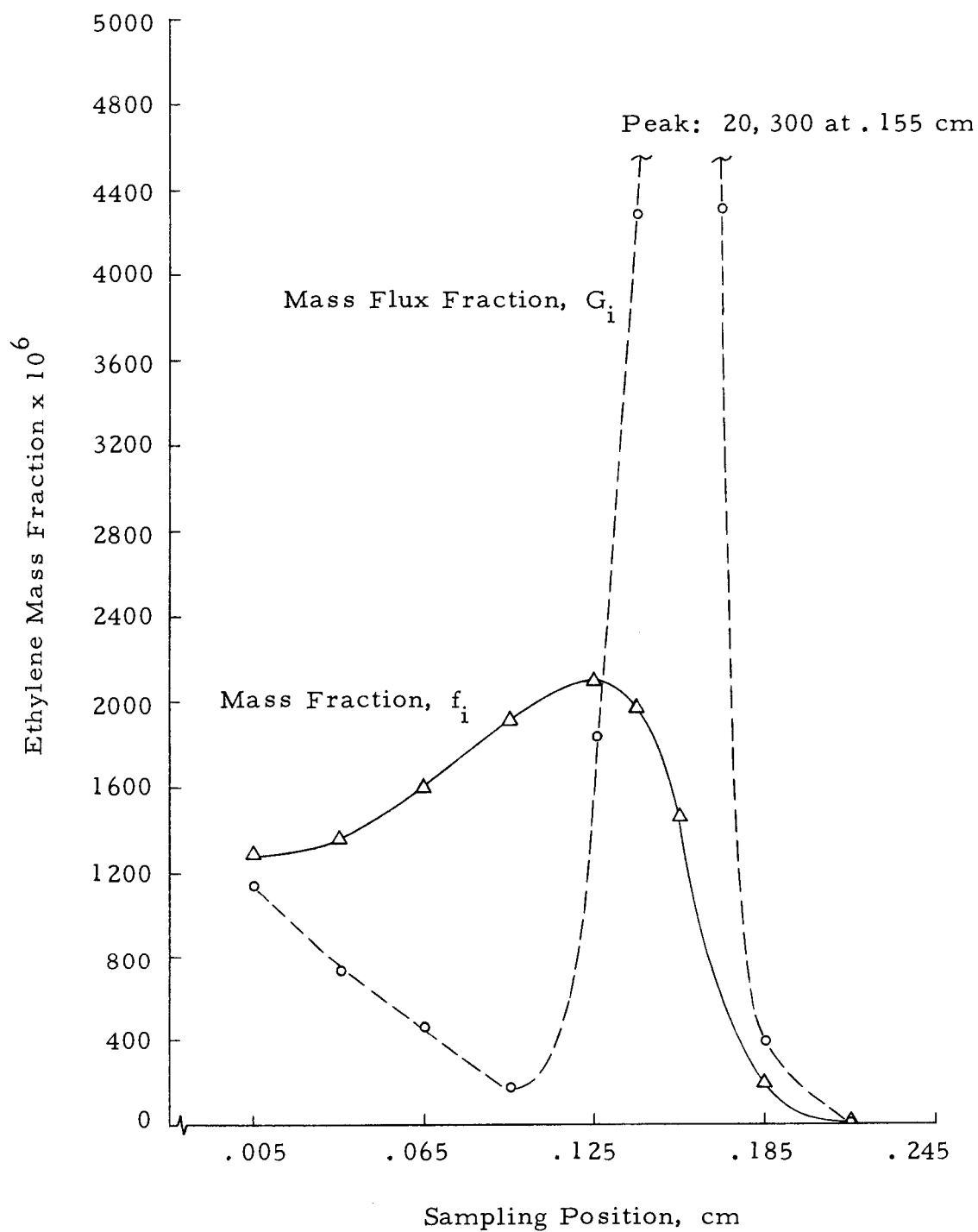


Figure 23. Ethylene response mass fraction profiles for operating conditions of fuel: propane; equivalence ratio: 1.05; plate temperature; 800° F.

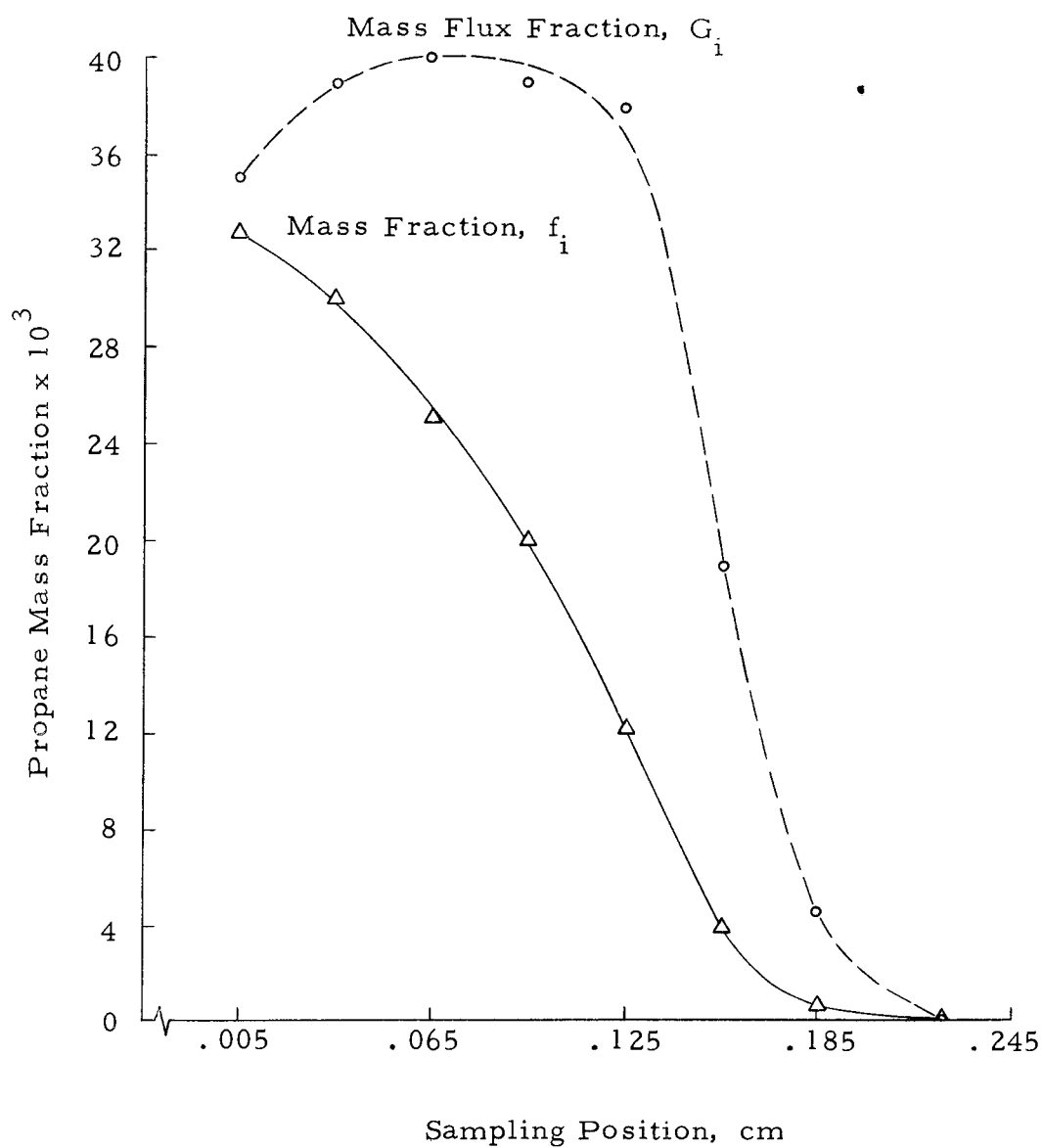


Figure 24. Propane response mass fraction profiles for operating conditions of fuel: propane; equivalence ratio: 1.05; plate temperature: 800° F.

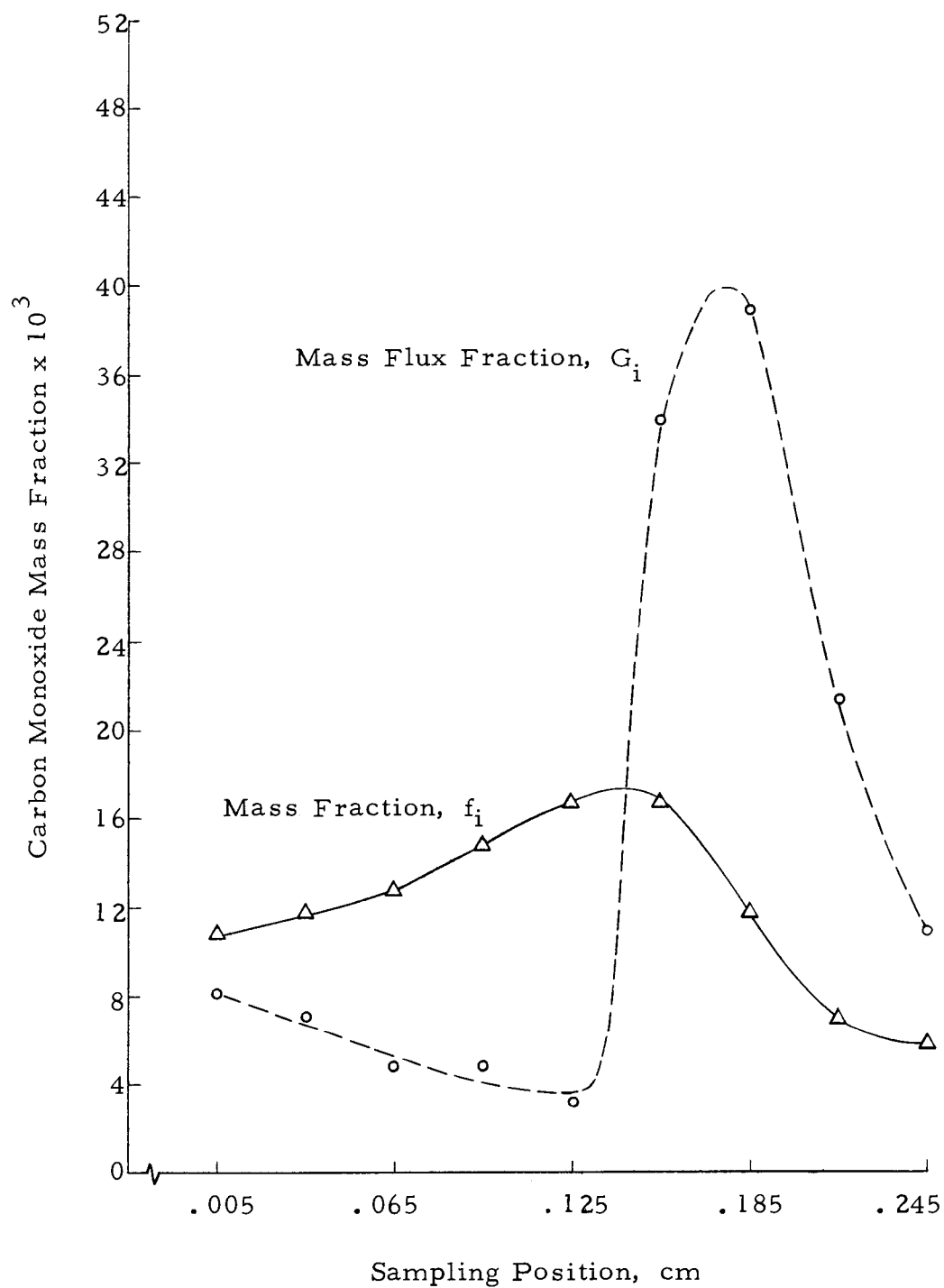


Figure 25. Carbon monoxide response mass fraction profiles for operating conditions of fuel: propane; equivalence ratio: 1.05; plate temperature: 800° F.

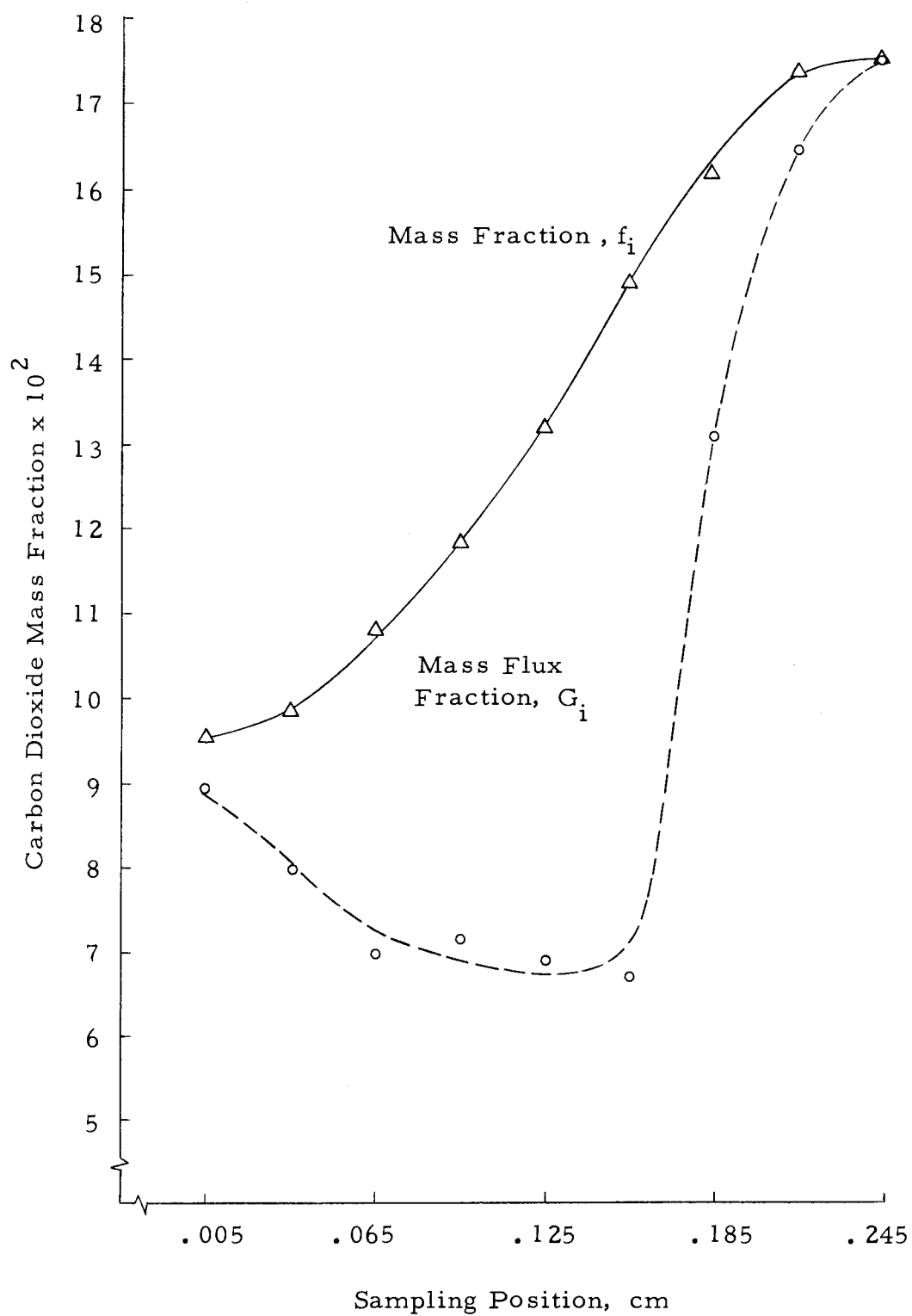


Figure 26. Carbon dioxide response mass fraction profiles for operating conditions of fuel: propane; equivalence ratio: 1.05; plate temperature: 800°F.

$$\frac{\rho_0 v_0}{M_i} \frac{dG_i}{dZ} = K_i A \quad (\text{I-4})$$

where,

K_i net molar rate of production or consumption of specie i per unit volume per unit time due to chemical reaction.

In order to make this calculation the derivatives of the G_i curves must be obtained. For this case, this calculation was not made.

The Energy Equation (I-5) and Heat Release Equation (I-7) cannot be applied to this data because, as mentioned previously, not all of the stable chemical specie profiles were measured.

A carbon balance was made through the reaction zone (0.005 to 0.210 cm) using Equation (I-9)

$$\sum_i \frac{n_i G_i}{M_i} = \text{constant} \quad (\text{I-9})$$

where,

n_i number of carbon atoms in specie i .

These calculations indicated the mean deviation from initial mixture values to be 16.3 percent with a standard deviation of 11.3. Using mass spectrometer analysis in a propane flame at 1/4-atmosphere, Fristrom (25) has reported similar results where carbon balance deviation values ranged from 5 to 22 percent. This type of

result is not completely unexpected if one recalls the number of unavoidable uncertainties and assumptions which are involved in making these calculations.

Discussion of Experimental Data

Significant Main Effects

The final products of combustion data confirmed several characteristics inherent in hydrocarbon-air combustion systems: (1) carbon monoxide increased for rich mixtures and decreased for lean mixtures, (2) maximum flame temperatures peaked-out on the slightly rich side of stoichiometric conditions and then decreased for richer or leaner conditions, (3) as predicted by theoretical calculations, propylene as fuel produced more carbon dioxide than propane, (4) as predicted by adiabatic flame calculations, propylene exhibited higher flame temperatures, and (5) carbon dioxide concentrations were maximum under stoichiometric conditions and decreased for richer or leaner mixtures.

The general species response curves are reasonable. As expected, fuel concentration decreased as other species increased. The other hydrocarbons and carbon monoxide built-up and then decreased sharply as the chemical reaction progressed. Carbon dioxide gradually increased and experienced a sharper increase as

carbon monoxide values decreased. Oxides of nitrogen concentrations sharply increased in the region of carbon monoxide and hydrocarbon drop-off.

Significant main effects of fuel type, equivalence ratio and sampling position were detected for all dependent variables. Main effect for plate temperature was found significant for ethane, propane, propylene, carbon monoxide, carbon dioxide and oxides of nitrogen but not for methane, ethylene, and acetylene.

The fuel effect for propane and propylene responses was definitely expected since these were the two fuels used. However, the situation is not so obvious for methane, ethane, ethylene and acetylene responses.

Although it was not done, three-factor A. O. V. calculations could be made for each fuel. This is justified since the fuel effect was significant in the four-factor A. O. V. calculations. Thus quantitative prediction equations could be obtained expressing each dependent response as a function of main and interaction effects of the defined experimental parameters.

Both fuels indicated ethylene as the major stable hydrocarbon component. The quantitative ranking of the other hydrocarbons differed not only with fuel type but with variations of equivalence ratio and plate temperature as well. In gross terms this would tend to indicate that the role of these stable species and, therefore, the

associated reaction process is not the same for all operating conditions investigated.

The effect of fuel type on oxides of nitrogen (NO_x) formation is complicated by the presence of the covariant parameter, flame temperature. It is a well-established fact that oxides of nitrogen (specifically nitric oxide) formation is an endothermic reaction and is strongly temperature dependent. These experimental data suggest that the temperature effect is very predominant because oxides of nitrogen concentrations increased at richer conditions and, therefore, accompanying higher temperatures, even though the apparent availability of oxygen for NO_x formation had decreased. In order to examine the true fuel effect one must somehow remove this predominant temperature effect. This could be accomplished by running a regression of NO_x on temperature and then adjusting response values to a common temperature in order to examine the fuel structure effect. Techniques for making these calculations are described by Li (38).

The presence of main effects of equivalence ratio and sampling position are logical. The dependent response curves for equivalence ratio are similar to those found for other types of combustion reactors. The sampling position effect was expected since this is a requirement of the laminar chemical reaction.

The plate temperature main effect for propane, propylene,

carbon monoxide and carbon dioxide indicates that chemical reaction takes place in the dead space adjacent to the burner wall. Appreciable carbon monoxide and carbon dioxide concentrations are found adjacent to the wall and fuel concentration is below its initial value. As will be discussed later, these phenomena cannot be completely explained by species diffusion effects and one must, therefore, conclude that chemical reaction is present within the dead space.

Significant Interaction Effects

A large number of two-factor interaction terms were found to be significant at the five percent level of significance. The (fuel) x (sampling position) interaction was significant for all of the dependent responses while the (equivalence ratio) x (sampling position) and (fuel) x (equivalence ratio) terms were significant for several of the dependent responses.

Proceed with caution concerning the meaning of these interaction effects. Use of graphical techniques is recommended for interpreting these interactions. For example, consider the (fuel) x (sampling position) interaction for ethylene response which has been illustrated in Figure 14. The physical meaning of the interaction term says that the response curves for the two fuels are not the same shape or slope. However, upon examination of the curves it is apparent that the major evidence of interaction takes place in a

very narrow region of the reaction zone. Here the concentration gradients are large and the likelihood of error is also somewhat greater. Further testing in this region would be desirable to verify this interaction.

Response Prediction Equations

Prediction equations have been formulated for dead space thickness and point of hydrocarbon disappearance. These expressions are estimates derived from the experimental data. No attempt should be made, using these expressions, to draw inference beyond the range of experimental parameters investigated.

Examples of prediction expressions for the dependent concentration profiles have been suggested. The obvious advantages of these expressions is that they represent an expedient and probably more accurate method for estimating concentrations, concentration gradients, diffusion velocities, mass flux fraction profiles and species rate constants.

Flame Equations

The one-dimensional flame equations may be applied to this experimental data. Therefore, as an example, sample calculations are presented for the data in Table K-12 for the conditions of propane as fuel, equivalence ratio of 1.05 and plate temperature of 800° F.

These calculations candidly illustrate the need to consider diffusion effects in the reacting system. Failure to do so will result in gross errors.

The derived mass flux fraction curves, G_i , for the sample calculations are similar to those given by Fristrom (25) using a 1/4-atmosphere, stoichiometric, propane-air flame. The G_i curve for propane indicated an apparent maximum. Fristrom (25) found the same phenomenon for oxygen response. In view of the number of assumptions and approximations, it must be realized that this effect may really be a result of the numerical treatment of the data.

Apparently for the above operating conditions, some species have sufficient diffusion velocities to produce a net upstream flow. However, further calculations indicate that the concentrations of carbon monoxide and carbon dioxide present at the plate surface cannot be totally explained in this manner. In addition, the fuel concentrations somewhat below initial values cannot be completely attributed to diffusion downstream. Therefore, it must be concluded that chemical reaction is present within the dead space. This conclusion is further substantiated by the significant temperature effect in the A.O.V. for propane, propylene, carbon monoxide and carbon dioxide responses.

If the carbon monoxide and carbon dioxide concentrations near the wall are attributed to chemical reaction then the obvious question

arises: Does all of this chemical reaction take place in the narrow .005 cm zone or does some portion actually take place within the porous media where the retention time of the gas mixture is about .25 seconds? Conditions are certainly conducive for reaction in the zone adjacent to the plate. Temperature is about 1000°F and temperature gradients are approximately 5×10^4 °F/cm. However, if the latter is true to a very large extent, then any usefulness of the steady-state data in drawing inference about a transient case is certainly reduced. The assumption that reaction within the porous media is negligible is frequently made. These test data suggest that some tests should be conducted under a wide range of plate temperature conditions in order to establish the region for which such an assumption would be valid.

Discussion of Experimental Design

The selected experimental design allowed adequate sensitivity for detecting main and interaction effects. In fact, in a number of cases significant two-factor interactions were found which actually were quite small in magnitude when compared to the main effects.

Sacrifices were made in the ranges of equivalence ratio and plate temperature in order that both fuels could be used and still maintain the required flame stability. In retrospect, it appears that it would have been better to further decrease the equivalence ratio

range and thereby be able to increase the range of plate temperatures investigated. Of course now that fuel main effects have been found for all of the intermediates, further testing would probably be made on each fuel separately. Using smaller experiments replication may then be feasible.

In the three-factor A. O. V. calculations for dependent responses of dead space thickness, flame zone thickness and point of hydrocarbon disappearance only main effects were found significant. The three-factor interaction term, (fuel) x (equivalence ratio) x (plate temperature), was used as an estimate of the error term. This same term was found to be significant for several of the dependent responses in the four-factor A. O. V. Thus one may be somewhat skeptical of its use because it may lead to making a Type II error, i. e., accepting a false hypothesis. Frequently, however, the three-factor term is significant only when one or more of the two-factor terms are quite significant. Since no two-factor terms were overwhelming then confidence is restored in the use of the three-factor term as an estimate of the error term.

Discussion of Experimental Equipment

This section discusses some problems and problem-solutions encountered in the course of the research project. It is hoped that this will provide some insight for improving experimental techniques

for future work.

Thermocouple Probe

Obtaining a microminiature thermocouple probe which would withstand an acceptable length of use proved to be a gross problem. The combination of vibration and high temperatures caused these delicate thermocouples to break rather easily. In spite of great efforts to eliminate sources of vibration, thermocouple life ranged from only 9 to 20 hours. It was this problem and the complicated difficulty of repairing the probes which precluded being able to obtain refined temperature profiles for all runs. Whenever a .001-inch couple was not available then a sturdier .003-inch couple was used but no attempt was made to obtain temperature profiles.

The basic idea of having the thermocouple leads in a constant temperature zone is desirable in that it eliminates the need to evaluate rather complicated corrections for conduction losses. It is felt that this basic probe design is acceptable and with some modification and extreme care to eliminate vibration sources, its life could be increased. Possibly some thought should be given to the idea of measuring the temperature profile first and then removing the probe prior to measuring the concentration profiles through the reaction zone.

Optical Measurements

During preliminary tests condensation on the inside of the quartz window impaired vision for optical measurements. A thin coating of silicone "defogging agent" proved to be helpful but the best method was an infrared lamp which cleared the window in a matter of a minute or two. Once cleared, condensation was not a problem during the remainder of the test.

Ignition System

The spark-type ignition system performed satisfactorily. However, it is now felt that a pilot-light type system may be inherently safer. On a few occasions mixture build-up occurred in the chamber while attempting to stabilize the flame on the porous burner. Excitement followed when the stabilized flame then ignited the accumulated mixture. This mixture build-up may not have happened with a continuous pilot-light ignition system.

Burner Plate Materials

Sintered copper was also tried as a burner material. After an extensive trial and error procedure the copper was successfully mounted using a heli-arc welder. Normal high temperature soldering techniques could not be used. The porous material acted as a capillary and the end result produced a copper plate filled with silver

solder. Also great care had to be taken not to mechanically seal the soft copper porous surface. Unfortunately this burner did not meet the requirement of producing a uniform flat flame. This occurred as a result of (1) not having sufficient uniform porosity initially and/or (2) not being able to construct the burner without altering the porosity of the copper.

V. CONCLUSIONS AND RECOMMENDATIONS

Conclusions

1. According to calculations using experimental data, chemical reaction takes place within the dead space. The concentrations of carbon monoxide and carbon dioxide at the plate surface cannot be completely explained by diffusion processes.
2. Stable species hydrocarbons exist in the reaction zone under all of the conditions investigated. Their concentration is a function of fuel type, equivalence ratio, sampling position and in some cases plate temperature. Several significant interaction terms are also present.
3. Ethylene is the major stable hydrocarbon species for both propane and propylene as fuels. The quantitative ranking of the other hydrocarbon species is a function of fuel type, equivalence ratio, and plate temperature.
4. Dead space thickness is a function of fuel type, equivalence ratio, and plate temperature but no significant two-factor interaction terms are present. Dead space response for propane and propylene may be expressed in the functional form of Equations (4-3) and (4-4) respectively.
5. Hydrocarbon disappearance point is a function of

equivalence ratio and plate temperature. For this experimental data, its response may be expressed in the functional form of Equation (4-5).

6. Luminous flame zone thickness is a function of fuel type only. Propylene exhibits a greater flame zone thickness than propane.

7. Oxides of nitrogen concentration is a function of fuel type, equivalence ratio, plate temperature, and sampling position. Several significant interaction terms are also present. In order to examine the true fuel structure effect, the predominant covariant flame temperature effect must be removed.

Recommendations

1. Since fuel effects were present for all of the dependent variables, study propane and/or propylene fuels in separate experiments. Reduce the range of equivalence ratio and thereby be able to decrease the minimum plate temperature at which a stable flame exists. This will effectively increase the available range of the plate temperature parameter.

2. Consider using lower than atmospheric chamber pressures. This would require exotic and expensive vacuum equipment but would result in greatly magnified vertical dimensions of the flame system. Thus the stringent requirements of the size of the

thermocouple probe would be somewhat reduced. This system would also facilitate being able to use chamber pressure as an independent variable.

3. Investigate diluents other than nitrogen, i. e. , argon or helium to determine if effects exist as predicted by various analytical expressions.

4. Conduct tests with other wall materials to determine if a material effect is present.

5. Conduct tests to determine for what range of operating conditions, the assumption concerning negligible reaction within the porous media is valid.

BIBLIOGRAPHY

1. Beckwith, T.G. and N. L. Buck. Mechanical measurements. Reading, Mass., Addison-Wesley, 1961. 559 p.
2. Belles, F.E. and A. L. Berlad. Chain breaking and branching in the active-particle diffusion concept of quenching. Washington, D. C., 1955. 37 p. (NACA Report TN 3409)
3. Blundell, R.V. et al. Rates of radical reaction in methane oxidation. In: Proceedings of the Tenth International Symposium on Combustion. Pittsburg, Combustion Institute, 1965. p. 445-452.
4. Box, G.E. The effects of errors in the factor levels and experimental design. Technometrics 5:247-261. 1963.
5. Boys, S.F. and J. Corner. Structure of the reaction zone in a flame. Proceedings of the Royal Society of London, ser. A, 197:90-108. 1949.
6. Bray, K. Atomic recombination in a hypersonic wind tunnel. Journal of Fluid Mechanics 6:1-32. 1959.
7. Cochran, W.G. and G.M. Cox. Experimental designs. 2d ed. New York, Wiley, 1957. 611 p.
8. Cornfield, J. and J. W. Tukey. Average values of mean squares in factorials. Annals of Mathematical Statistics 27: 906-941. 1956.
9. Daniel, C. Use of half-normal plots in interpreting factorial two-level experiments. Technometrics 1:311-341. 1959.
10. Daniell, P. J. The theory of flame motion. Proceedings of the Royal Society of London, ser. A, 126:393-405. 1930.
11. Davies, O. L., ed. The design and analysis of industrial experiments. London, Oliver and Boyd, 1954. 636 p.
12. Eschenroeder, D.W. Boyer and J.G. Hall. Nonequilibrium expansions of air with coupled chemical reactions. Physics of Fluids 5:615-624. 1962.

13. Evans, M. W. Current theoretical concepts of steady-state flame propagation. *Chemical Reviews* 51:363-429. 1952.
14. Everett, A. J. and G. J. Minkoff. Some aspects of the combustion of methane at low pressures. In: *Proceedings of the Third Symposium on Combustion and Flame and Explosion Phenomena (Third international symposium on combustion)* Baltimore, Williams and Wilkins, 1949. p. 390-397.
15. Fiock, E. F., L. O. Olsen and P. D. Freeze. The use of thermocouples in streaming exhaust gas. In: *Proceedings of the Third Symposium on Combustion and Flame and Explosion Phenomena (Third international symposium on combustion)* Baltimore, Williams and Wilkins, 1959. p. 655-662.
16. Friedman, R. The quenching of laminar oxyhydrogen flames by solid surfaces. In: *Proceedings of the Third Symposium on Combustion and Flame and Explosion Phenomena (Third international symposium on combustion)* Baltimore, Williams and Wilkins, 1953. p. 110-120.
17. Friedman, R. Measurement of the temperature profile in a laminar flame. In: *Proceedings of the Fourth Symposium on Combustion and Flame and Explosion Phenomena (Fourth international symposium on combustion)* Baltimore, Williams and Wilkins, 1953. p. 259-263.
18. Friedman, R. and E. Burke. Measurement of temperature distribution in a low-pressure flat flame. *Journal of Chemical Physics* 22:824-830. 1954.
19. Friedman, R. and J. A. Cyphers. Flame structure studies. III. Gas sampling in a low-pressure propane-air flame. *Journal of Chemical Physics* 23:1875-1880. 1955.
20. Friedman, R. and W. C. Johnston. The wall quenching of laminar propane flames as a function of pressure, temperature, and air-fuel ratio. *Journal of Applied Physics* 21:791-795. 1950.
21. Fristrom, R. M. The structure of laminar flames. In: *Proceedings of the Sixth International Symposium on Combustion*. New York, Reinhold, 1957. p. 96-110.

22. Fristrom, R.M. Radical concentrations and reactions in a methane-oxygen flame. In: Proceedings of the Ninth International Symposium on Combustion. New York, Academic, 1963. p. 560-575.
23. Fristrom, R.M., C. Grunfelder and S. Favin. Methane-oxygen flame structure. I. Characteristic profiles in a low-pressure laminar, lean, premixed methane-oxygen flame. Journal of Physical Chemistry 64:1386-1392. 1960.
24. Fristrom, R.M., R. Prescott and C. Grunfelder. Flame zone studies. III. Techniques for the determination of composition profiles for flame fronts. Combustion and Flame 1:102-113. 1957.
25. Fristrom, R.M. and A.A. Westenberg. Flame zone studies. IV. Microstructure and material transport in a laminar propane-air front. Combustion and Flame 1:217-228. 1957.
26. Fristrom, R.M. and A.A. Westenberg. Experimental chemical kinetics from methane-oxygen laminar flame structure. In: Proceedings of the Eighth International Symposium on Combustion. Baltimore, Williams and Wilkins, 1962. p. 438-448.
27. Fristrom, R.M. and A.A. Westenberg. Flame structure. New York, McGraw-Hill, 1965. 424 p.
28. Gad El-Mawla, Ahmed E. -Said M. A study of hydrocarbon concentration and temperature profiles through a steady-state flame adjacent to a wall. Ph. D. thesis. Ann Arbor, University of Michigan, 1965. 165 numb. leaves.
29. Gloss, G.P., et al. The oxidation reaction of acetylene and methane. In: Proceedings of the Tenth International Symposium on Combustion. Pittsburg, Combustion Institute, 1965. p. 513-522.
30. Hirschfelder, J.O. and C.F. Curtiss. Theory of flame propagation. In: Proceedings of the Third Symposium on Combustion, and Flame and Explosion Phenomena (Third international symposium on combustion) Baltimore, Williams and Wilkins, 1949. p. 390-397.
31. Hirschfelder, J.O., C.F. Curtiss and R.B. Bird. Molecular theory of gases and liquids. 2d ed. New York, Wiley, 1964. 1249 p.

32. Hoare, D.E. and A.D. Walsh. The oxidation of methane. In: Proceedings of the Fifth International Symposium on Combustion. New York, Reinhold, 1955. p. 467-484.
33. Johnstone, H.F., R.L. Pigford and J. H. Chapin. Heat transfer to clouds of falling particles. Urbana, 1941. 55 p. (University of Illinois. Engineering Experiment Station. Station Bulletin No. 330.)
34. Kaskan, W.E. The dependence of flame temperature on mass burning velocity. In: Proceedings of the Sixth International Symposium on Combustion. New York, Reinhold, 1957. p. 134-143.
35. Klaukens, H. and H. G. Wolfhard. Measurements in the reaction zone of a bunsen flame. Proceedings of the Royal Society of London, ser. A, 193:512-524. 1948.
36. Kreith, F. Principles of heat transfer. Scranton, International Textbook, 1958. 536 p.
37. Lewis, B. and G. von Elbe. Combustion, flames and explosions of gases. 2d ed. Academic, New York, 1961. 731 p.
38. Li, J.R. Statistical inference. Ann Arbor, Edwards Brothers, 1964. 658 p.
39. Minkoff, G.J. and C.F. Tipper. Chemistry of combustion reactions. London, Butterworths, 1962. 393 p.
40. Needham, D.P. and J. Powling. The flame decomposition of ethyl nitrate. Proceedings of the Royal Society of London, ser. A, 232:337-350. 1955.
41. Potter, A.E. and A.L. Berlad. A thermal equation for flame quenching. 1956. 7 p. (NACA Report 1264)
42. Potter, A.E. and A.L. Berlad. The quenching of flames of propane-oxygen-argon and propane-oxygen-helium mixtures. Journal of Physical Chemistry 60:97-101. 1956.
43. Prescott, R. et al. Composition profiles in pre-mixed laminar flames. Journal of Chemical Physics 22:145-146. 1954.

44. Quenouille, M. H. Introductory statistics. London, Pergamon, 1950. 248 p.
45. Rosen, P. Potential flow of a fluid into a sampling probe. Silver Springs, Maryland, John Hopkins Applied Physics Laboratory. 1954. (Report No. CF-2248) (Cited in: Fristrom, R. M. and A. A. Westenberg. Flame structure. New York, McGraw-Hill, 1965. 424 p.)
46. Saltsman, B. E. Determination of nitrogen dioxide and nitric oxide: Saltsman method. Selected methods for the measurement of air pollutants. Washington, D. C., 1965. 54 p. (U. S. Public Health Service. P. H. S. Publication No. 999-AP-1.)
47. Simon, D. M. Flame propagation: active particle diffusion theory. Industrial Engineering Chemistry 42:2718-2721. 1951.
48. Simon, D. M. and F. E. Belles. An active particle diffusion theory of flame quenching for laminar flames. 1952. 24 p. (NACA Report RM 51 L18)
49. Smith, S. R. and A. S. Gordon. Studies of diffusion flames. I. The methane diffusion flame. Journal of Physical Chemistry 60:759-763. 1956.
50. Tine, G. Gas sampling and chemical analysis in combustion processes. London, Pergamon, 1961. 94 p. (North Atlantic Treaty Organization, Advisory Group for Aeronautical Research and Development. AGARDograph 47)
51. von Karman, T. The present status of the theory of laminar flame propagation. In: Proceedings of the Sixth International Symposium on Combustion. New York, Reinhold, 1957. p. 1-11.
52. von Karman, T. and G. Millan. Thermal theory of a laminar flame front near a cold wall. In: Proceedings of the Fourth International Symposium on Combustion. Baltimore, Williams and Wilkins, 1953. p. 173-177.
53. von Karman, T. and S. S. Penner. Fundamental approach to laminar flame propagation. In: Selected combustion problems. Part 1. Fundamentals and aeronautical applications. London, North Atlantic Treaty Organization, Advisory Group for Aeronautical Research and Development, 1954. p. 5-41.

54. Westenberg, A. A. and S. Favin. Complex chemical kinetics in supersonic nozzle flow. In: Proceedings of the Ninth International Symposium on Combustion. New York, Academic, 1963. p. 785-798.
55. Westenberg, A. A. and R. M. Fristrom. Methane-oxygen flame structure. II. Conservation of matter and energy in the one-tenth atmosphere flame. Journal of Physical Chemistry 23:1875-1880. 1960.
56. Westenberg, A. A., S. D. Raezer and R. M. Fristrom. Interpretation of the sample taken by a probe in a laminar concentration gradient. Combustion and Flame 1:467-478. 1957.
57. Wohl, K. Quenching, flash-back, blow-off--theory and experiment. In: Proceedings of the Fourth International Symposium on Combustion. Baltimore, Williams and Wilkins, 1953. p. 68-89.

APPENDICES

APPENDIX A

QUARTZ SAMPLING PROBE TECHNIQUE

The basic requirements of a sampling probe are: (1) must not disturb flame structure and (2) must quench gas sample rapidly to prevent further chemical reaction.

Aerodynamic Disturbance

Aerodynamic flow in the flame front may be disturbed by the wake of the probe and by the fact that there is sample withdrawal. Actually, these effects tend to cancel so that a small tapered probe introduced along the streamlines from the hot side of the flame gives no visual disturbance.

Rosen (45) has considered, using a disc-sink model and incompressible flow approximation, the disturbance due to sample withdrawal alone. This theoretical treatment indicated that the disturbance would be about 0.05 millimeters, which is not a serious aerodynamic disturbance. This general behavior has been confirmed experimentally by Fristrom (24) using Schlieren photography of the flow into a probe.

Westenberg (56) has considered the probe orifice to act theoretically as a point-sink rather than a disc-sink. The results indicated only a very slight aerodynamic disturbance; the sample

entering the sink has a composition which differs only very slightly from that at the same point in the unperturbed (no sink) case.

Thermal Effects

A probe represents a heat sink which can disturb the flame by reducing the temperature and enthalpy in the region being sampled. Since the thermal conductivity of quartz is low, radiation is the primary heat-loss mechanism. According to Fristrom (27), at 2000°K in the region of the tip, rough calculations indicate that less than one percent of the sample enthalpy would be extracted prior to sampling. This would lower the temperature by less than 20°K. Since the effect varies at T^4 , it would be less than 1°K at 1000°K and negligible below that point. Fristrom (24) confirmed the qualitative correctness of these calculations by measuring the surface temperature of a quartz probe, which was only 50°K below the gas temperature of 2000°K.

Catalytic Effects

A probe is a solid surface in a gaseous reacting system. Its presence might accelerate or inhibit chemical reactions and thus affect the flame structure and chemical composition of the gas samples. The subject of heterogeneous catalysis is very complex. However, Fristrom and Westenberg (27) point out that for the specific

catalysis of the recombination of labile atoms such as are present in flames, quartz is known to have a very low activity even at high temperatures. Thus, a quartz probe would probably have little or no effect in this way.

Quenching of Reactions

The probe must quench chemical reactions if it is to provide a meaningful sample. This is accomplished by rapidly reducing the sample pressure and temperature to conditions where the kinetic rate constants are extremely small. Critical flow sampling through a small orifice satisfies this requirement.

The internal aerodynamic considerations of probe sampling as related to quenching are quite complex, involving such areas as viscous effects, boundary layer, effects of wall reactions, and heat transfer. Fristrom, Prescott and Grunfelder (24) have considered this problem for sampling from a 1/4-atmosphere flame. It was assumed that the orifice was sonic and the sample was in thermal equilibrium with the walls. It was reported that the sample pressure dropped to 0.1 of its initial value in five microseconds and that the sample entered the cold part of the probe in a fraction of a millisecond. It was, therefore, concluded that such a sampling process should have only a negligible effect on stable flame species.

Minkoff (39) has indicated that the overall reaction to be quenched

is regarded as having a half-life of the order of 500 microseconds. Since the quenching lag is only of the order of five microseconds, there appears to be no difficulty.

The justification of an experimental technique is usually demonstrated when experimental data compare favorably to some accepted theory. For a sampling probe the latter does not exist. However, analytical work which has some elements in common and would therefore support the probe technique, has been reported for flow of reacting gases in supersonic nozzles and wind tunnels (6, 12, 54). Westenberg and Favin (54) cite an example in supersonic nozzle flow where quenching of carbon monoxide and hydrogen occurs after about 50 microseconds. At this point, the gas temperature was one-half its original value and the pressure had dropped 20-fold.

Sample Interpretation

The sample taken by a quartz probe represents the composition at the sampling point. This has been verified by direct comparison with known values (19, 23, 24).

APPENDIX B

RADIATION LOSS CORRECTION FOR
THERMOCOUPLE READINGS

The following expression for radiation loss correction is closely derived from those of Friedman (17) and Klaukens (35).

Since the thermocouple wires adjacent to the thermocouple junction are exposed to the same temperature region in the flat flame, conduction losses for the junction are minimized and, therefore, neglected in this development. The energy balance then can be written as:

$$\begin{array}{lcl} \text{Heat transferred to the} & & \text{Heat radiated from the} \\ \text{thermocouple from the} & = & \text{thermocouple to the} \\ \text{flame} & & \text{surroundings} \end{array}$$

Assuming that heat is transferred from the flame to the thermocouple by convection only and neglecting conduction losses, then

$$hA(T_{\text{flame}} - T_{\text{couple}}) = \sigma AFe (T_{\text{couple}}^4 - T_{\text{surroundings}}^4) \quad (\text{B-1})$$

where,

h convective heat transfer coefficient.

σ Stefan-Boltzman constant.

F view factor of couple to surroundings.

e emissivity of junction.

A area of couple.

T absolute temperature.

Now noting that $T_{\text{couple}} \gg T_{\text{surroundings}}$ then $T_{\text{couple}}^4 \gg T_{\text{surroundings}}^4$.

Therefore, $T_{\text{surroundings}}$ may be neglected.

Since,

$$F = 1.0$$

then,

$$h(T_{\text{flame}} - T_{\text{couple}}) = e \sigma T_{\text{couple}}^4 \quad (\text{B-2})$$

If the thermocouple bead is assumed to be a sphere, the Nusselt Number can be taken equal to 2.0 when the Reynolds Number is less than 3.0. This has been obtained analytically by Johnstone (33).

$$\text{Nu} = \frac{hd}{k} \text{ by definition}$$

therefore

$$h = \frac{2.0 k}{d} \quad (\text{B-3})$$

where,

d diameter of couple.

k thermal conductivity of gas.

Substituting Equation (B-3) into Equation (B-2) we obtain Equation (B-4). Rearranging terms gives Equation (B-5).

$$\frac{2.0k}{d} (T_{\text{flame}} - T_{\text{couple}}) = e \sigma T_{\text{couple}}^4 \quad (\text{B-4})$$

$$T_{\text{flame}} = T_{\text{couple}} + \frac{e \sigma d}{2k} T_{\text{couple}}^4 \quad (\text{B-5})$$

where,

$e = 0.50$ for green ceramic NBS A-418.

$e = 0.80$ for silica.

Equation (B-5) was used to correct thermocouple readings for radiation loss. Thermal conductivity values from Kreith (36) for nitrogen were used. This is justified in that nitrogen is the predominant specie present. Furthermore, carbon dioxide and carbon monoxide, the other two major species present, possess thermal conductivities almost identical to that of nitrogen.

APPENDIX C

CALIBRATION OF DISA MODEL 55 A01
HOT-WIRE ANEMOMETER

The Disa Model 55 A01 anemometer equipped with a Type 55 A22 probe was calibrated using a Scott Model 9005A wind tunnel, a small pitot tube, and a Pace Model KP15 pressure transducer. Applying Bernoulli's theorem to the pitot tube, Equation (C-1) is obtained.

$$V = \sqrt{\frac{2gP_s}{W}} \quad (C-1)$$

where,

V velocity, fps.

g gravity term.

W unit weight of gas, lbs/ft³.

P_s stagnation pressure, lbs/ft².

The pitot technique is not sensitive at air velocities below about ten feet per second. Fortunately, a linear relationship exists for the hot-wire instrument. Thus a hot-wire may be calibrated at higher velocities with a pitot tube and then used directly as a flow velocity indicator in the very low velocity range. This technique was used to determine the linear relationship between (bridge voltage)² and (velocity)^{1/2}.

Calibration data for the Disa instrument are given in Table C-1. The standard statistical linear regression method described by Li (38) was used to obtain the estimated line of regression. The estimated regression line and the 95 percent confidence limits for the two population parameters are as follows:

Population equation:

$$\mu_{y \cdot x} = \alpha + \beta(x - \bar{x})$$

Estimated line of regression:

$$\bar{Y}_x = 58.20 + 6.09(x - \bar{x})$$

95 percent confidence interval for α :

$$57.58 < \alpha < 58.82$$

95 percent confidence interval for β :

$$5.39 < \beta < 6.79$$

Table C-1. Calibration data for Disa Model 55 A01 anemometer.

$(\text{Bridge Voltage})^2$	$(\text{Air Velocity})^{1/2}$
46.24	3.68
49.70	3.89
51.84	4.24
53.29	4.51
54.02	4.74
55.50	4.89
57.00	5.02
58.22	5.32
59.29	5.54
60.68	5.71
61.62	5.88
62.57	6.04
63.84	6.28
64.80	6.44
65.93	6.65
66.74	6.82

APPENDIX D

OPERATION AND CALIBRATION OF PERKIN-ELMER
MODEL 810 GAS CHROMATOGRAPH

The flame ionization detector (FID) of the Perkin-Elmer Model 810 gas chromatograph gives a linear response to hydrocarbons. Thus only one upscale calibration point is needed. Upscale calibration gases for methane, ethane, ethylene, propane, propylene and acetylene were obtained from Scott Research Laboratories in Perkasié, Pennsylvania.

As illustrated in Figure 7, known quantities of calibration gas were metered to the gas sampling valve and then sent to the gas chromatograph. The chromatograph output signal drove the Honeywell Electronik 15 recorder. A Disc Model 201-B instrument integrated this signal with time. This integrated output is directly proportional to the hydrocarbon concentration. Thus, the instrument is effectively calibrated if (1) sample size, (2) sample pressure and temperature, and (3) constituent concentrations are all known. Typical calibration curve is shown in Figure D-1.

Unfortunately the FID response is sensitive to the hydrogen and air flow rates. All combinations of hydrogen at 5, 7.5, 10, 12.5, 15 and 20 psig and air at 30, 35, 40 and 45 psig were tested. The optimum performance occurred with the hydrogen regulator set

22 November 1967

Operating conditions:

oven 75°C
detector 100°C
air 40 psig
hydrogen 7.5 psig
nitrogen 80 psig

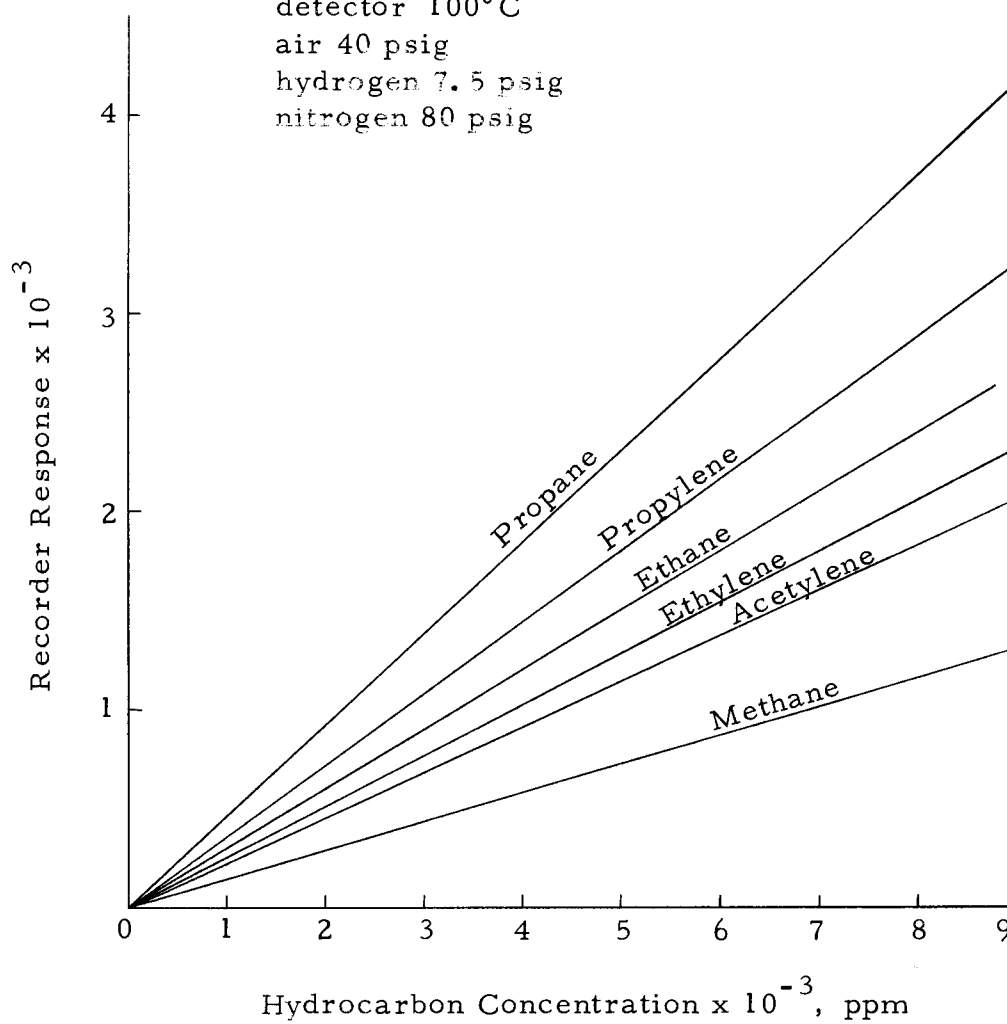


Figure D-1. Hydrocarbon calibration curves for Perkin-Elmer Model 810 gas chromatograph.

at 7.5 psig and the air at 40 psig. These conditions, which were typical of the range suggested by the manufacturer, were used throughout the test program.

A column containing di-2-ethylhexyl sebacate liquid phase, 1.5 weight percent on 30 - 60 mesh silica gel, was used to separate the various hydrocarbons in the gas sample. Nitrogen carrier gas flow rate was set at the manufacturer's recommended value of 35 ml per minute. A number of tests were made to determine the best isothermal oven temperature for adequate component separation and minimal analysis time. It was found that 75°C provided satisfactory hydrocarbon separation and yielded an acceptable total analysis time of 16 minutes.

APPENDIX E

CALIBRATION OF BECKMAN CARBON MONOXIDE
AND CARBON DIOXIDE ANALYZERS

The calibration curves for Beckman carbon monoxide and carbon dioxide analyzers are not expected to be linear. It is, therefore, important to be able to produce several calibration points. Since the infrared analyzers count molecules and are insensitive to the partial pressures of other species, this was achieved with the use of one upscale calibration gas. The mixture, containing carbon monoxide, carbon dioxide and nitrogen, was obtained from Scott Research Laboratories in Perkasie, Pennsylvania.

Referring to Figure 7, the upscale calibration gas was metered into the analytical system to give different total pressures of the same gaseous mixture. This produced the same instrument response as if several different calibration mixtures were available and were each in turn put into the system at the same total pressure. Typical calibration curves obtained in this manner are shown in Figures E-1 and E-2.

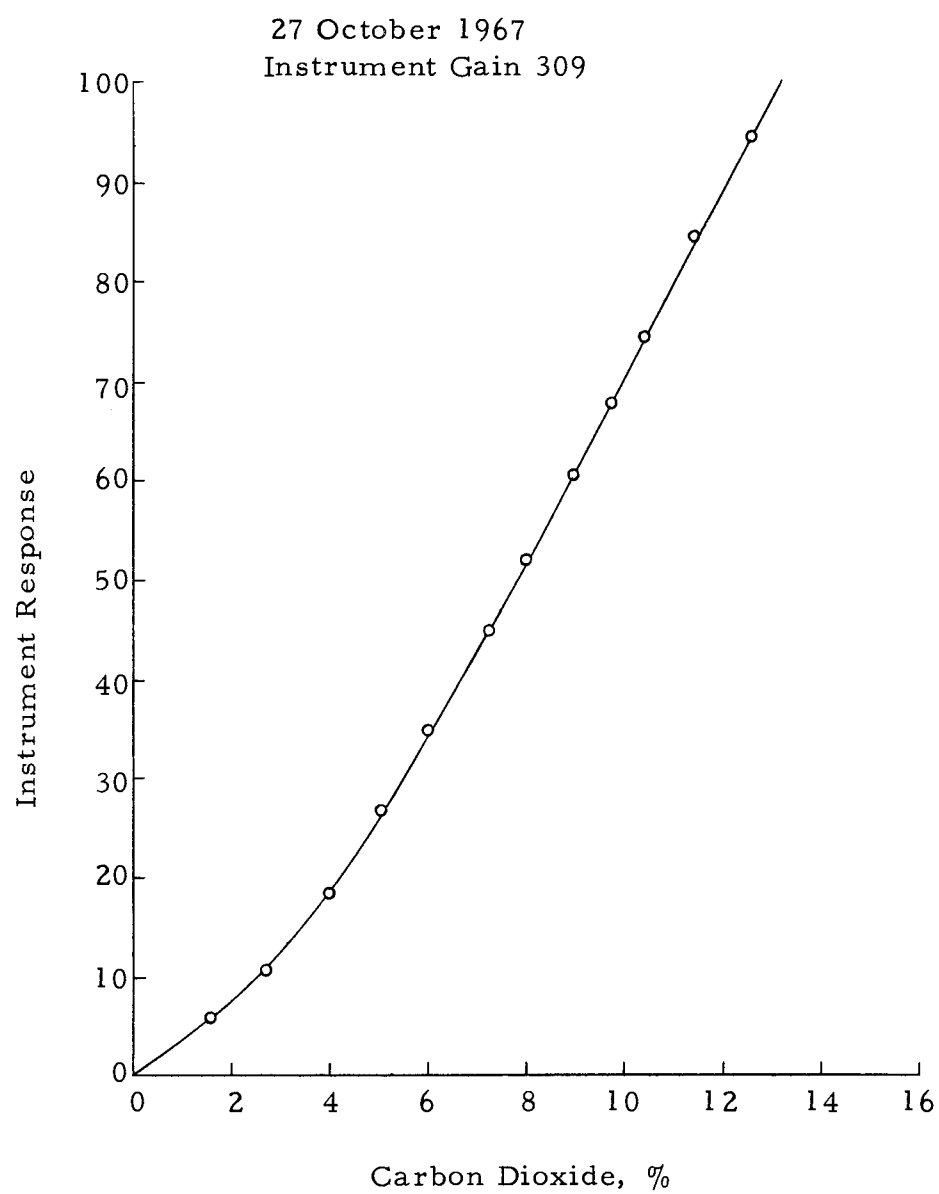


Figure E-1. Carbon dioxide calibration curve.
Beckman IR-215.

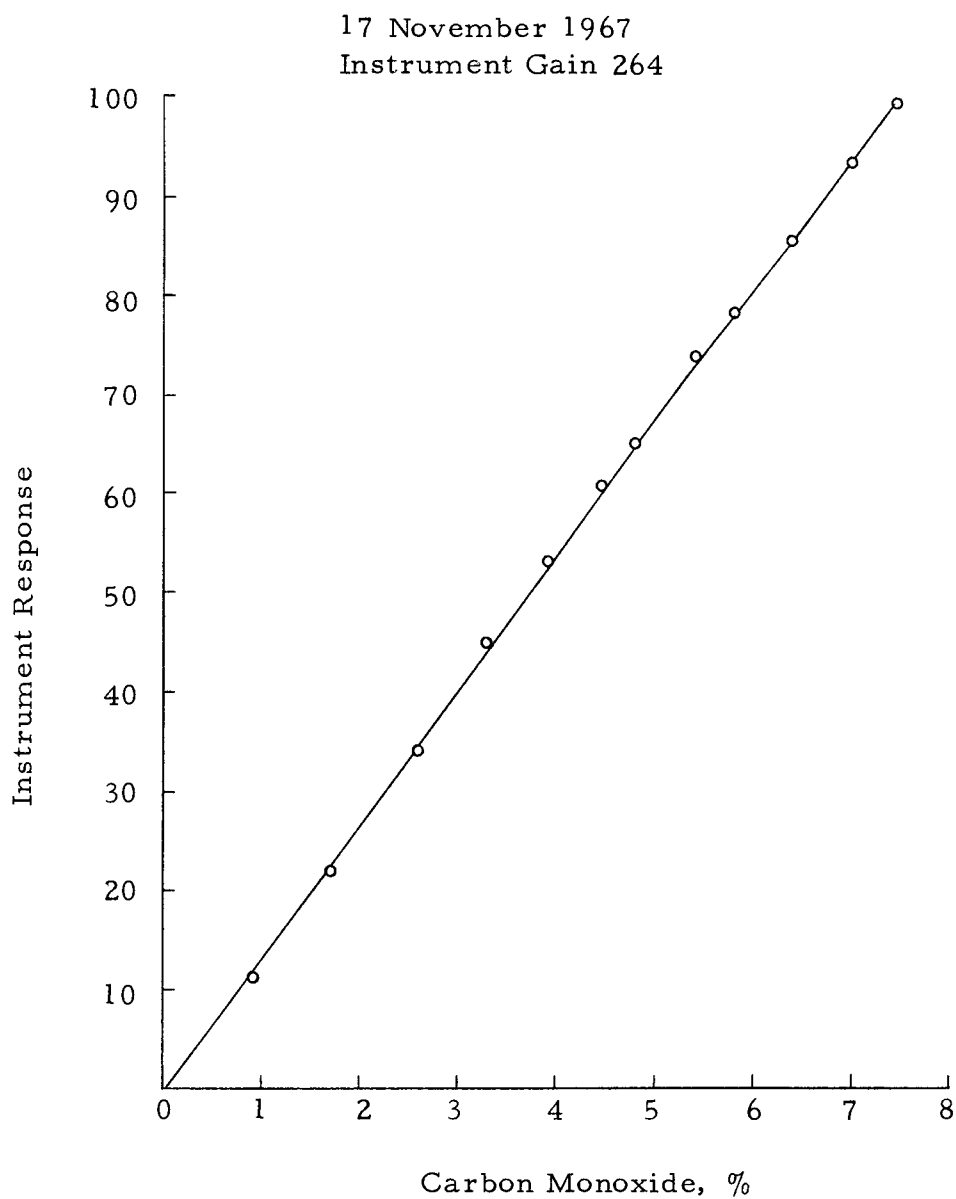


Figure E-2. Carbon monoxide calibration curve.
Beckman IR-15A.

CONSTRUCTION DETAILS OF TEST EQUIPMENT

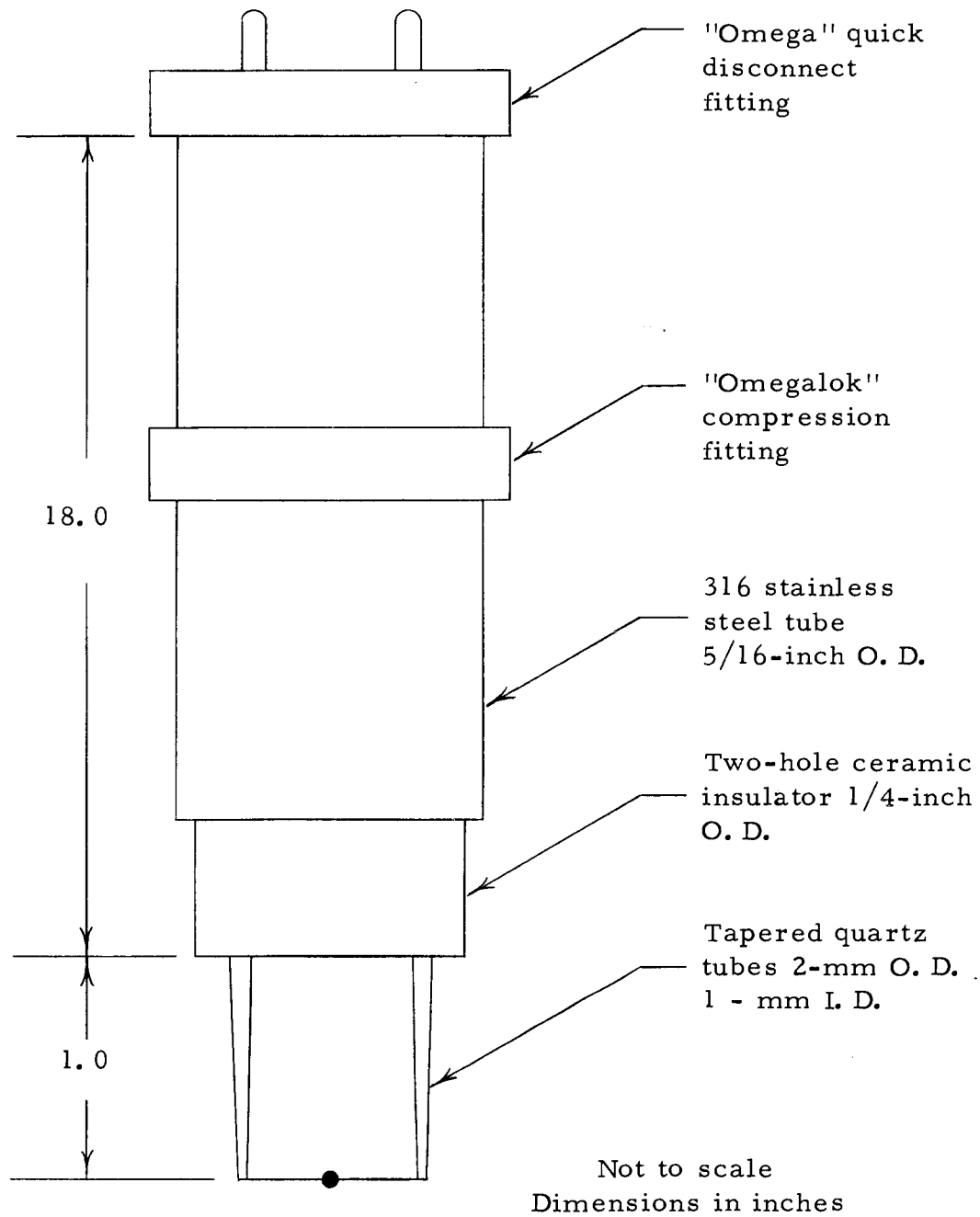


Figure F-1. Details of thermocouple probe.

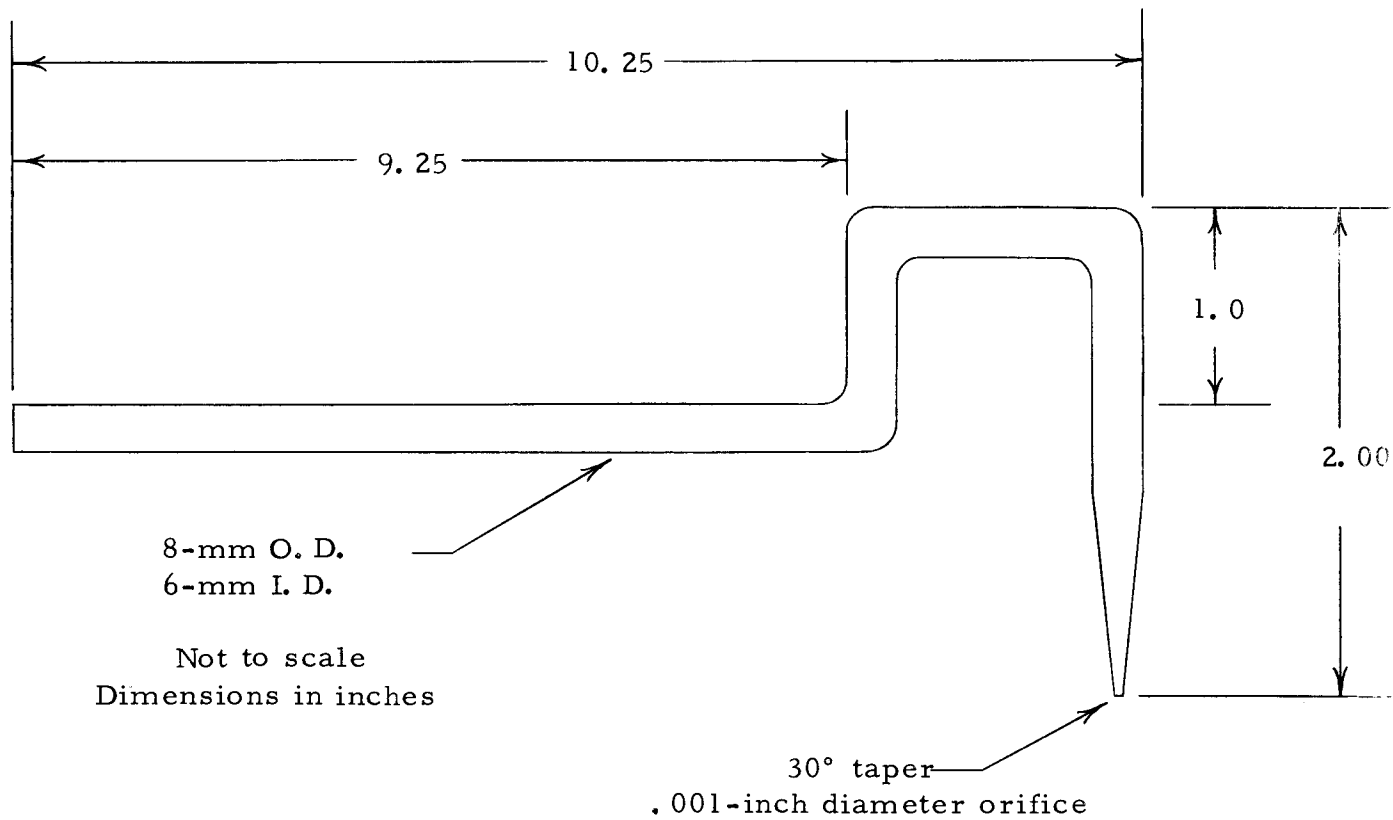
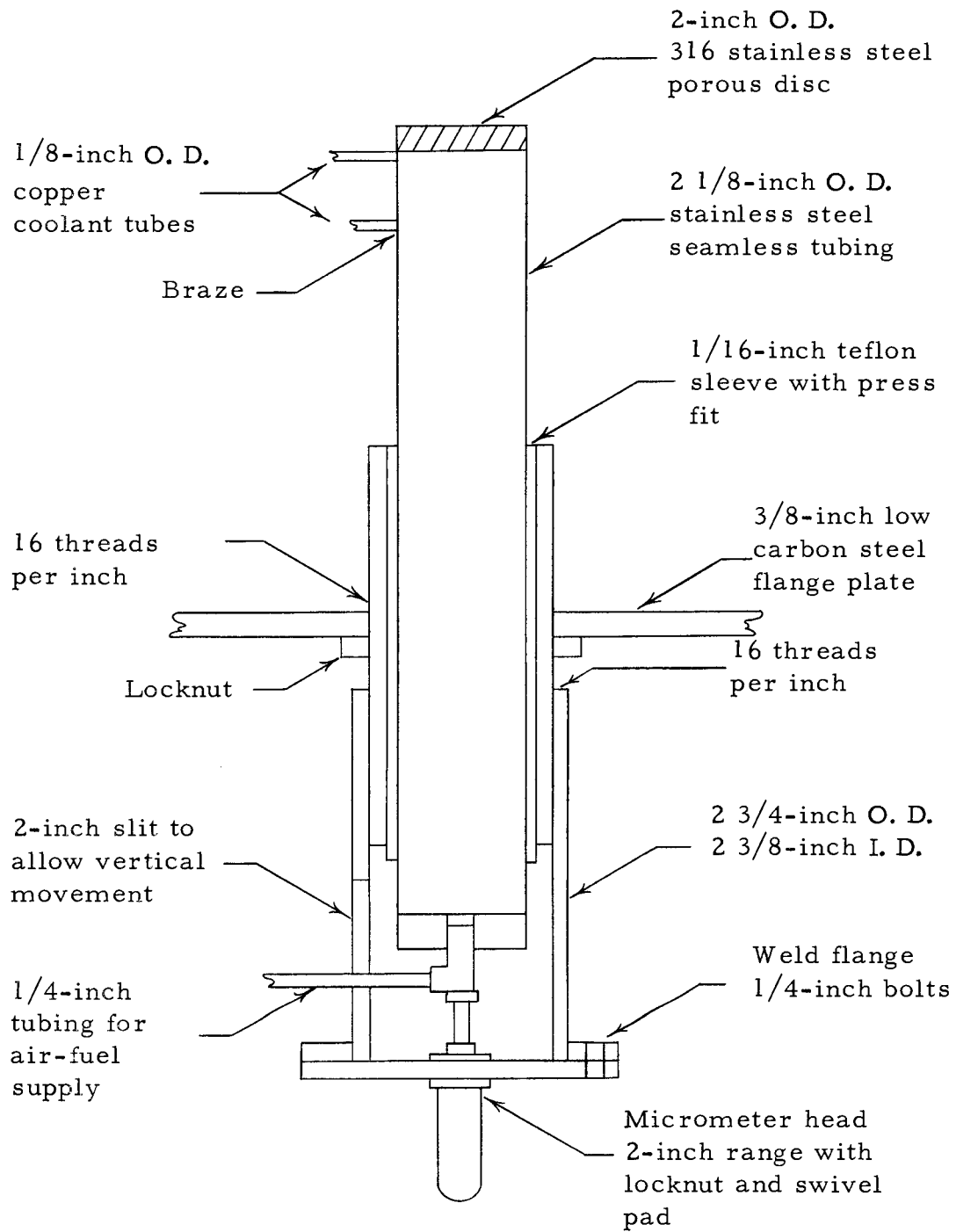


Figure F-2. Details of quartz sampling probe.



Not to scale

Figure F-3. Details of burner assembly.

APPENDIX G

DETERMINATION OF AIR AND FUEL MASS FLOW RATES

Equation (3-1) is derived from Bernoulli's equation by basing the energy relation on the specific weight at the upstream condition and introducing an expansion factor. This development is described by Beckwith and Buck (1).

Although a number of orifice plates were used in preliminary tests, the 0.010 and 0.035 inch diameter orifices were used for the fuel and air flowmeter respectively. These plates were very satisfactory in that they (1) allowed the desired flowrates, (2) produced measurable pressure drops and (3) allowed critical flow conditions to be maintained across the metering valves. The orifice flowmeters were calibrated with bubble flowmeters which were fabricated from laboratory burettes. The calibration data are given in Tables G-1 and G-2.

Table G-1. Calibration of air flowmeter for Equation (3-1).

Run	$m \times 10^4 \text{ lbs/sec}$	$K \times 10^4$
1	1.061	1.643
2	1.165	1.655
3	1.253	1.652
4	1.285	1.638
5	1.358	1.654
6	1.450	1.655
7	1.475	1.647
8	1.580	1.652
9	1.684	1.648
10	1.709	1.651
11	1.832	1.642
12	1.936	1.649
13	2.083	1.644
Mean:	$\bar{x}_K = 1.648 \times 10^{-4}$	
Standard deviation:	$S = 0.005 \times 10^{-4}$	
95 percent confidence limits:	$1.645 \times 10^{-4} < \mu_K < 1.651 \times 10^{-4}$	

Table G-2. Calibration of fuel flowmeter for Equation (3-1).

Run	$m \times 10^5 \text{ lb/sec}$	$K \times 10^5$
1	1.345	1.745
2	1.378	1.750
3	1.399	1.749
4	1.456	1.754
5	1.510	1.760
6	1.542	1.763
7	1.562	1.751
8	1.610	1.763
9	1.639	1.771
10	1.689	1.776
11	1.743	1.771
Mean:	$\bar{x}_K = 1.759 \times 10^{-5}$	
Standard deviation:	$S = 0.010 \times 10^{-5}$	
95 percent confidence limits:	$1.752 \times 10^{-5} < \mu_K < 1.766 \times 10^{-5}$	

APPENDIX H

CALIBRATION OF PACE MODEL KP 15
PRESSURE TRANSDUCERS

The Pace Model KP 15 pressure transducer gives a linear output and, therefore, need be calibrated at only one upscale point. A hydraulic dead weight tester provided the upscale value for the Pace unit which monitored the fuel and air upstream pressures. A column of water provided the known upscale value for the Pace unit which monitored the pressure drop across the orifice plates. A vacuum manometer was used to calibrate the Pace unit which measured the gas pressure in the sampling system. The following general procedure was used to calibrate the Pace transducers.

1. Place appropriate diaphragm in KP 15 transducer.
2. Turn on instrument.
3. Set "zero" on CD 25 transducer indicator panel meter.
4. Set meter sensitivity switch to "suppression in" 100.
5. Apply known fullscale pressure and set null meter to read 1000.
6. Adjust "span" to give zero meter reading.
7. Change meter sensitivity to "suppression in" 10.
8. Make fine adjustment to give zero meter reading.
9. Record "zero" and "span" settings.

APPENDIX I

ONE-DIMENSIONAL FLAME EQUATIONS

The one-dimensional flame equations have been obtained and presented by Fristrom and Westenberg (27). They are summarized here mainly so that one may view the presented experimental data in light of an analytical model. No attempt is made to detail the derivations here, however, the main assumptions are listed.

Assumptions

The laminar flame is conveniently described by considering the following basic equations: (1) conservation of mass, (2) conservation of momentum, (3) conservation of energy, and (4) equation of state for ideal gas. In applying these equations to a flame a number of assumptions and approximations must be used. The major ones are briefly as follows:

1. Steady-state flow exists.
2. Effects due to external forces such as gravity, electric and magnetic fields, etc. are neglected.
3. Radiation heat loss from flame by either thermal origin or chemiluminescence is negligible.
4. Velocity gradients are small and may be neglected; therefore, viscosity terms in momentum and energy

equations may be neglected.

5. Since velocities are low, pressure gradients may be ignored. Thus treat as constant pressure system.
6. High temperature gradients exist and, therefore, heat conduction term in energy equation must be included.
7. Concentration gradients exist and, therefore, diffusion should be included in equations of continuity and energy.
8. Pressure diffusion may be neglected.
9. Thermal diffusion is neglected. This is done because of the complexity of the subject and the lack of data for thermal diffusion coefficients.

Notation for Flame Equations

a_0	area of flame at flame zone.
ρ_0	gas density at flame zone.
v_0	flame velocity.
m	mass flow rate.
A	area ratio, a/a_0 .
R	molar gas constant.
P	pressure.
T	temperature.
Z	distance, independent variable.
N_i	moles of specie i per unit volume.

X_i	mole fraction of specie i.
V_i	diffusion velocity of specie i.
D_{ij}	binary diffusion coefficient.
λ	thermal conductivity.
f_i	mass fraction of specie i.
Q	volumetric heat release rate.
n_i	number of a particular kind of atom in specie i.
\overline{M}	mean molecular weight.
M_i	molecular weight of specie i.
G_i	mass flux fraction of specie i.
K_i	net molar rate of production or consumption of specie i per unit volume per unit time due to chemical reaction.
H_i	molar enthalpy of specie i.
\hat{H}_∞	specific enthalpy at $Z = \infty$.

One-dimensional Laboratory Flame Equations

Conservation of Mass:

$$\rho v a = \rho_0 v_0 a_0 \quad (I-1)$$

or

$$\rho v A = \rho_0 v_0 = m$$

Species Continuity Equation: .

$$\frac{d}{dZ} [N_i(v + V_i)A] = K_i A \quad (I-2)$$

if G_i , the mass flux fraction, is defined as:

$$G_i = \frac{N_i M_i (v + V_i)}{\rho v} \quad (I-3)$$

then,

$$\frac{\rho_0 v_0}{M_i} \frac{dG_i}{dZ} = K_i A \quad (I-4)$$

where G_i represents the fraction of the total mass flux per unit area which is due to species i and it includes the contribution of diffusion as well as convection.

Energy Equation:

$$\rho_0 v_0 \sum \frac{H_i G_i}{M_i} - A \lambda \frac{dT}{dZ} = \rho_0 v_0 \hat{H}_\infty \quad (I-5)$$

Diffusion Equation:

$$V_i = - \frac{D_{ij}}{X_i} \frac{dX_i}{dZ} \quad (I-6)$$

Heat Release Rate:

$$Q = \sum H_i K_i \quad (I-7)$$

Equation of State:

$$P = NR T \quad (I-8)$$

Equation for Atom Balance:

$$\sum_i \frac{n_i G_i}{M_i} = \text{constant} \quad (I-9)$$

Equation for Mass Fraction:

$$f_i = X_i \frac{M_i}{\overline{M}} \quad (I-10)$$

APPENDIX J

METHOD FOR CALCULATING BINARY
DIFFUSION COEFFICIENTS

The following expressions were taken from the works of
Fristrom and Westenberg (27) and Hirschfelder (31).

Chapman-Enskog Equation

The Chapman-Enskog kinetic theory of dilute gases provides
Equation (J-1).

$$D_{ij} = \frac{3(kT)^2}{16 P \mu \Omega_{ij}^{(1,1)}} \quad (J-1)$$

where

k Boltzmans constant.

T Temperature, °K.

P pressure, atmospheres.

μ reduced mass of pair of molecules.

D_{ij} binary diffusion coefficient, cm^2/sec .

$\Omega_{ij}^{(1,1)}$ collision integral.

Assumptions of Chapman-Enskog Theory

1. The gradients in the macroscopic variables of the flame
(temperature, density, etc.) are small over distances
which are large when compared with the mean free path.

2. The densities of the gases are low enough that only the binary collisions need be considered (i. e. no appreciable amount of three body or higher multicomponent reactions).
3. The gas is composed of particles which undergo elastic collisions.
4. Particle collisions may be treated according to classical mechanics.

Calculation of Diffusion Coefficients

The collision integral in Equation(J-1) involves the potential energy of interaction between molecules. The potential function most widely used for transport property calculations is the Lennard-Jones (12-6) Potential which is shown as Equation J-2.

$$\phi(r) = 4e \left[\left(\frac{\sigma}{r}\right)^{12} - \left(\frac{\sigma}{r}\right)^6 \right] \quad (J-2)$$

where

r intermolecular separation distance.

σ value of r for which $\phi = 0$.

e depth of potential "well".

These two terms are illustrated graphically in Figure J-1.

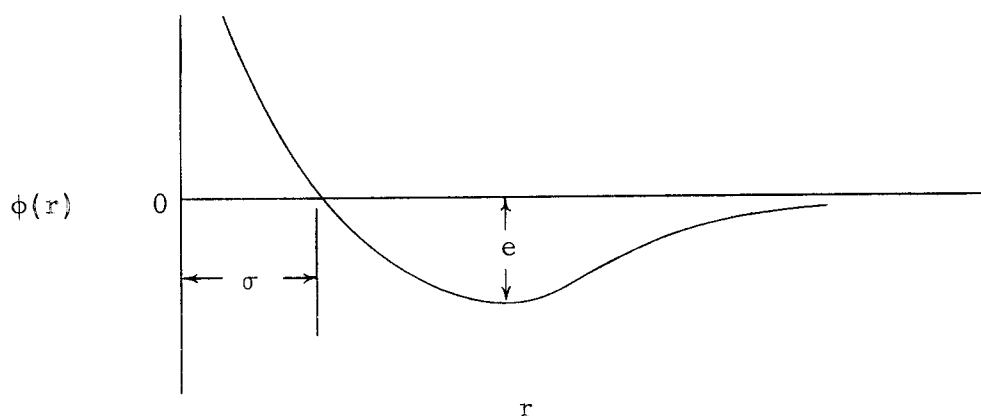


Figure J-1. Parameters of Lennard-Jones Potential

The collision integrals for the Lennard-Jones Potential have been evaluated by Hirschfelder (31) in terms of the reduced quantity $\Omega_{ij}^{(1,1)*}$ obtained by dividing $\Omega_{ij}^{(1,1)}$ by

$$\sigma^2 \left(\frac{\pi kT}{2\mu} \right)^{1/2}$$

which is the corresponding integral for the rigid sphere model.

$$\Omega_{ij}^{(1,1)*} = \left(\frac{2\mu}{\pi kT} \right)^{1/2} \frac{\Omega_{ij}^{(1,1)}}{\sigma^2} \quad (\text{J-3})$$

The above is given as a function of the reduced temperature

$$T^* = \frac{kT}{e}$$

Thus,

$$D_{ij} = \frac{1.86 \times 10^{-3} \left[\frac{M_i + M_j}{M_i M_j} \right]^{1/2} T^{3/2}}{P \sigma_{ij}^2 \Omega^{(1,1)*}} \quad (J-4)$$

where M_i and M_j are molecular weights.

In order to make use of this equation it is necessary to have values of parameters for the potential characteristic for the particular pair of gases being considered. The commonly used method for combustion work is to use potential parameters for the pure gases which have been determined from viscosity data and certain combining rules by which the parameters for the interaction of unlike molecules may be estimated from those for the respective species making up the diffusion pair. Hirschfelder (21) has used experimental gas viscosity data to derive values for the potential parameters in the Lennard-Jones Potential. These are shown in Table J-1. The potential parameters determined in this manner are characteristic of like molecule interactions ($i - i$, $j - j$). It is assumed that an unlike potential ϕ_{ij} is related to the potential for the pure species by

$$\phi_{ij} = (\phi_{ii} \phi_{jj})^{1/2} \quad (J-5)$$

Table J-1. Potential parameters for Lennard-Jones (12-6) Potential.

Gas	σ , Angstroms	e/k , °K
Methane	3.80	144
Ethane	4.42	230
Ethylene	4.23	205
Propane	5.06	254
Acetylene	4.22	185
Propylene	4.68	299
Carbon Monoxide	3.71	88
Carbon Dioxide	3.90	213
Nitric Oxide	3.60	91
Oxygen	3.54	88
Nitrogen	3.79	80
Water Vapor	2.64	809

With this assumption it may be shown that for the Lennard-Jones Potential

$$e_{ij} = (e_{ii}e_{jj})^{1/2} \quad (J-6)$$

$$\sigma_{ij} = \frac{1}{2} (\sigma_{ii} + \sigma_{jj}) \quad (J-7)$$

now, binary diffusion coefficients for flame conditions may be calculated using Equation (J-4).

APPENDIX K

EXPERIMENTAL DATA

Table K-1. Dependent variable responses for fuel: propane; equivalence ratio: 0.90; and wall temperature: 600°F.

Dead Space Thickness <u>0.083</u> cm				Flame Zone Thickness <u>0.082</u> cm			Hydrocarbon Distance <u>0.255</u> cm			
Position cm	Methane ppm	Ethane ppm	Ethylene ppm	Propane ppm	Acetylene ppm	Propylene ppm	Carbon Monoxide %	Carbon Dioxide %	Oxides of Nitrogen ppm	Gas Temperature °F
.005	800	125	1525	27750	175	201	2.5	5.3	1.5	----
.035	1025	225	1925	25000	225	250	2.9	6.1	2.5	----
.065	1225	275	2250	22000	302	303	3.3	6.3	2.0	----
.095	1400	287	2600	18250	525	325	3.6	6.8	2.0	----
.125	1570	300	3020	13200	932	410	4.0	7.6	2.5	----
.140	1655	280	3270	10100	1172	483	4.1	7.9	2.0	----
.155	1710	264	3480	7250	1370	553	4.3	8.4	2.5	----
.170	1560	220	3490	4900	1215	530	4.5	8.9	3.0	2135
.185	1010	185	3075	3100	760	380	4.6	9.6	3.5	2125
.200	505	105	1210	1700	355	223	4.7	10.1	6.0	2120
.215	155	43	270	650	80	70	4.8	10.5	16.5	2110
.230	65	25	105	330	45	50	4.7	10.7	21.0	2110
.245	24	15	44	190	21	23	4.7	10.8	22.0	2100
.255	Trace	Trace	Trace	Trace	Trace	Trace	4.6	10.8	23.0	2100
.275	0	0	0	0	0	0	4.6	10.9	24.0	2090
.305	0	0	0	0	0	0	4.5	10.9	26.0	2070
.335	0	0	0	0	0	0	4.3	10.9	27.5	2060
.385	0	0	0	0	0	0	4.2	11.0	29.5	2050

Table K-2. Dependent variable responses for fuel: propane; equivalence ratio: 0.90; and wall temperature: 700°F.

Dead Space Thickness <u>0.060</u> cm				Flame Zone Thickness <u>0.081</u> cm			Hydrocarbon Distance <u>0.220</u> cm			
Probe Position cm	Methane ppm	Ethane ppm	Ethylene ppm	Propane ppm	Acetylene ppm	Propylene ppm	Carbon Monoxide %	Carbon Dioxide %	Oxides of Nitrogen ppm	Gas Temperature °F
.005	705	210	1610	25250	105	100	2.3	5.5	1.0	----
.035	820	255	1870	23200	207	170	2.6	6.0	1.5	----
.065	955	280	2120	20750	323	295	3.0	6.4	1.5	----
.095	1153	365	2515	15500	486	445	3.3	7.0	2.0	----
.110	1305	418	2910	12100	566	506	3.5	7.4	2.5	----
.125	1395	472	3250	8300	705	655	3.7	7.8	2.5	----
.140	1440	470	3320	7340	805	812	3.8	8.2	3.0	----
.155	1360	374	2900	4900	795	815	3.9	8.6	3.5	2245
.170	920	247	1250	3040	515	564	4.0	9.2	4.5	2230
.185	280	110	453	1500	195	200	4.0	9.9	7.0	2220
.200	45	25	80	400	45	52	4.1	10.3	12.5	2210
.215	Trace	Trace	Trace	Trace	Trace	Trace	4.1	10.5	19.0	2200
.230	0	0	0	0	0	0	4.0	10.7	23.0	2200
.245	0	0	0	0	0	0	3.9	10.8	25.5	2195
.275	0	0	0	0	0	0	3.6	10.8	26.0	2190
.305	0	0	0	0	0	0	3.5	10.8	26.0	2180
.335	0	0	0	0	0	0	3.5	10.8	25.5	2175
.385	0	0	0	0	0	0	3.4	10.8	26.5	2170

Table K-3. Dependent variable responses for fuel: propane; equivalence ratio: 0.90; and wall temperature: 800°F.

Dead Space Thickness <u>0.045</u> cm				Flame Zone Thickness <u>0.098</u> cm				Hydrocarbon Distance <u>0.225</u> cm		
Probe Position cm	Methane ppm	Ethane ppm	Ethylene ppm	Propane ppm	Acetylene ppm	Propylene ppm	Monoxide %	Dioxide %	Oxides of Nitrogen ppm	Gas Temperature °F
.005	895	150	1870	25750	210	280	2.6	5.3	0.5	----
.035	1015	223	2095	22300	387	305	2.8	5.8	0.5	----
.065	1070	328	2200	19100	497	358	2.9	6.1	0.5	----
.095	1215	377	2677	15550	618	436	3.2	6.6	0.5	----
.110	1365	380	2900	12700	702	495	3.5	6.9	1.0	----
.125	1500	375	3210	10100	745	518	3.8	7.4	0.5	----
.140	1673	365	3440	7200	837	500	4.0	7.7	1.0	----
.155	1805	360	3655	6450	857	480	4.3	8.0	2.0	----
.170	1847	355	3750	4490	927	438	4.5	8.4	5.0	----
.185	1620	320	3380	2720	905	365	4.6	8.8	16.0	2175
.200	1370	230	2710	1490	827	246	4.6	9.4	19.5	2170
.215	780	97	1410	700	506	145	4.5	9.9	21.0	2170
.230	Trace	Trace	Trace	Trace	Trace	Trace	4.5	10.3	21.5	2160
.245	0	0	0	0	0	0	4.4	10.4	22.5	2150
.275	0	0	0	0	0	0	4.4	10.5	23.0	2140
.305	0	0	0	0	0	0	4.3	10.5	23.0	2125
.335	0	0	0	0	0	0	4.3	10.5	24.5	2100
.385	0	0	0	0	0	0	4.2	10.5	26.0	2075

Table K-4. Dependent variable responses for fuel: propane; equivalence ratio: 0.95; and wall temperature: 600°F.

Dead Space Thickness <u>0.073</u> cm				Flame Zone Thickness <u>0.082</u> cm			Hydrocarbon Distance <u>0.200</u> cm			
Probe Position cm	Methane ppm	Ethane ppm	Ethylene ppm	Propane ppm	Acetylene ppm	Propylene ppm	Carbon Monoxide %	Carbon Dioxide %	Oxides of Nitrogen ppm	Gas Temperature °F
.005	472	202	1372	25100	0	305	1.5	5.9	0	----
.035	563	247	1583	24260	0	344	1.7	6.2	0	----
.065	624	259	1791	22100	20	398	1.9	6.7	0	----
.095	695	341	2035	16800	105	520	2.0	7.3	0.5	----
.110	743	383	2191	14280	348	584	2.1	7.8	0.5	----
.125	817	415	2383	11420	522	638	2.3	8.3	0.5	----
.140	946	434	2577	8210	634	714	2.5	8.7	1.0	----
.155	1051	453	2684	4350	756	773	2.8	9.1	1.0	2320
.170	1004	346	2505	1520	790	648	3.1	9.8	1.5	2310
.185	703	202	1630	470	741	234	2.8	10.3	4.0	2295
.200	Trace	Trace	Trace	Trace	Trace	Trace	1.9	11.4	10.0	2290
.215	0	0	0	0	0	0	1.7	11.7	10.5	2283
.245	0	0	0	0	0	0	1.5	11.9	11.0	2271
.275	0	0	0	0	0	0	1.4	11.9	10.5	2249
.305	0	0	0	0	0	0	1.4	11.9	10.5	2221
.335	0	0	0	0	0	0	1.4	11.9	10.5	2201
.385	0	0	0	0	0	0	1.4	11.9	10.0	2162

Table K-5. Dependent variable responses for fuel: propane; equivalence ratio: 0.95; and wall temperature: 700°F.

Dead Space Thickness <u>0.058</u> cm				Flame Zone Thickness <u>0.085</u> cm			Hydrocarbon Distance <u>0.200</u> cm			
Probe Position cm	Methane ppm	Ethane ppm	Ethylene ppm	Propane ppm	Acetylene ppm	Propylene ppm	Carbon Monoxide %	Carbon Dioxide %	Oxides of Nitrogen ppm	Gas Temperature °F
.005	592	247	1670	23960	0	474	1.7	5.9	0	----
.035	621	259	1746	22100	15	485	1.8	6.4	0	----
.065	636	277	1841	19650	117	492	1.9	6.9	0	----
.095	683	310	2094	17020	259	506	2.0	7.4	0.5	----
.110	796	361	2323	14830	348	553	2.2	7.8	0.5	----
.125	902	397	2573	12300	391	615	2.4	8.2	1.0	----
.140	1005	502	2735	9240	421	741	2.5	8.6	1.5	----
.155	987	548	2682	5420	424	982	2.7	9.2	2.0	----
.170	884	647	2410	1120	345	484	2.9	9.9	3.5	2295
.185	602	681	1094	190	94	72	3.0	10.5	10.0	2284
.200	Trace	Trace	25	Trace	22	15	1.9	11.5	20.5	2272
.215	0	0	0	0	0	0	1.9	11.7	25.0	2261
.245	0	0	0	0	0	0	1.9	11.7	27.0	2247
.275	0	0	0	0	0	0	1.9	11.7	28.0	2233
.305	0	0	0	0	0	0	1.9	11.7	27.5	2218
.335	0	0	0	0	0	0	1.9	11.7	27.5	2197
.385	0	0	0	0	0	0	1.9	11.7	28.0	2158

Table K-6. Dependent variable responses for fuel: propane; equivalence ratio; 0.95; and wall temperature: 800°F.

Dead Space Thickness <u>0.048</u> cm				Flame Zone Thickness <u>0.095</u> cm			Hydrocarbon Distance <u>0.210</u> cm			
Probe Position cm	Methane ppm	Ethane ppm	Ethylene ppm	Propane ppm	Acetylene ppm	Propylene ppm	Carbon Monoxide %	Carbon Dioxide %	Oxides of Nitrogen ppm	Gas Temperature °F
.005	620	255	1672	23250	0	490	1.8	6.5	0.0	----
.035	625	275	1750	21430	0	515	1.9	6.8	0.5	----
.065	652	286	1807	19350	0	554	2.0	7.1	0.5	----
.095	727	322	2227	15850	0	582	2.1	7.6	1.0	----
.125	848	397	2510	11750	15	752	2.3	8.4	1.5	----
.140	902	419	2680	7700	70	857	2.4	8.9	1.7	----
.155	986	447	2803	4420	355	806	2.5	9.3	2.0	----
.170	1070	381	2615	1720	758	522	2.7	9.9	2.5	2260
.185	941	274	1595	510	850	127	3.0	10.2	4.0	2245
.200	606	106	503	Trace	590	Trace	2.6	10.9	15.0	2230
.215	0	0	0	0	0	0	1.8	11.4	26.0	2225
.245	0	0	0	0	0	0	1.4	11.8	27.0	2217
.275	0	0	0	0	0	0	1.3	11.8	27.5	2200
.305	0	0	0	0	0	0	1.3	11.9	26.5	2189
.335	0	0	0	0	0	0	1.3	11.9	27.0	2171
.385	0	0	0	0	0	0	1.3	11.9	27.5	----

Table K-7. Dependent variable responses for fuel: propane; equivalence ratio: 1.00; and wall temperature: 600°F.

Dead Space Thickness <u>0.058</u> cm				Flame Zone Thickness <u>0.083</u> cm			Hydrocarbon Distance <u>0.270</u> cm			
Probe Position cm	Methane ppm	Ethane ppm	Ethylene ppm	Propane ppm	Acetylene ppm	Propylene ppm	Carbon Monoxide %	Carbon Dioxide %	Oxides of Nitrogen %	Gas Temperature °F
.005	350	325	1320	24800	0	525	1.3	6.1	0	----
.035	380	334	1369	23600	0	545	1.4	6.4	0	----
.065	420	352	1482	22100	0	562	1.4	6.7	0	----
.095	465	379	1640	20200	18	604	1.5	7.1	0	----
.125	502	426	1853	17800	68	637	1.7	7.6	0.5	----
.155	582	465	2076	13650	195	870	1.8	8.4	0.5	----
.170	606	480	2195	11040	242	942	1.9	8.9	1.0	2305
.185	651	504	2325	8800	297	965	2.0	9.3	1.5	2285
.200	700	544	2450	6350	372	941	2.1	9.8	2.5	2275
.215	748	582	2502	3570	453	839	2.3	10.2	3.0	2267
.230	708	620	2305	1060	532	560	2.5	10.8	4.0	2259
.245	500	602	1200	300	562	151	2.4	11.3	10.5	2248
.260	225	210	265	170	225	44	1.5	11.5	18.0	2235
.275	0	0	0	0	0	0	0.9	11.7	19.5	2227
.305	0	0	0	0	0	0	0.8	11.7	18.5	2220
.335	0	0	0	0	0	0	0.8	11.7	19.0	2205
.385	0	0	0	0	0	0	0.7	11.7	19.5	2152

Table K-8. Dependent variable responses for fuel: propane; equivalence ratio: 1.00; and wall temperature: 700°F.

Dead Space Thickness <u>0.053</u> cm				Flame Zone Thickness <u>0.082</u> cm			Hydrocarbon Distance <u>0.205</u> cm			
Probe Position cm	Methane ppm	Ethane ppm	Ethylene ppm	Propane ppm	Acetylene ppm	Propylene ppm	Carbon Monoxide %	Carbon Dioxide %	Oxides of Nitrogen ppm	Gas Temperature °F
.005	370	198	1403	21820	0	570	1.2	6.8	0	----
.035	397	218	1475	20600	0	615	1.4	7.0	0	----
.065	442	235	1560	19030	0	648	1.5	7.3	0	----
.095	505	254	1784	16000	51	745	1.7	8.1	0.5	----
.125	610	302	2140	10700	177	837	1.9	9.3	0.5	----
.140	658	333	2302	4500	204	830	2.1	10.2	0.5	----
.155	599	310	2280	1550	235	603	2.2	10.8	1.5	----
.170	398	201	1530	650	254	240	2.0	11.3	2.0	2270
.185	220	101	510	150	185	76	1.7	11.6	4.5	2257
.200	58	45	104	0	57	28	1.0	11.7	8.0	2250
.215	0	0	0	0	0	0	0.7	11.7	11.0	2244
.245	0	0	0	0	0	0	0.6	11.8	13.0	2230
.275	0	0	0	0	0	0	0.6	11.8	15.5	2215
.305	0	0	0	0	0	0	0.6	11.8	16.0	2185
.335	0	0	0	0	0	0	0.5	11.8	17.5	2171
.385	0	0	0	0	0	0	0.5	11.8	17.0	2137

Table K-9. Dependent variable responses for fuel: propane; equivalence ratio: 1.00; and wall temperature: 800°F.

Dead Space Thickness <u>0.044</u> cm				Flame Zone Thickness <u>0.096</u> cm			Hydrocarbon Distance <u>0.170</u> cm			
Probe Position cm	Methane ppm	Ethane ppm	Ethylene ppm	Propane ppm	Acetylene ppm	Propylene ppm	Carbon Monoxide %	Carbon Dioxide %	Oxides of Nitrogen ppm	Gas Temperature °F
.005	396	210	1495	24300	0	540	1.3	6.9	0	1051
.020	---	---	----	-----	---	---	---	----	----	1585
.035	425	230	1572	23250	0	594	1.4	7.3	0.5	1847
.050	---	---	----	-----	---	---	---	----	----	1977
.065	452	246	1730	16800	17	670	1.5	7.9	0.5	2056
.080	---	---	----	-----	---	---	---	----	----	2105
.095	510	281	1925	11100	35	805	1.7	8.7	1.0	2151
.110	583	316	2155	8670	50	880	1.9	9.2	2.0	2202
.125	651	351	2410	5700	70	952	2.1	9.8	2.5	2230
.140	647	320	2615	3020	142	875	2.2	10.3	3.0	2241
.155	552	217	2200	510	260	440	2.3	11.0	3.0	2252
.170	Trace	Trace	Trace	Trace	Trace	Trace	1.3	11.5	4.5	2247
.185	0	0	0	0	0	0	0.9	11.7	8.0	2236
.200	0	0	0	0	0	0	0.6	11.7	12.5	2225
.215	0	0	0	0	0	0	0.5	11.7	11.5	2212
.245	0	0	0	0	0	0	0.5	11.7	12.0	2192
.275	0	0	0	0	0	0	0.5	11.7	12.5	2175
.305	0	0	0	0	0	0	0.5	11.7	12.5	2163
.335	0	0	0	0	0	0	0.5	11.7	12.0	2150
.385	0	0	0	0	0	0	0.4	11.7	13.0	2124

Table K-10. Dependent variable responses for fuel: propane; equivalence ratio: 1.05; and wall temperature: 600° F.

Dead Space Thickness <u>0.068</u> cm				Flame Zone Thickness <u>0.094</u> cm			Hydrocarbon Distance <u>0.260</u> cm			
Probe Position cm	Methane ppm	Ethane ppm	Ethylene ppm	Propane ppm	Acetylene ppm	Propylene ppm	Carbon Monoxide %	Carbon Dioxide %	Oxides of Nitrogen ppm	Gas Temperature °F
.005	304	155	1080	23700	0	202	1.0	5.6	0	----
.035	300	160	1135	22650	0	265	1.1	5.9	0	----
.065	320	185	1251	21300	0	360	1.2	6.3	0	----
.095	405	220	1515	19200	17	477	1.4	6.9	0	----
.110	442	255	1660	17700	30	504	1.5	7.2	0	----
.125	485	275	1765	16300	42	560	1.6	7.5	0	----
.140	515	285	1880	14550	75	625	1.6	7.9	0.5	----
.155	550	290	2015	12100	102	672	1.7	8.4	0.5	----
.170	567	275	2030	8540	130	651	1.8	9.0	0.5	2280
.185	479	245	1822	4900	98	504	1.8	9.5	1.0	2276
.200	345	200	1100	1600	75	153	1.7	10.3	1.5	2270
.215	220	104	490	450	65	97	1.5	10.8	3.0	2250
.245	55	10	210	0	15	16	1.0	11.3	6.5	2225
.275	0	0	85	0	0	0	0.6	11.6	8.0	2200
.305	0	0	0	0	0	0	0.5	11.6	8.5	2184
.335	0	0	0	0	0	0	0.5	11.6	8.5	2162
.385	0	0	0	0	0	0	0.5	11.6	10.0	2130

Table K-11. Dependent variable responses for fuel: propane; equivalence ratio: 1.05; and wall temperature: 700°F.

Dead Space Thickness <u>0.057</u> cm				Flame Zone Thickness <u>0.092</u> cm			Hydrocarbon Distance <u>0.220</u> cm			
Probe Position cm	Methane ppm	Ethane ppm	Ethylene ppm	Propane ppm	Acetylene ppm	Propylene ppm	Carbon Monoxide %	Carbon Dioxide %	Oxides of Nitrogen ppm	Gas Temperature °F
.005	370	202	1320	23200	30	425	1.1	5.9	0.5	----
.035	422	225	1510	20750	44	452	1.3	6.7	0.5	----
.065	500	252	1745	17800	102	535	1.4	7.2	1.0	----
.095	564	305	1985	13550	130	410	1.5	7.8	0.5	----
.110	580	320	2105	11100	185	715	1.6	8.2	1.0	----
.125	587	334	2200	8200	190	705	1.7	8.7	1.5	----
.140	530	305	2110	5400	155	580	1.8	9.2	2.0	----
.155	452	253	1715	3050	110	495	1.9	9.7	2.5	2250
.170	395	185	1255	1300	65	260	1.7	10.1	3.0	2225
.185	280	115	805	550	35	175	1.2	10.6	3.5	2210
.200	157	75	335	200	Trace	100	0.7	11.0	5.5	2190
.215	45	30	70	0	0	30	0.6	11.3	9.5	2175
.245	0	0	0	0	0	0	0.5	11.4	10.5	2155
.275	0	0	0	0	0	0	0.5	11.4	10.0	2125
.305	0	0	0	0	0	0	0.5	11.5	11.5	2100
.335	0	0	0	0	0	0	0.4	11.5	12.0	2065
.385	0	0	0	0	0	0	---	----	11.5	2025

Table K-12. Dependent variable responses for fuel: propane; equivalence ratio: 1.05; and wall temperature: 800°F.

Dead Space Thickness <u>0.054</u> cm				Flame Zone Thickness <u>0.096</u> cm			Hydrocarbon Distance <u>0.210</u> cm			
Probe Position cm	Methane ppm	Ethane ppm	Ethylene ppm	Propane ppm	Acetylene ppm	Propylene ppm	Carbon Monoxide %	Carbon Dioxide %	Oxides of Nitrogen ppm	Gas Temperature °F
.005	320	195	1310	21250	0	355	1.1	6.2	0	1070
.020	---	---	----	-----	---	---	---	----	----	1568
.035	370	215	1380	19150	0	405	1.2	6.4	0	1791
.050	---	---	----	-----	---	---	---	----	0	1925
.065	485	284	1622	16400	20	480	1.3	7.0	0	2030
.080	---	---	----	-----	---	---	---	----	----	2101
.095	525	345	1881	13000	152	617	1.5	7.7	0.5	2152
.110	564	345	2001	10800	256	672	1.6	8.1	0.5	2200
.125	575	310	2105	7950	230	700	1.7	8.6	1.0	2220
.140	510	277	1978	5500	95	630	1.8	9.1	1.5	2240
.155	380	227	1475	2550	52	460	1.7	9.2	1.5	2250
.170	260	172	550	1300	30	300	1.5	10.3	2.0	2245
.185	135	64	185	440	18	185	1.2	10.9	3.0	2230
.200	30	17	55	0	0	45	1.0	11.2	5.0	2221
.215	0	0	0	0	0	0	0.7	11.3	5.5	2210
.245	0	0	0	0	0	0	0.6	11.4	7.0	2185
.275	0	0	0	0	0	0	0.6	11.4	8.5	2160
.305	0	0	0	0	0	0	0.5	11.4	10.0	2145
.335	0	0	0	0	0	0	0.5	11.4	10.5	2125
.385	0	0	0	0	0	0	0.5	11.4	10.0	2082

Table K-13. Dependent variable responses for fuel: propane; equivalence ratio: 1.10; and wall temperature: 600° F.

Dead Space Thickness <u>0.074</u> cm				Flame Zone Thickness <u>0.096</u> cm			Hydrocarbon Distance <u>0.290</u> cm			
Probe Position cm	Methane ppm	Ethane ppm	Ethylene ppm	Propane ppm	Acetylene ppm	Propylene ppm	Carbon Monoxide %	Carbon Dioxide %	Oxides of Nitrogen ppm	Gas Temperature ° F
.005	155	75	852	22300	0	245	0.9	5.8	0	----
.035	220	130	950	21250	0	320	1.0	6.0	0	----
.065	272	183	1080	19750	0	410	1.2	6.4	0.5	----
.095	312	202	1245	16300	0	425	1.4	7.0	0.5	----
.125	340	205	1382	9400	0	315	1.5	8.3	1.0	----
.140	364	197	1375	6570	0	253	1.5	8.9	1.5	----
.155	320	177	1280	5040	0	201	1.5	9.3	2.0	2220
.185	245	122	954	3540	0	105	1.3	10.1	2.5	2195
.215	105	60	525	2310	0	35	1.2	10.6	3.0	2175
.245	45	15	200	1100	0	0	0.9	10.8	4.5	2154
.275	0	0	75	350	0	0	0.6	11.0	5.5	2100
.305	0	0	0	0	0	0	0.4	11.1	5.0	2075
.335	0	0	0	0	0	0	0.4	11.1	5.5	2063
.385	0	0	0	0	0	0	0.4	11.1	5.0	2053

Table K-14. Dependent variable responses for fuel: propane; equivalence ratio: 1.10; and wall temperature: 700°F.

Dead Space Thickness <u>0.062</u> cm				Flame Zone Thickness <u>0.104</u> cm			Hydrocarbon Distance <u>0.270</u> cm			
Probe Position cm	Methane ppm	Ethane ppm	Ethylene ppm	Propane ppm	Acetylene ppm	Propylene ppm	Carbon Monoxide %	Carbon Dioxide %	Oxides of Nitrogen ppm	Gas Temperature °F
.005	210	145	980	20450	0	327	1.0	6.2	0	955
.020	---	---	----	-----	---	---	---	----	----	1407
.035	260	165	1125	19470	0	355	1.1	6.4	0	1693
.050	---	---	----	-----	---	---	---	----	----	1846
.065	275	182	1167	17970	0	395	1.1	6.7	0	1936
.080	---	---	----	-----	---	---	---	----	----	2005
.095	296	197	1280	15560	0	462	1.2	7.2	0	2046
.110	321	205	1373	13500	0	510	1.2	7.7	0.5	2076
.125	340	210	1460	11550	0	563	1.3	8.1	0.5	2105
.140	380	225	1561	9320	0	580	1.4	8.5	1.0	2140
.155	402	230	1631	7210	0	682	1.5	8.9	1.0	2150
.185	351	197	1310	4100	0	480	1.5	9.7	1.5	2175
.215	243	136	857	1750	0	252	1.4	10.4	2.5	2155
.245	63	39	358	270	0	54	1.1	10.9	3.5	2140
.260	21	15	84	100	0	18	0.8	11.1	3.5	2125
.275	0	0	0	0	0	0	0.5	11.2	4.0	2110
.305	0	0	0	0	0	0	0.4	11.3	4.0	2085
.335	0	0	0	0	0	0	0.3	11.4	4.5	2060
.385	0	0	0	0	0	0	0.2	11.4	4.0	2030

Table K-15. Dependent variable responses for fuel: propane; equivalence ratio: 1.10; and wall temperature: 800°F.

Dead Space Thickness <u>0.055</u> cm				Flame Zone Thickness <u>0.100</u> cm			Hydrocarbon Distance <u>0.240</u> cm			
Probe Position cm	Methane ppm	Ethane ppm	Ethylene ppm	Propane ppm	Acetylene ppm	Propylene ppm	Carbon Monoxide %	Carbon Dioxide %	Oxides of Nitrogen ppm	Gas Temperature °F
.005	185	130	1055	17350	0	385	1.0	6.2	0	----
.035	245	153	1105	14550	0	505	1.1	6.6	0	----
.065	335	190	1295	14870	0	535	1.2	7.2	0.5	----
.095	384	220	1550	12050	0	610	1.3	8.0	0.5	----
.110	378	225	1648	9930	0	665	1.4	8.4	1.0	----
.125	361	194	1672	7520	0	640	1.5	8.8	1.0	----
.140	332	187	1564	5510	0	521	1.5	9.2	1.0	----
.155	281	152	1326	3820	0	401	1.4	9.6	1.5	2185
.170	250	131	1110	2800	0	310	1.3	9.9	2.5	2175
.185	215	110	905	1550	0	164	1.3	10.3	4.0	2160
.200	163	85	700	540	0	65	1.2	10.5	5.5	2150
.215	104	52	425	300	0	35	0.9	10.9	6.5	2125
.230	35	15	130	Trace	0	15	0.7	11.1	6.0	2105
.245	0	0	0	0	0	0	0.5	11.2	6.0	2080
.275	0	0	0	0	0	0	0.4	11.3	5.5	2065
.305	0	0	0	0	0	0	0.3	11.3	5.5	2054
.335	0	0	0	0	0	0	0.3	11.3	5.5	2040
.385	0	0	0	0	0	0	0.3	11.3	5.0	2025

Table K-16. Dependent variable responses for fuel: propylene; equivalence ratio: 0.90; and wall temperature: 600°F.

Dead Space Thickness <u>0.075</u> cm				Flame Zone Thickness <u>0.095</u> cm			Hydrocarbon Distance <u>0.250</u> cm			
Probe Position cm	Methane ppm	Ethane ppm	Ethylene ppm	Propane ppm	Acetylene ppm	Propylene ppm	Carbon Monoxide %	Carbon Dioxide %	Oxides of Nitrogen ppm	Gas Temperature °F
.005	459	151	1074	51	643	39100	2.0	6.3	3.5	857
.020	---	---	----	-----	-----	-----	---	----	----	1489
.035	521	172	1288	44	692	36540	2.1	6.6	5.0	1786
.050	---	---	----	-----	-----	-----	---	----	----	1947
.065	567	178	1381	48	787	34480	2.3	7.0	6.5	2050
.080	---	---	----	-----	-----	-----	---	----	----	2146
.095	702	181	1498	24	874	30710	2.7	7.5	7.0	2198
.110	762	211	1706	16	947	27040	3.0	7.9	6.5	2251
.125	818	232	1908	12	1071	22840	3.2	8.4	7.5	2282
.140	909	249	2066	Trace	1221	16650	3.5	8.9	7.5	2310
.155	971	256	2155	0	1303	14980	3.7	9.3	7.0	2333
.170	1026	251	2224	0	1401	10520	3.9	9.8	7.5	2361
.185	1032	234	2149	0	1552	6030	4.0	10.3	8.0	2345
.200	971	202	1801	0	1751	1210	4.3	10.7	9.0	2325
.215	857	183	1409	0	1926	280	4.6	11.2	9.5	2311
.230	751	108	744	0	1618	170	4.9	11.7	10.0	2302
.245	Trace	Trace	Trace	0	Trace	Trace	3.8	12.0	16.0	2291
.275	0	0	0	0	0	0	3.8	12.1	31.5	2269
.305	0	0	0	0	0	0	3.8	12.1	36.5	2247
.335	0	0	0	0	0	0	3.8	12.1	39.0	2230
.385	0	0	0	0	0	0	3.8	12.1	41.5	2208

Table K-17. Dependent variable responses for fuel: propylene; equivalence ratio: 0.90; and wall temperature: 700°F.

Dead Space Thickness <u>0.062</u> cm				Flame Zone Thickness <u>0.101</u> cm			Hydrocarbon Distance <u>0.250</u> cm			
Probe Position cm	Methane ppm	Ethane ppm	Ethylene ppm	Propane ppm	Acetylene ppm	Propylene ppm	Carbon Monoxide %	Carbon Dioxide %	Oxides of Nitrogen ppm	Gas Temperature °F
.005	494	176	1105	74	640	39200	1.9	6.6	1.0	----
.035	506	185	1170	68	672	37200	2.0	6.8	2.5	----
.065	552	188	1252	65	685	32840	2.2	7.6	4.0	----
.095	677	237	1570	68	865	27950	2.6	8.2	5.5	----
.125	754	252	1864	70	1078	22000	3.0	8.9	7.0	----
.155	883	318	2127	38	1277	10810	3.4	9.9	8.5	----
.170	959	353	2225	24	1359	7020	3.7	10.3	9.0	2410
.185	1030	337	2253	17	1481	4520	4.0	10.7	9.0	2391
.200	1064	298	2021	0	1602	1980	4.3	11.0	11.0	2365
.215	951	231	1308	0	1673	470	4.5	11.4	13.0	2320
.230	582	127	641	0	1511	Trace	4.6	11.7	20.5	2301
.245	Trace	Trace	Trace	0	Trace	0	4.5	12.0	30.0	2258
.275	0	0	0	0	0	0	3.7	12.2	47.5	2219
.305	0	0	0	0	0	0	3.4	12.3	50.5	2181
.335	0	0	0	0	0	0	3.4	12.3	52.0	2154
.385	0	0	0	0	0	0	3.4	12.3	53.0	----

Table K-18. Dependent variable responses for fuel: propylene; equivalence ratio: 0.90; and wall temperature: 800°F.

Dead Space Thickness <u>0.042</u> cm				Flame Zone Thickness <u>0.104</u> cm			Hydrocarbon Distance <u>0.250</u> cm			
Probe Position cm	Methane ppm	Ethane ppm	Ethylene ppm	Propane ppm	Acetylene ppm	Propylene ppm	Carbon Monoxide %	Carbon Dioxide %	Oxides of Nitrogen ppm	Gas Temperature °F
.005	497	142	1151	70	594	32100	2.0	6.5	1.0	----
.035	548	151	1204	65	647	31700	2.2	6.9	1.5	----
.065	597	154	1263	72	749	30750	2.3	7.3	2.5	----
.095	677	183	1449	68	938	28450	2.5	7.8	4.0	----
.110	744	224	1617	64	1022	26040	2.7	8.1	5.0	----
.125	851	238	1768	63	1110	23150	2.9	8.3	5.5	----
.140	898	257	1902	55	1220	20000	3.2	8.5	5.5	----
.155	950	266	2013	47	1305	16640	3.5	9.0	6.5	----
.170	1003	263	2174	35	1418	13470	3.7	9.4	7.5	2352
.185	1105	324	2356	28	1550	10080	4.1	9.7	7.5	2340
.200	1210	337	2425	21	1834	5530	4.5	10.1	8.0	2322
.215	1347	264	2247	15	2205	2890	4.8	10.5	11.0	2310
.230	371	45	784	Trace	694	510	4.7	11.1	25.5	2280
.245	17	Trace	46	0	53	Trace	3.9	12.0	32.0	2254
.275	0	0	0	0	0	0	3.9	12.1	38.0	2230
.305	0	0	0	0	0	0	3.9	12.2	40.0	2177
.335	0	0	0	0	0	0	3.9	12.2	42.0	2134
.385	0	0	0	0	0	0	3.9	12.2	43.0	----

Table K-19. Dependent variable responses for fuel: propylene; equivalence ratio: 0.95; and wall temperature: 600°F.

Dead Space Thickness <u>0.065</u> cm				Flame Zone Thickness <u>0.108</u> cm			Hydrocarbon Distance <u>0.225</u> cm			
Probe Position cm	Methane ppm	Ethane ppm	Ethylene ppm	Propane ppm	Acetylene ppm	Propylene ppm	Carbon Monoxide %	Carbon Dioxide %	Oxides of Nitrogen ppm	Gas Temperature °F
.005	304	131	881	32	481	33850	1.3	6.3	3.0	----
.035	312	142	902	27	472	31220	1.4	6.6	5.5	----
.065	321	144	956	30	489	28710	1.4	6.9	6.0	----
.095	374	165	1110	19	564	25880	1.6	7.6	7.0	----
.125	428	202	1351	22	679	21000	2.0	8.5	8.0	----
.155	526	229	1420	14	762	7530	2.2	9.6	7.5	----
.170	573	224	1452	Trace	812	4010	2.4	10.0	7.5	2402
.185	589	124	1362	0	871	2280	2.6	10.4	9.0	2385
.200	572	184	1122	0	912	1080	2.7	10.9	10.0	2372
.215	381	113	759	0	943	370	2.6	11.3	18.5	2360
.230	Trace	Trace	22	0	28	Trace	1.0	12.2	28.0	2349
.245	0	0	0	0	0	0	0.9	12.3	29.5	2332
.275	0	0	0	0	0	0	0.9	12.4	32.5	2317
.305	0	0	0	0	0	0	0.9	12.4	31.5	2301
.335	0	0	0	0	0	0	0.9	12.4	34.0	2282
.385	0	0	0	0	0	0	0.9	12.4	----	----

Table K-20. Dependent variable responses for fuel: propylene; equivalence ratio: 0.95; and wall temperature: 700°F.

Dead Space Thickness <u>0.055</u> cm				Flame Zone Thickness <u>0.098</u> cm			Hydrocarbon Distance <u>0.200</u> cm			
Probe Position cm	Methane ppm	Ethane ppm	Ethylene ppm	Propane ppm	Acetylene ppm	Propylene ppm	Carbon Monoxide %	Carbon Dioxide %	Oxides of Nitrogen ppm	Gas Temperature °F
.005	267	130	825	40	453	31250	1.2	6.5	3.5	----
.035	278	142	889	25	459	29780	1.3	6.9	4.5	----
.065	332	151	951	22	474	27510	1.5	7.3	5.0	----
.095	380	153	1026	15	501	24200	1.7	7.9	6.0	----
.125	432	172	1139	18	587	19030	1.8	8.5	5.5	----
.155	497	180	1348	12	726	11150	2.1	9.5	7.0	----
.170	525	217	1496	0	832	6560	2.3	9.9	7.0	----
.185	507	203	1582	0	884	2040	2.4	11.2	8.5	2365
.190	250	102	335	0	270	520	1.8	11.9	9.5	----
.200	22	12	42	0	27	0	0.8	12.2	10.0	2342
.215	0	0	0	0	0	0	0.7	12.3	26.0	2325
.245	0	0	0	0	0	0	0.7	12.3	28.0	2318
.275	0	0	0	0	0	0	0.7	12.3	28.5	2305
.305	0	0	0	0	0	0	0.7	12.3	30.0	2285
.335	0	0	0	0	0	0	0.7	12.3	29.5	2268
.385	0	0	0	0	0	0	0.7	12.3	30.0	----

Table K-21. Dependent variable responses for fuel: propylene; equivalence ratio: 0.95; and wall temperature: 800°F.

Dead Space Thickness 0.036 cm				Flame Zone Thickness 0.104 cm			Hydrocarbon Distance 0.205 cm			
Probe Position cm	Methane ppm	Ethane ppm	Ethylene ppm	Propane ppm	Acetylene ppm	Propylene ppm	Carbon Monoxide %	Carbon Dioxide %	Oxides of Nitrogen ppm	Gas Temperature %
.005	304	102	882	22	401	30040	1.5	6.6	3.5	981
.020	---	---	---	--	---	---	---	---	---	1548
.035	349	120	1026	25	449	28420	1.6	7.1	4.0	1882
.050	---	---	---	--	---	---	---	---	---	2043
.065	392	131	1129	37	551	25950	1.7	7.7	3.5	2165
.080	---	---	---	--	---	---	---	---	---	2215
.095	418	169	1210	24	575	22100	1.8	8.4	4.5	2325
.125	448	197	1368	15	625	16340	1.9	9.0	5.0	2402
.140	502	205	1431	12	698	13080	2.1	9.5	5.5	2421
.155	537	194	1521	0	749	8520	2.2	10.1	7.0	2423
.170	548	199	1510	0	872	4230	2.4	10.7	10.0	2416
.185	496	175	1300	0	1039	720	2.6	11.3	13.0	2406
.200	419	35	54	0	27	150	0.9	12.3	22.0	2389
.215	0	0	0	0	0	0	0.8	12.5	24.0	2378
.245	0	0	0	0	0	0	0.6	12.6	24.5	2347
.275	0	0	0	0	0	0	0.6	12.6	26.0	2318
.305	0	0	0	0	0	0	0.5	12.6	24.5	2301
.335	0	0	0	0	0	0	0.5	12.6	26.5	2282
.385	0	0	0	0	0	0	0.5	12.6	27.0	---

Table K-22. Dependent variable responses for fuel: propylene; equivalence ratio: 1.00; and wall temperature: 600°F.

Dead Space Thickness <u>0.056</u> cm				Flame Zone Thickness <u>0.107</u> cm			Hydrocarbon Distance <u>0.245</u> cm			
Probe Position cm	Methane ppm	Ethane ppm	Ethylene ppm	Propane ppm	Acetylene ppm	Propylene ppm	Carbon Monoxide %	Carbon Dioxide %	Oxides of Nitrogen ppm	Gas Temperature °F
.005	220	110	672	27	304	34840	1.1	5.9	1.0	----
.035	231	105	814	29	314	33100	1.1	6.2	1.0	----
.065	252	120	927	21	336	30150	1.2	6.7	1.5	----
.095	270	148	998	20	361	25840	1.3	7.3	2.0	----
.125	338	186	1096	15	448	20750	1.5	8.0	2.0	----
.140	361	204	1132	18	465	17270	1.6	8.6	2.5	----
.155	375	210	1156	13	489	13210	1.7	9.1	3.0	----
.170	349	194	1121	0	475	9510	1.8	9.7	4.0	----
.185	296	168	1049	0	420	6190	1.8	10.3	5.0	2352
.200	228	127	861	0	338	4210	1.6	10.9	6.0	2331
.215	166	74	602	0	222	2250	1.3	11.5	7.5	2317
.230	103	42	300	0	102	790	1.1	12.0	9.5	2302
.245	37	16	39	0	28	110	0.9	12.4	11.5	2286
.275	0	0	0	0	0	0	0.6	12.6	11.0	2267
.305	0	0	0	0	0	0	0.5	12.6	12.0	2242
.335	0	0	0	0	0	0	0.4	12.7	12.5	2218
.385	0	0	0	0	0	0	0.3	12.7	12.0	2169

Table K-23. Dependent variable responses for fuel: propylene; equivalence ratio: 1.00; and wall temperature: 700°F.

Dead Space Thickness <u>0.046</u> cm				Flame Zone Thickness <u>0.110</u> cm			Hydrocarbon Distance <u>0.220</u> cm			
Probe Position cm	Methane ppm	Ethane ppm	Ethylene ppm	Propane ppm	Acetylene ppm	Propylene ppm	Carbon Monoxide %	Carbon Dioxide %	Oxides of Nitrogen ppm	Gas Temperature °F
.005	198	88	697	31	424	33550	1.0	6.1	0.5	994
.020	---	---	----	--	---	-----	---	----	----	1516
.035	236	105	743	24	446	31720	1.1	6.5	1.0	1802
.050	---	---	----	--	---	-----	---	----	----	1953
.065	271	122	862	19	454	28150	1.3	7.0	1.0	2062
.080	---	---	----	--	---	-----	---	----	----	2129
.095	300	151	1052	22	450	23250	1.4	7.8	2.0	2181
.110	312	159	1137	17	473	20050	1.5	8.2	2.5	2217
.125	335	155	1180	12	508	16270	1.6	8.6	3.0	2246
.140	352	172	1203	0	562	13030	1.7	9.1	3.5	2262
.155	367	182	1189	0	578	9980	1.8	9.6	4.0	2276
.170	351	175	1129	0	557	6890	1.8	10.1	4.0	2273
.185	310	168	1005	0	510	3760	1.7	10.7	4.5	2268
.200	221	136	715	0	353	1240	1.6	11.3	7.5	2255
.215	69	34	230	0	102	150	0.9	12.0	11.0	2241
.220	Trace	Trace	18	0	15	0	0.7	12.2	12.0	2226
.230	0	0	0	0	0	0	0.6	12.8	11.5	2210
.245	0	0	0	0	0	0	0.5	12.8	13.0	2187
.275	0	0	0	0	0	0	0.5	12.8	14.0	2160
.305	0	0	0	0	0	0	0.4	12.8	14.0	2132
.335	0	0	0	0	0	0	0.4	12.8	15.5	2119
.385	0	0	0	0	0	0	0.4	12.8	15.0	----

Table K-24. Dependent variable responses for fuel: propylene; equivalence ratio: 1.00; and wall temperature: 800°F.

Dead Space Thickness <u>0.041</u> cm				Flame Zone Thickness <u>0.098</u> cm			Hydrocarbon Distance <u>0.205</u> cm			
Probe Position cm	Methane ppm	Ethane ppm	Ethylene ppm	Propane ppm	Acetylene ppm	Propylene ppm	Carbon Monoxide %	Carbon Dioxide %	Oxides of Nitrogen ppm	Gas Temperature °F
.005	272	80	826	24	318	32500	1.1	6.3	0.5	1040
.020	---	---	----	--	---	-----	---	----	----	1610
.035	302	127	902	26	370	29450	1.2	6.8	1.0	1927
.050	---	---	----	--	---	-----	---	----	----	2088
.065	301	162	1019	23	443	25850	1.3	7.3	1.5	2200
.080	---	---	----	--	---	-----	----	----	----	2286
.095	335	179	1203	16	555	20030	1.5	8.1	2.0	2334
.110	437	182	1377	12	584	13820	1.7	8.8	4.0	2362
.125	476	195	1398	0	590	8470	1.8	9.1	3.0	2378
.140	484	204	1361	0	564	4040	1.9	9.4	3.5	2385
.155	403	209	1328	0	515	2160	2.0	9.9	4.0	2374
.170	317	200	1124	0	489	1190	1.8	10.5	6.0	2358
.185	177	102	505	0	205	480	1.4	11.9	10.0	2339
.200	36	Trace	Trace	0	Trace	Trace	0.7	12.3	14.0	2316
.215	0	0	0	0	0	0	0.4	12.5	15.5	2301
.245	0	0	0	0	0	0	0.4	12.7	17.0	2267
.275	0	0	0	0	0	0	0.4	12.7	16.0	2238
.305	0	0	0	0	0	0	0.3	12.7	17.0	2202
.335	0	0	0	0	0	0	0.3	12.7	17.5	2172
.385	0	0	0	0	0	0	0.3	12.7	16.5	----

Table K-25. Dependent variable responses for fuel: propylene; equivalence ratio: 1.05; and wall temperature: 600°F.

Dead Space Thickness <u>0.060</u> cm				Flame Zone Thickness <u>0.100</u> cm			Hydrocarbon Distance <u>0.255</u> cm			
Probe Position cm	Methane ppm	Ethane ppm	Ethylene ppm	Propane ppm	Acetylene ppm	Propylene ppm	Carbon Monoxide %	Carbon Dioxide %	Oxides of Nitrogen ppm	Gas Temperature °F
.005	201	81	622	32	177	34000	1.0	5.5	0	----
.035	226	92	668	24	190	32200	1.1	6.0	0	----
.065	272	109	759	22	254	28300	1.2	6.5	0.5	----
.095	289	125	887	16	325	23850	1.3	7.2	0.5	----
.125	330	152	1055	0	418	18350	1.5	7.9	1.0	----
.140	362	148	1115	0	453	15100	1.7	8.2	1.5	----
.155	398	165	1137	0	468	11520	1.7	8.7	1.0	----
.170	427	162	1079	0	434	8030	1.8	9.2	1.5	----
.185	354	135	926	0	350	5180	1.7	9.7	2.0	2275
.200	251	118	702	0	244	2670	1.6	10.1	2.5	2262
.215	157	97	501	0	150	750	1.5	10.6	4.0	2248
.230	72	43	247	0	76	Trace	1.2	10.9	4.5	2227
.245	30	17	77	0	36	0	0.8	11.0	6.5	2215
.275	0	0	0	0	0	0	0.4	11.2	8.0	2198
.305	0	0	0	0	0	0	0.3	11.2	10.5	2182
.335	0	0	0	0	0	0	0.3	11.2	12.0	2164
.385	0	0	0	0	0	0	0.3	11.2	12.5	2147

Table K-26. Dependent variable responses for fuel: propylene; equivalence ratio: 1.05; and wall temperature: 700°F.

Dead Space Thickness <u>0.053</u> cm				Flame Zone Thickness <u>0.107</u> cm			Hydrocarbon Distance <u>0.250</u> cm			
Probe Position cm	Methane ppm	Ethane ppm	Ethylene ppm	Propane ppm	Acetylene ppm	Propylene ppm	Carbon Monoxide %	Carbon Dioxide %	Oxides of Nitrogen ppm	Gas Temperature °F
.005	177	82	604	37	208	24500	0.9	5.8	0	----
.035	184	93	647	25	235	31850	1.0	6.2	0.5	----
.065	204	102	702	20	254	33240	1.1	6.6	0.5	----
.095	229	104	851	17	317	24480	1.2	7.0	1.0	----
.125	284	121	954	0	384	19520	1.4	7.7	1.0	----
.140	325	128	1025	0	457	16550	1.5	8.1	1.5	----
.155	351	154	1053	0	500	12500	1.7	8.7	2.0	----
.170	298	179	977	0	426	8270	1.6	9.1	1.5	2275
.185	237	168	854	0	329	5020	1.5	9.6	2.0	2262
.200	198	125	698	0	247	2520	1.4	10.0	2.5	2251
.215	154	77	501	0	179	890	1.3	10.4	2.0	2241
.230	117	51	175	0	121	220	1.0	10.9	5.0	2230
.245	34	19	54	0	44	0	0.7	11.1	9.0	2220
.275	0	0	0	0	0	0	0.4	11.3	10.5	2204
.305	0	0	0	0	0	0	0.4	11.3	11.0	2185
.335	0	0	0	0	0	0	0.3	11.3	10.0	2159
.385	0	0	0	0	0	0	0.3	11.3	10.5	----

Table K-27. Dependent variable responses for fuel: propylene; equivalence ratio: 1.05; and wall temperature: 800°F.

Dead Space Thickness <u>0.038</u> cm				Flame Zone Thickness <u>0.108</u> cm			Hydrocarbon Distance <u>0.200</u> cm			
Probe Position cm	Methane ppm	Ethane ppm	Ethylene ppm	Propane ppm	Acetylene ppm	Propylene ppm	Carbon Monoxide %	Carbon Dioxide %	Oxides of Nitrogen ppm	Gas Temperature °F
.005	200	89	654	23	264	30840	1.1	5.9	0.5	----
.035	205	85	689	18	270	28500	1.2	6.3	1.0	----
.065	239	109	737	16	307	24100	1.3	6.9	1.5	----
.095	277	130	951	0	374	19290	1.4	7.7	2.5	----
.125	354	157	1127	0	500	14270	1.6	8.3	4.0	----
.140	382	172	1202	0	535	10550	1.7	8.8	4.5	----
.155	328	162	1148	0	498	6580	1.7	9.2	5.5	----
.170	252	147	927	0	401	3030	1.6	9.8	7.0	2255
.185	159	84	521	0	220	1100	1.2	10.3	7.5	2245
.200	72	14	54	0	35	150	0.8	10.7	9.0	2239
.215	Trace	0	0	0	0	0	0.7	10.9	10.5	2228
.245	0	0	0	0	0	0	0.4	11.0	10.5	2220
.275	0	0	0	0	0	0	0.4	11.1	11.0	2211
.305	0	0	0	0	0	0	0.3	11.1	10.0	2202
.335	0	0	0	0	0	0	0.3	11.1	10.5	2178
.385	0	0	0	0	0	0	0.3	11.1	11.0	2161

Table K-28. Dependent variable responses for fuel: propylene; equivalence ratio: 1.10; and wall temperature: 600°F.

Dead Space Thickness <u>0.068</u> cm				Flame Zone Thickness <u>0.105</u> cm			Hydrocarbon Distance <u>0.300</u> cm			
Probe Position cm	Methane ppm	Ethane ppm	Ethylene ppm	Propane ppm	Acetylene ppm	Propylene ppm	Carbon Monoxide %	Carbon Dioxide %	Oxides of Nitrogen ppm	Gas Temperature °F
.005	132	79	527	27	196	30400	0.9	6.0	0.5	----
.035	151	74	563	29	224	29150	1.0	6.4	1.5	----
.065	177	81	587	25	246	27010	1.1	6.7	2.0	----
.095	224	89	671	17	261	24240	1.2	7.0	2.0	----
.125	236	103	779	19	301	20320	1.4	7.9	2.5	----
.155	251	117	898	14	338	14520	1.5	8.8	2.5	----
.170	253	122	926	12	353	11410	1.6	9.4	3.0	2252
.185	247	101	901	Trace	341	9060	1.5	9.8	4.0	2241
.200	227	83	838	0	299	7050	1.5	10.3	5.0	2226
.215	203	76	776	0	257	5250	1.4	10.6	5.0	2205
.245	138	54	585	0	203	2510	1.3	11.2	5.5	2190
.275	78	31	306	0	104	690	0.8	11.3	4.5	2151
.305	Trace	Trace	Trace	0	Trace	Trace	0.4	11.4	5.0	2104
.335	0	0	0	0	0	0	0.3	11.4	5.5	2074
.385	0	0	0	0	0	0	0.2	11.4	5.0	2002

Table K-29. Dependent variable responses for fuel: propylene; equivalence ratio: 1, 10; and wall temperature: 700°F.

Dead Space Thickness <u>0, 060</u> cm				Flame Zone Thickness <u>0, 106</u> cm			Hydrocarbon Distance <u>0, 290</u> cm			
Probe Position cm	Methane ppm	Ethane ppm	Ethylene ppm	Propane ppm	Acetylene ppm	Propylene ppm	Carbon Monoxide %	Carbon Dioxide %	Oxides of Nitrogen ppm	Gas Temperature °F
.005	149	65	442	20	101	26250	1.1	6.0	0.5	----
.035	157	63	474	22	108	25020	1.1	6.2	0.5	----
.065	164	71	503	19	123	23710	1.2	6.4	1.0	----
.095	181	73	568	17	155	21690	1.2	6.8	1.0	----
.125	203	76	659	19	173	18400	1.3	7.5	1.5	----
.140	207	78	696	12	184	15720	1.4	7.9	2.5	----
.155	198	80	701	Trace	201	12500	1.5	8.3	2.0	----
.170	184	79	687	0	200	9470	1.5	8.9	2.5	----
.185	137	64	645	0	192	6460	1.4	9.6	3.0	2240
.215	89	52	498	0	168	3300	1.2	10.2	4.0	2204
.245	65	31	317	0	89	990	1.1	10.6	4.5	2181
.275	37	14	68	0	41	Trace	0.8	11.1	4.5	2158
.290	Trace	Trace	Trace	0	Trace	0	0.5	11.2	5.5	2137
.305	0	0	0	0	0	0	0.3	11.3	5.0	2110
.335	0	0	0	0	0	0	0.2	11.4	5.5	2084
.385	0	0	0	0	0	0	0.2	11.4	5.0	----

Table K-30. Dependent variable responses for fuel: propylene; equivalence ratio: 1.10; and wall temperature: 800°F.

Dead Space Thickness <u>0.039</u> cm				Flame Zone Thickness <u>0.109</u> cm			Hydrocarbon Distance <u>0.270</u> cm			
Probe Position cm	Methane ppm	Ethane ppm	Ethylene ppm	Propane ppm	Acetylene ppm	Propylene ppm	Carbon Monoxide %	Carbon Dioxide %	Oxides of Nitrogen ppm	Gas Temperature °F
.005	110	53	505	28	104	25840	1.0	6.3	0.5	----
.035	128	52	542	23	105	23440	1.1	6.9	0.5	----
.065	149	58	577	18	99	20810	1.2	7.3	1.0	----
.095	187	65	693	21	105	15010	1.3	7.9	1.0	----
.110	174	74	707	15	115	10720	1.3	8.3	1.0	----
.125	138	79	752	12	119	5970	1.4	8.6	1.5	----
.140	98	85	720	Trace	132	4240	1.5	9.0	1.5	----
.155	72	67	615	0	110	2990	1.4	9.5	2.0	----
.185	61	49	414	0	58	1510	1.3	10.2	2.0	2181
.215	44	37	201	0	42	870	1.1	10.7	3.0	2150
.245	37	18	88	0	21	420	0.7	11.1	3.5	2132
.260	13	Trace	39	0	Trace	Trace	0.4	11.3	4.0	2118
.275	0	0	0	0	0	0	0.3	11.5	4.0	2107
.305	0	0	0	0	0	0	0.2	11.7	4.5	2085
.335	0	0	0	0	0	0	0.2	11.7	5.5	2061
.385	0	0	0	0	0	0	0.2	11.7	6.0	----

APPENDIX L

TWO-WAY TABLES OF MEANS FOR THREE-FACTOR AND FOUR-FACTOR ANALYSES OF VARIANCE

Table L-1. Three-factor two-way tables of means for dead space response.

A \ B	.90	.95	1.00	1.05	1.10	Mean
Propane	.063	.060	.050	.060	.063	.059
Propylene	.060	.057	.050	.050	.057	.055

C \ B	.90	.95	1.00	1.05	1.10	Mean
600°F	.080	.070	.060	.065	.070	.069
700°F	.060	.060	.050	.055	.060	.057
800°F	.045	.045	.040	.045	.050	.045

A \ C	600°F	700°F	800°F	Mean
Propane	.070	.058	.050	.059
Propylene	.068	.056	.040	.055

Table 1-2. Three-factor two-way tables of means for flame zone responses.

A \ B	.90	.95	1.00	1.05	1.10	Mean
Propane	.087	.083	.087	.093	.100	.090
Propylene	.097	.103	.107	.107	.107	.104

C \ B	.90	.95	1.00	1.05	1.10	Mean
600°F	.085	.095	.095	.095	.100	.094
700°F	.090	.090	.095	.100	.105	.096
800°F	.100	.095	.100	.105	.105	.101

A \ C	600°F	700°F	800°F	Mean
Propane	.086	.086	.098	.090
Propylene	.102	.106	.104	.104

Table L-3. Three-factor two-way tables of means for hydrocarbon distance response.

A \ B	.90	.95	1.00	1.05	1.10	Mean
Propane	.230	.203	.217	.230	.267	.229
Propylene	.250	.210	.223	.233	.287	.241

C \ B	.90	.95	1.00	1.05	1.10	Mean
600°F	.250	.210	.255	.255	.295	.253
700°F	.235	.200	.215	.235	.280	.233
800°F	.235	.210	.190	.205	.255	.219

A \ C	600°F	700°F	800°F	Mean
Propane	.254	.224	.210	.229
Propylene	.252	.242	.228	.241

Table L-4. Four-factor two-way tables of means for methane response.

A \ B	.90	.95	1.00	1.05	1.10	Mean
Propane	708	426	300	253	182	373
Propylene	510	246	182	163	115	423

C \ B	.90	.95	1.00	1.05	1.10	Mean
600°F	619	340	283	224	160	325
700°F	521	322	218	211	159	286
800°F	687	348	219	189	127	314

C \ A	Propane	Propylene	Mean
600°F	393	257	325
700°F	342	231	286
800°F	386	243	314

A \ D	.005	.035	.065	.095	.125	.155	.185	.215	.245	.275	.305	.335	Mean
Propane	450	513	576	656	766	801	515	160	46	0	0	0	373
Propylene	266	289	319	368	428	474	449	295	24	8	0	0	423

C \ D	.005	.035	.065	.095	.125	.155	.185	.215	.245	.275	.305	.335	Mean
600°F	340	393	445	514	586	673	561	299	83	8	0	0	325
700°F	353	388	433	497	584	610	395	155	16	4	0	0	286
800°F	380	421	465	526	620	629	491	228	5	0	0	0	314

B \ D	.005	.035	.065	.095	.125	.155	.185	.215	.245	.275	.305	.335	Mean
.90	642	739	828	971	1148	1280	1013	682	7	0	0	0	609
.95	427	458	493	546	646	764	640	64	0	0	0	0	336
1.00	301	329	356	398	485	480	276	164	90	0	0	0	240
1.05	262	285	332	382	436	410	274	96	20	0	0	0	208
1.10	157	194	229	264	270	254	209	131	58	19	0	0	149
Mean	358	401	448	512	597	637	482	228	35	4	0	0	308

Table L-5. Four-factor two-way tables of means for ethane response.

A \ B	.90	.95	1.00	1.05	1.10	Mean
Propane	167	197	198	139	108	162
Propylene	145	99	89	75	52	92

C \ B	.90	.95	1.00	1.05	1.10	Mean
600°F	138	144	213	109	82	137
700°F	166	160	109	109	87	127
800°F	165	139	108	102	70	117

C \ A	Propane	Propylene	Mean
600°F	177	97	137
700°F	160	93	127
800°F	148	86	117

A \ D	.005	.035	.065	.095	.125	.155	.185	.215	.245	.275	.305	.335	Mean
Propane	188	221	254	294	331	318	215	74	45	0	0	0	162
Propylene	104	114	125	143	168	186	168	83	10	3	0	0	92

C \ D	.005	.035	.065	.095	.125	.155	.185	.215	.245	.275	.305	.335	Mean
600°F	143	168	189	214	250	263	211	133	80	3	0	0	137
700°F	154	171	186	215	249	263	214	56	9	2	0	0	127
800°F	141	163	195	227	249	230	150	45	2	0	0	0	117

B \ D	.005	.035	.065	.095	.125	.155	.185	.215	.245	.275	.305	.335	Mean
.90	159	202	234	272	312	306	252	136	3	0	0	0	156
.95	178	198	208	243	297	342	292	19	0	0	0	0	148
1.00	169	187	206	232	269	266	174	155	103	0	0	0	143
1.05	134	145	174	205	225	209	135	51	8	0	0	0	107
1.10	91	106	128	141	145	137	107	69	26	8	0	0	80
Mean	146	167	190	219	249	252	192	78	28	2	0	0	127

Table L-6. Four-factor two-way tables of means for ethylene response.

A \ B	.90	.95	1.00	1.05	1.10	Mean
Propane	1483	1154	1063	908	779	1077
Propylene	1084	693	597	519	440	667

C \ B	.90	.95	1.00	1.05	1.10	Mean
600°F	1294	926	963	750	631	913
700°F	1140	894	755	733	627	830
800°F	1416	950	771	658	572	873

C \ A	Propane	Propylene	Mean
600°F	1122	703	913
700°F	1018	641	830
800°F	1091	655	873

A \ D	.005	.035	.065	.095	.125	.155	.185	.215	.245	.275	.305	.335	Mean
Propane	1369	1506	1663	1930	2262	2280	1336	437	134	11	0	0	1077
Propylene	764	835	907	1049	1227	1321	1188	602	80	25	0	0	667

C \ D	.005	.035	.065	.095	.125	.155	.185	.215	.245	.275	.305	.335	Mean
600°F	993	1120	1246	1420	1659	1830	1620	783	236	47	0	0	913
700°F	1066	1165	1270	1473	1742	1763	1051	346	73	7	0	0	830
800°F	1142	1227	1338	1577	1832	1808	1116	428	13	0	0	0	873

B \ D	.005	.035	.065	.095	.125	.155	.185	.215	.245	.275	.305	.335	Mean
.90	1389	1592	1744	2052	2503	2722	2278	1107	15	0	0	0	1284
.95	1217	1316	1413	1617	1887	2076	1427	127	0	0	0	0	923
1.00	1069	1146	1263	1434	1680	1705	899	556	207	0	0	0	830
1.05	932	1006	1136	1345	1534	1424	852	260	57	14	0	0	713
1.10	727	793	868	1001	1117	1075	855	547	258	75	0	0	610
Mean	1067	1171	1285	1490	1744	1800	1262	519	107	18	0	0	873

Table L-7. Four-factor two-way tables of means for propane response.

A \ B	.90	.95	1.00	1.05	1.10	Mean
Propane	8874	8381	8509	8125	7547	8287
Propylene	28	11	9	7	9	13

C \ B	.90	.95	1.00	1.05	1.10	Mean
600°F	4899	4360	5623	5198	4228	4861
700°F	4158	4199	3748	3633	4101	3968
800°F	4296	4028	3406	3367	3005	3620

C \ A	Propane	Propylene	Mean
600°F	9712	11	4861
700°F	7922	14	3968
800°F	7227	13	3620

A \ D	.005	.035	.065	.095	.125	.155	.185	.215	.245	.275	.305	.335	Mean
Propane	23349	21571	19265	15729	10813	5485	2168	919	124	23	0	0	8287
Propylene	36	32	30	24	18	9	3	1	0	0	0	0	13

C \ D	.005	.035	.065	.095	.125	.155	.185	.215	.245	.275	.305	.335	Mean
600°F	12382	11691	10740	9085	6818	4243	2081	1103	159	35	0	0	4861
700°F	11488	10628	9535	7777	5117	2218	651	175	27	0	0	0	3968
800°F	11207	10084	8669	6768	4311	1780	525	102	0	0	0	0	3620

B \ D	.005	.035	.065	.095	.125	.155	.185	.215	.245	.275	.305	.335	Mean
.90	13158	11780	10339	8243	5291	3114	1228	228	32	0	0	0	4451
.95	12067	11311	10198	8288	5921	2369	195	0	0	0	0	0	4196
1.00	11834	11255	9666	7893	5705	2621	1492	595	50	0	0	0	4259
1.05	11375	10436	9260	7631	5408	2950	982	750	0	0	0	0	4066
1.10	10029	9224	8775	7327	4753	2681	1532	727	228	58	0	0	3778
Mean	11692	10801	9648	7876	5416	2747	1086	460	62	12	0	0	4650

Table L-8. Four-factor two-way tables of means for acetylene response.

A \ B	.90	.95	1.00	1.05	1.10	Mean
Propane	331	130	73	40	0	115
Propylene	733	382	261	201	127	341

C \ B	.90	.95	1.00	1.05	1.10	Mean
600°F	552	309	188	113	103	253
700°F	466	224	172	129	56	209
800°F	578	234	141	121	32	221

C \ A	Propane	Propylene	Mean
600°F	141	365	253
700°F	90	329	209
800°F	113	329	221

A \ D	.005	.035	.065	.095	.125	.155	.185	.215	.245	.275	.305	.335	Mean
Propane	35	59	93	160	272	367	278	74	40	0	0	0	115
Propylene	354	377	417	481	573	655	667	524	32	10	0	0	341

C \ D	.005	.035	.065	.095	.125	.155	.185	.215	.245	.275	.305	.335	Mean
600°F	198	212	243	305	448	578	543	410	87	10	0	0	253
700°F	196	219	253	321	419	485	391	212	13	4	0	0	209
800°F	189	223	268	335	400	470	485	275	7	0	0	0	221

B \ D	.005	.035	.065	.095	.125	.155	.185	.215	.245	.275	.305	.335	Mean
.90	395	472	557	718	940	1151	1074	1065	12	0	0	0	532
.95	223	233	275	334	470	629	747	157	0	0	0	0	256
1.00	174	188	208	245	310	379	270	130	98	0	0	0	167
1.05	113	123	156	219	294	288	175	66	16	0	0	0	121
1.10	67	73	78	87	99	108	99	78	52	24	0	0	64
Mean	194	218	255	321	423	511	473	299	36	5	0	0	228

Table L-9. Four-factor two-way tables of means for propylene response.

A \ B	.90	.95	1.00	1.05	1.10	Mean
Propane	225	296	383	266	247	283
Propylene	14830	11881	12005	12245	11065	12406

C \ B	.90	.95	1.00	1.05	1.10	Mean
600°F	7811	6419	7172	6554	6884	6968
700°F	7403	6191	6289	6884	5912	6536
800°F	7369	5656	5123	5328	4172	5530

C \ A	Propane	Propylene	Mean
600°F	277	13659	6968
700°F	287	12785	6536
800°F	287	10773	5530

A \ D	.005	.035	.065	.095	.125	.155	.185	.215	.245	.275	.305	.335	Mean
Propane	362	408	466	531	633	616	269	100	16	0	0	0	283
Propylene	32551	30607	28104	23798	17658	10373	4295	1165	269	46	0	0	12406

C \ D	.005	.035	.065	.095	.125	.155	.185	.215	.245	.275	.305	.335	Mean
600°F	17367	16393	15068	13287	10582	6483	3093	994	281	69	0	0	6968
700°F	16665	15765	14782	12414	9860	6052	2280	509	104	0	0	0	6536
800°F	15337	14365	13006	10793	6996	3948	1473	394	42	0	0	0	5530

B \ D	.005	.035	.065	.095	.125	.155	.185	.215	.245	.275	.305	.335	Mean
.90	18497	17694	16504	14719	11296	7380	3596	643	4	0	0	0	7528
.95	16068	15907	13936	12298	9729	4960	912	62	0	0	0	0	6089
1.00	17088	16004	14338	11879	7986	4544	1912	540	44	0	0	0	6194
1.05	16720	15612	14503	11521	9018	5371	2027	295	3	0	0	0	6256
1.10	13908	13132	12145	10406	7701	5216	2963	1624	662	115	0	0	5656
Mean	16456	15508	14285	12165	9146	5494	2282	632	142	23	0	0	6144

Table L-10. Four-factor two-way tables of means for carbon monoxide response.

A \ B	.90	.95	1.00	1.05	1.10	Mean
Propane	3.8	1.9	1.3	1.1	1.0	1.8
Propylene	3.3	1.4	1.1	1.0	1.0	1.6

C \ B	.90	.95	1.00	1.05	1.10	Mean
600°F	3.7	1.7	1.3	1.1	1.0	1.8
700°F	3.3	1.7	1.1	1.0	1.0	1.6
800°F	3.6	1.6	1.1	1.0	0.9	1.6

C \ A	Propane	Propylene	Mean
600°F	1.9	1.6	1.8
700°F	1.8	1.5	1.6
800°F	1.8	1.5	1.6

A \ D	.005	.035	.065	.095	.125	.155	.185	.215	.245	.275	.305	.335	Mean
Propane	1.5	1.6	1.8	2.0	2.2	2.4	2.3	1.9	1.7	1.5	1.4	1.4	1.8
Propylene	1.3	1.4	1.5	1.6	1.9	2.1	2.2	1.9	1.4	1.2	1.1	1.1	1.6

C \ D	.005	.035	.065	.095	.125	.155	.185	.215	.245	.275	.305	.335	Mean
600°F	1.4	1.5	1.6	1.8	2.1	2.3	2.4	2.3	1.8	1.5	1.4	1.3	1.8
700°F	1.3	1.5	1.6	1.8	2.0	2.3	2.2	1.7	1.6	1.3	1.2	1.2	1.6
800°F	1.5	1.6	1.7	1.8	2.1	2.3	2.2	1.6	1.3	1.3	1.2	1.2	1.6

B \ D	.005	.035	.065	.095	.125	.155	.185	.215	.245	.275	.305	.335	Mean
.90	2.2	2.4	2.7	3.0	3.4	3.9	4.2	4.6	4.2	4.0	3.9	3.9	3.5
.95	1.5	1.6	1.7	1.9	2.1	2.4	2.7	1.6	1.2	1.1	1.1	1.1	1.7
1.00	1.2	1.3	1.4	1.5	1.8	2.0	1.6	1.0	0.9	0.6	0.5	0.5	1.2
1.05	1.0	1.2	1.3	1.4	1.6	1.7	1.4	1.0	0.7	0.5	0.4	0.4	1.0
1.10	1.0	1.1	1.2	1.3	1.4	1.5	1.4	1.2	1.0	0.6	0.3	0.3	1.0
Mean	1.4	1.5	1.6	1.8	2.1	2.3	2.3	1.9	1.6	1.4	1.3	1.2	1.2

Table L-11. Four-factor two-way tables of means for carbon dioxide response.

A \ B	.90	.95	1.00	1.05	1.10	Mean
Propane	8.6	9.5	9.7	9.3	9.1	9.2
Propylene	10.0	10.0	9.9	9.0	9.1	9.6

C \ B	.90	.95	1.00	1.05	1.10	Mean
600°F	9.1	9.6	9.3	8.9	9.0	9.2
700°F	9.3	9.7	10.0	9.2	8.9	9.4
800°F	9.3	9.9	10.2	9.3	9.4	9.6

C \ A	Propane	Propylene	Mean
600°F	9.0	9.4	9.2
700°F	9.3	9.5	9.4
800°F	9.4	9.9	9.6

A \ D	.005	.035	.065	.095	.125	.155	.185	.215	.245	.275	.305	.335	Mean
Propane	6.0	6.4	6.8	7.4	8.3	9.2	10.2	11.0	11.3	11.4	11.4	11.4	9.2
Propylene	6.2	6.6	7.0	7.6	8.3	9.3	11.0	11.2	11.8	12.0	12.0	12.0	9.6

C \ D	.005	.035	.065	.095	.125	.155	.185	.215	.245	.275	.305	.335	Mean
600°F	5.9	6.3	6.6	7.2	8.0	8.9	9.9	10.9	11.5	11.7	11.7	11.7	9.2
700°F	6.1	6.5	6.9	7.5	8.3	9.3	10.4	11.2	11.5	11.7	11.7	11.7	9.4
800°F	6.3	6.7	7.2	7.9	8.6	9.5	11.5	11.2	11.6	11.7	11.7	11.7	9.6

B \ D	.005	.035	.065	.095	.125	.155	.185	.215	.245	.275	.305	.335	Mean
.90	5.9	6.4	6.8	7.3	8.1	8.9	11.5	10.7	11.3	11.4	11.5	11.5	9.3
.95	6.3	6.7	7.1	7.7	8.5	9.5	10.7	11.8	12.1	12.1	12.1	12.1	9.7
1.00	6.4	6.7	7.2	7.9	8.7	9.8	10.9	11.6	12.1	12.2	12.2	12.2	9.8
1.05	5.8	6.3	6.8	7.4	8.1	9.1	10.1	10.9	11.2	11.3	11.4	11.4	9.1
1.10	6.1	6.4	6.8	7.3	8.2	9.1	10.0	10.6	10.9	11.2	11.4	11.4	9.1
Mean	6.1	6.5	6.9	7.5	8.3	9.3	10.6	11.1	11.5	11.7	11.7	11.7	9.4

Table L-12. Four-factor two-way tables of means for oxides of nitrogen response.

A \ B	.90	.95	1.00	1.05	1.10	Mean
Propane	11.3	9.8	6.4	4.1	2.4	6.8
Propylene	16.9	15.0	7.2	4.7	2.8	9.3

C \ B	.90	.95	1.00	1.05	1.10	Mean
600°F	12.9	10.5	6.0	3.4	2.9	7.1
700°F	15.9	13.8	6.8	4.7	2.3	8.7
800°F	13.6	12.9	7.5	5.1	2.7	8.4

C \ A	Propane	Propylene	Mean
600°F	5.5	8.8	7.1
700°F	7.6	9.8	8.7
800°F	7.3	9.4	8.4

A \ D	.005	.035	.065	.095	.125	.155	.185	.215	.245	.275	.305	.335	Mean
Propane	0.2	0.4	0.5	0.7	1.1	1.8	4.9	11.6	13.9	15.2	15.4	15.8	6.8
Propylene	1.3	2.0	2.5	3.2	3.9	4.6	6.3	11.0	16.7	19.2	20.1	21.2	9.3

C \ D	.005	.035	.065	.095	.125	.155	.185	.215	.245	.275	.305	.335	Mean
600°F	1.0	1.6	1.9	2.2	2.6	2.8	4.1	8.1	12.4	15.5	16.4	17.4	7.1
700°F	0.7	1.1	1.4	1.9	2.4	3.4	5.4	12.3	17.4	18.9	19.6	20.0	8.7
800°F	0.7	1.0	1.2	1.8	2.6	3.5	7.5	13.5	16.2	17.2	17.4	18.2	8.4

B \ D	.005	.035	.065	.095	.125	.155	.185	.215	.245	.275	.305	.335	Mean
.90	1.4	2.3	2.8	3.5	4.3	5.0	8.5	15.0	26.0	31.7	33.7	35.1	14.1
.95	1.7	2.4	2.5	3.3	3.6	4.4	8.1	21.7	24.5	25.5	25.1	25.8	12.4
1.00	0.3	0.6	0.8	1.3	1.9	2.7	5.6	9.9	12.8	14.8	15.0	15.7	6.8
1.05	0.2	0.3	0.6	0.8	1.4	2.2	3.2	5.8	8.3	9.3	10.3	10.6	4.4
1.10	0.3	0.4	0.8	0.8	1.3	1.8	2.8	4.0	4.6	4.7	4.8	5.3	2.6
Mean	0.8	1.2	1.5	1.9	2.5	3.2	5.6	11.3	15.3	17.2	17.8	18.5	8.1